Abstract

Title of dissertation: PROTEIN PERMEABILITY PATHWAYS IN THE MITOCHONDRIAL OUTER MEMBRANE DURING APOPTOSIS – MECHANISTIC INSIGHTS INTO THEIR STRUCTURE AND DYNAMICS

Vidyaramanan Ganesan, Doctor of Philosophy, 2012

Dissertation directed by: Dr. Marco Colombini
Department of Biology

Apoptosis, a form of programmed cell death is a physiological process that guides the systematic removal of unwanted cells from the body. A key step in apoptosis is the irreversible release of mitochondrial intermembrane space (IMS) proteins into the cytosol by a process called **M**itochondrial **O**uter **M**embrane **P**ermeabilization (MOMP). MOMP is regulated by a class of proteins called Bcl-2 family and a sphingolipid called ceramide. The pro-apoptotic Bcl-2 proteins, especially Bax and Bak can cooperate with ceramide to form channels in mitochondria that cause protein efflux during MOMP. The ability of ceramide to form protein-permeable channels in MOM is established. Bax and ceramide enhanced MOMP synergistically. The ability of Bax to stimulate ceramide channels was investigated. It was found that the apparent affinity of Bax for a ceramide channel increases with the ceramide channel size. The results indicate that Bax binds a small ceramide channel and drives its growth until the Bax molecule finds the best fit to the channel. This interaction between Bax and a ceramide channel does not require of the presence of other Bcl-2 proteins or mitochondrion-specific factors. The structural features of ceramide were investigated for their role in channel formation. Analogs of ceramide bearing modifications in the functional groups were analyzed for their ability to form channels to assess stability and also to interact with native ceramide to form channels to

assess compatibility between interacting groups. The C1-hydroxyl was found to be indispensable for channel formation while the C3-hydroxyl was inconsequential. The amide nitrogen with its ability to donate hydrogen was important for stability. Similarly, converting the carbonyl oxygen to a urea group, now more polar resulted in more stable permeabilization. Phytoceramide, which has a C4 hydroxyl instead of the C4-C5 *trans* double bond formed stable channels but phytoceramide inhibited channel formation by ceramide suggesting incompatibility in structure.

Bax activation involves translocation of Bax from the cytosol to the MOM, conformational changes and subsequent channel formation. All steps involved in Bax activation are not well-understood. We have used ionic strength as a modulating tool to dissect the different steps in Bax mediated MOMP. Increasing the ionic strength was found to delay formation of real-time permeability by Bax. Increasing the ionic strength resulted in smaller channels that grew in size slowly. The high permeability induced by low ionic strength was not reversed by raising the ionic strength suggesting that Bax channels are not in dynamic equilibrium with Bax monomers. Ionic strength also altered the sensitivity of Bax mediated MOMP to inhibition by Bcl-xL. Ionic strength, however did not affect Bax insertion into membranes. Thus, ionic strength presents a good diagnostic tool to modulate Bax mediated channel formation downstream of Bax insertion into membranes.

PROTEIN PERMEABILITY PATHWAYS IN THE MITOCHONDRIAL OUTER MEMBRANE DURING APOPTOSIS – MECHANISTIC INSIGHTS INTO THEIR STRUCTURE AND DYNAMICS

By

Vidyaramanan Ganesan

Dissertation submitted to the faculty of the graduate school of the
University of Maryland, College Park in partial fulfillment
of the requirements for the degree of
Doctor of Philosophy
2012

Advisory committee:

Dr. Marco Colombini, chair
Dr. Heven Sze
Dr. Ricardo Araneda
Dr. Richard Stewart
Dr. Volker Briken

Preface

This dissertation describes my research on the protein permeability pathways formed in the mitochondrial outer membrane (MOM) during apoptosis by two distinct classes of molecules. The first is a class of lipids called sphinogolipids, especially ceramide. The second is a family of proteins called Bcl-2 with emphasis on Bax. The interactions between ceramide and Bax were also investigated.

Chapter 1 is a general introduction to the field of apoptosis of Programmed Cell Death (PCD) where these permeability pathways operate. A thorough review of the literature summarizing our present understanding of apoptosis, the role of mitochondria in apoptosis, the different hypotheses about the possible MOM permeability pathways in apoptosis and the necessity and relevance of the research of this dissertation in the big picture of apoptosis are presented.

Chapter 2 describes in detail those methods common to all the different lines of research undertaken in this dissertation. Emphasis of the description is on the detail necessary to reproduce the experimental conditions used in the various experiments in this research. The appropriateness of the choice of experiments to the research problem in question is also addressed.

Chapter 3 describes the research that dealt with the interaction of Bax with ceramide in inducing MOMP. A synergistic interaction between Bax and ceramide in inducing MOMP was discovered. Further, the structural mechanism of this interaction was investigated in detail. We found that Bax causes expansion of the ceramide channels by

varying its apparent affinity for the channel based on the channel size. This work was performed in collaboration with Meenu Perera and published in the journal *Apoptosis*.

Chapter 4 describes the research on the role of different functional groups in determining the ability of ceramide to form channels. Analogs with changes in the critical functional groups of ceramide were tested for their ability to form channels in mitochondria and planar membranes. It was found that the C1-hydroxyl is critical for channel formation while the C3-hydroxyl is not. The hydrogen bonding ability of amide nitrogen is crucial for the channel stability. The chain length of the hydrocarbon chains was inconsequential to channel formation by ceramide. Phytoceramide was capable of forming channels but was incompatible with native ceramide. This work was performed in collaboration with Meenu Perera and published in the journal *BBA- Biomembranes*.

Chapter 5 describes insights into Bax channel formation in the MOM using ionic strength as a modulating tool. Ionic strength slowed the formation of real-time permeability without affecting Bax insertion into the MOM. Ionic strength resulted in the formation of smaller channels resulting in a slower rate of release of bigger proteins from mitochondria during MOMP. Ionic strength also enhanced the ability of Bcl-xL to inhibit MOMP. This work has been accepted for publication in the *Biophysical Journal*.

Chapter 6 provides a discussion of the scope of the results in the light of the big picture of apoptosis and MOMP. It also provides a brief vision for the future, some questions that merit investigation to gather a better understanding of apoptosis.

Acknowledgements

First and foremost, I would like to extend my most sincere gratitude to my advisor Dr. Marco Colombini who has been more than a mentor, literally a scientific father, in my graduate life. Graduate research has been a telling exercise in learning, research, curiosity, anxiety, discovery and accomplishment. To describe Dr. Colombini's role in seeing me emerge from each phase of graduate school as a better researcher cannot be put down in words. More than the scientific question I addressed for my graduate dissertation, it is the training in scientific thinking that I received from Dr. Colombini that has made the whole effort worthwhile and meaningful.

I would also like to thank my committee advisors Dr. Heven Sze, Dr. Richard Stewart, Dr. Volker Briken, Dr. Sergei Sukharev and Dr. Richardo Araneda whose advice guided my research direction.

I am also thankful to my parents Geetha and Ganesan, who have stood by me at all times and lifted me when I slipped and made sure I continued the journey. Without them, … Sorry I cannot even imagine anything without them.

I met some of the best people as lab mates who have left a deep impression in me by their creativity, knowledge, commitment and motivation. Most significant of them is Meenu N. Perera with whom I found a very successful and productive collaboration. There were extended periods when we were the only graduate students in the lab and to think that we led the ship of research in the lab from the front thrills me even now. Later came along Soumya Samanta, with whom I share a deep personal rapport and friendship. He has

been my savior at many exigencies and the thought the he has been present did motivate me to try both my legs in many an adventure.

Shang and Kaiti, the knowledge tanks, have been always up with fruitful suggestions and have had a significant influence in my pursuit of research.

My last project would have not been possible without this undergraduate honors student Timothy Walsh. In spite of heavy coursework, he was around, racing with time, doing multiple assays, generating data with almost nil error. He did not have to be told twice. Often he creatively guided the work through new productive routes. His hands would make no mistakes in science. His dedication indeed motivated me when the going was tough. I wish him all the best in all his pursuits in the future.

Many people in the graduate school, faculty and administrators, have made my time at UMD pleasant. I would also like to thank Dr. Destefano, who was a great guiding force in my first year at UMD and on many occasions subsequently. Among the other office-bearers, I would like to thank Sarah Biancardi, who took every care that I needed as a new student in 2006; I had a smooth transition adjusting to a radically different education system here. Lois Reid also saved me a lot of time and effort by helping me with the necessary paperwork so I could better focus on research. I also thank the various members of the administrative staff: James Parker, Wan Chen, KeCia Harper, Lindsey Johnson, Larry Shetler and Douglas Downing.

Off lab, Sriram Krishnan, Anand Giridhar, Sivaprakash Agastin and Krishna Kannan have been friends for a long time have given me a lot of support and companionship in my scientific pursuits. I thank my many roommates, especially Praveen Vaddadi, my

faithful companion in every road trip, movie, restaurant and my journey into the realms of religion and philosophy. Kazi Rajibul Islam was another such roommate whose company I count as memorable.

I also thank my mentors and friends in my extra-academic pursuits. Important among them are Guru Sri. Ananthakrishnan, Dr. Swarup, Rajesh Rachabattuni, Dr. Avinash Varna, Sri. Visweswaran, Dr. Mouna Selvam, Mr. Vayudeva and Dr. Nigel Siva. Narendar Chandrashekar, Anand Seetharaman, Raghuraman Janamanchi, Vishy Mahadevan, Vaidyanathan Anantharaman and Ganesh Sivaraman were my partners in the Veda circle.

Hemavathy, my soon to be my better half, brought with her all the positive changes in my life at the closing stages of this thesis that are defining my future. My gratitude to her is suffused in our love.

Last, I am in complete devotion to Kanchi Paramacharya, the divine force, who has stood by me in soul.

Table of contents

List of Tables

List of figures

List of abbreviations

MOMP: **M**itochondrial **O**uter **M**embrane **P**ermeability

MOM**: M**itochondrial **O**uter **M**embrane

Bcl-2: **B C**ell **L**ymphoma

BH: **B**cl-2 **H**omology

AK: **A**denylate **K**inase

ER: **E**ndoplasmic **R**eticulum

Ac-Bax: **Ac**tivated Bax

SOX: **S**ulfite **Ox**idase

PROTEIN PERMEABILITY PATHWAYS IN THE MITOCHONDRIAL OUTER MEMBRANE DURING APOPTOSIS – MECHANISTIC INSIGHTS INTO THEIR STRUCTURE AND DYNAMICS

CHAPTER 1 GENERAL INTRODUCTION

Apoptosis, a form of programmed cell death, is a complex, systematic process by which the multicellular organism eliminates damaged cells from its system. Cells constantly divide and renew themselves. Old cells are eliminated to make way for new cells. Cells could be damaged by infection by bacteria or viruses or various chemicals could induce DNA damage. In such circumstances, if the microbes cannot be destroyed or if the DNA damage cannot be corrected, the safest option for a cell is to undergo apoptosis to prevent the infection from spreading to other cells or in the case of DNA damage, stop the formation of cancer. Apoptosis is classified as intrinsic or extrinsic based on the nature of the mode of apoptotic induction (1).

Internal apoptotic signals like DNA damage or microbial infection induce intrinsic apoptosis. This process is mediated by a special class or proteins called the Bcl-2 family. In this mode of apoptosis, an upstream caspase called caspase 8 cleaves the Bcl-2 family protein Bid into its active form called tBid (truncated Bid) which in turn activates the pro-apoptotic Bcl-2 family proteins Bax and Bak which induce **M**itochondrial **O**uter **M**embrane **P**ermeabilization (MOMP). Experimental apoptosis inducers such as ultraviolet light (UV), ceramide, etoposide and doxorubicin can also induce intrinsic apoptosis. The proteins released from mitochondria activate the downstream caspases like caspase 9 which initiate the execution phase of apoptosis.

In extrinsic apoptosis, signals from neighboring cells like CD95L, TNF-α engage death receptors on the plasma membrane which in turn activate caspase 8. Active caspase 8 can either activate tBid mediated MOMP or directly activate the downstream caspases bypassing the mitochondrial step. Chemicals like staurosporine or cyclohexamide can induce extrinsic apoptosis.

Apoptosis as a protective mechanism

An important role of apoptosis is to protect the host multicellular organism from microbial infections and cancer. Many a time, cells can be infected by bacteria or viruses that escape the immune surveillance in the blood. Such infected cells undergo apoptosis to not only prevent the infection from spreading to other cells but also to present the antigens of the microorganisms to the immune system. The apoptotic bodies resulting from the disbanded apoptotic cells are consumed by the macrophages that digest the microorganisms and produce antigens from the degradation of the microbial proteins. These macrophages act as antigen presenting cells to prime the immune T cells to the microorganisms. Prevention of host cell apoptosis is an important mechanism by which many bacteria and viruses evade the immune system (2 - 5). Alternatively, some pathogens induce apoptosis to aggravate the infection (5). The T cell apoptosis induced by HIV is one example.

Another significant role of apoptosis is to eliminate cells with DNA damage. DNA damage can result in such mutations that can cause cancer. Damaged DNA stimulates the cellular apoptotic machinery through p53 (6). P53 up regulates Puma and a host of other apoptotic proteins.

Apoptosis as a homeostatic mechanism

Apoptosis is also an integral part of the embryonic developmental program of the multicellular organism. It is apoptosis that causes digitation of the fingers by removing the inter-digital cells in our hands and toes. But for apoptosis that removes a line of cells in the eyelid and enables the lid's opening and closure, we would have never been able to perceive the world around us in its multitude of colors and shapes. Indeed, apoptosis is an eye opener (7).

The cellular mechanism of apoptosis initiation

The upstream processes of apoptosis converge at the activation of a class of proteases called the caspases. Caspases are classified as either upstream or downstream based on their temporal role in the apoptotic timeline. Once the death receptor mediated signaling is initiated, these receptors dimerize to form a signaling complex called the Death Inducing Signaling complex which activates an upstream caspase called caspase 8. This is accomplished by the proteolytic cleavage of pro-caspase or zymogen into active caspase by the signaling complex. The active caspase 8 can in turn activate either downstream caspases 3, 7 and 9 (the executioner caspases) by proteolytic cleavage directly leading to the execution phase of apoptosis or activate the Bcl-2 family protein Bid into its active version (tBid) engaging the mitochondria in the subsequent phase of apoptosis. Mitochondria release certain pro-apoptotic proteins that stimulate the downstream caspases leading the cell forward into the execution phase (1, 8). Cells are classified at type I or type II based on whether the upstream caspase engages the downstream caspases directly or through the role of mitochondria respectively (1, 8).

Apoptosis execution

The direct activation of downstream caspases occurs in extrinsic apoptosis. In intrinsic apoptosis, the caspase 8 mediated activation of Bid results in the release of pro-apoptotic proteins from the mitochondria. Of these, cytochrome *c* forms a heptameric complex called apoptosome with a cytosolic protein called Apaf-1. The apoptosome acts as the activator of the executioner caspase namely caspase – 9 (Fig 1.1). Once the downstream caspases are activated, they accomplish the digestion of all other cellular proteins and packaging of the cell into apoptotic bodies.

Mitochondria in apoptosis

Mitochondria, the powerhouse of the cells, have a crucial role in apoptosis. Mitochondria consist of an outer membrane that is freely permeable to small solutes but impermeable to proteins. The inner membrane, which is folded into cristae has a greater surface area and houses the respiratory complexes that are used to generate the energy. The inner membrane is impermeable to all solutes. The mitochondria are dynamic structures that are constantly undergoing fission and fusion with other mitochondria (9, 10, 11). The fission of mitochondria is regulated by GTPases called Drp1 (dynamin Related Protein 1) and Fis1 (Fission Protein 1) (9, 10, 11). The fusion of the outer membrane is regulated by the Mitofusins (Mfn1 and 2) (9, 10, 11). The fusion of the inner membrane is regulated by another dynamin related GTPase called Opa1 (9, 10, 11). The inter-membrane space is the volume between the 2 membranes that contains many proteins. Important among these is the cytochrome *c* which shuttles electrons between the respiratory complexes. Other proteins include SMAC/Diablo, endonuclease G and AIF which have important

functions in apoptosis. Matrix is the volume enclosed by the inner membrane and contains metabolic enzymes.

A crucial step in apoptosis is MOMP (fig 1.1) which is considered the point of no return. In this step, the mitochondrial outer membrane which is normally impermeable to proteins is breached and the **I**nter-**M**embrane **S**pace (IMS) proteins translocate to the cytosol and activate the downstream caspases, importantly caspase 9 and caspase 3. This step is tightly regulated by the Bcl-2 family of proteins (12, 13). This family of proteins consists of 3 classes classified based on their role in apoptosis and the number of defining **B**cl-2 **H**omology (BH) domains they possess. While the outer membrane changes determine the commitment to apoptosis, changes to the inner membrane occur downstream of the MOMP and caspase activation. Especially, the permeability transition of the inner membrane occurs downstream of caspase activation.

Bcl-2 family proteins: Classification, location and function

Pro-apoptotic BH1-3 type proteins: These proteins have 3 of the 4 BH domains and are pro-apoptotic in their action. They directly engage with the MOM to induce MOMP. Bax, Bak are the most studied BH1-3 type proteins.

Pro-apoptotic BH3 only proteins: These proteins contain only one BH domain namely BH3. They act indirectly to induce MOMP by either favoring the insertion of BH1-3 pro-apoptotic proteins into the MOM or interfering with the activity of the anti-apoptotic proteins. Bid, Bim, PUMA, Bad and Bik are the best known members of this family.

Anti-apoptotic Bcl-2 proteins: These proteins inhibit MOMP. Structurally they contain all 4 BH domains. The members of this group include Bcl-2, Bcl-xL, Mcl-1, and A1.

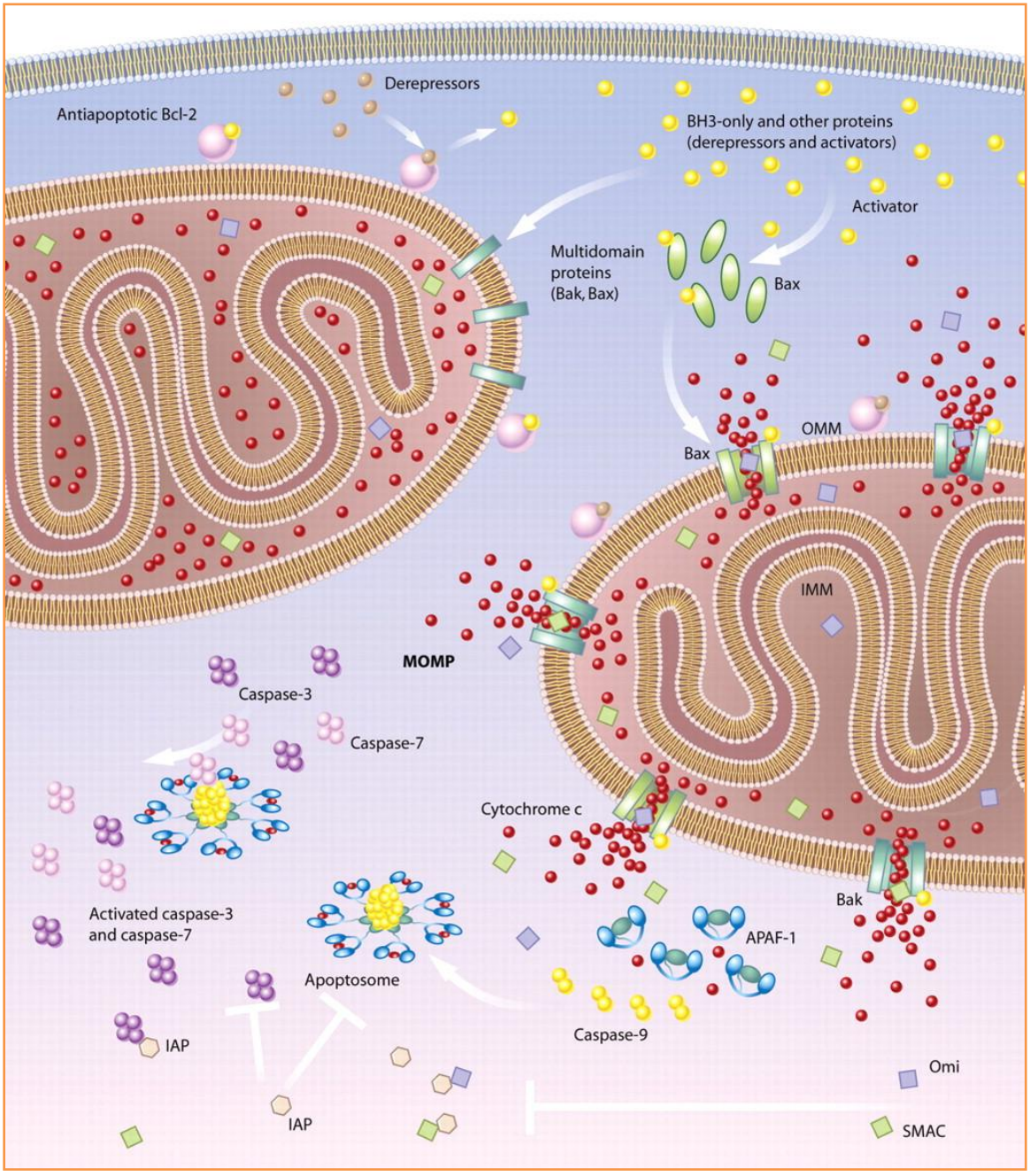

Fig 1.1 (reproduced from Spierings, D., McStay, G., Saleh, M., Bender, C., Chipuk, J., U. Maurer, U and D. R. Green. 2005. Connected to death: the (unexpurgated) mitochondrial pathway of apoptosis. Science 310:66-67. (14) Reprinted with permission from AAAS): During apoptosis, BH3 only proteins induce conformational changes in BH1-3 type proteins and cause the translocation of Bax from the cytosol to the MOM. In the MOM, Bax and Bak enable the formation of the MOMP pore that allows the IMS proteins to efflux into the cytosol which activates downstream effectors of apoptosis. In normal cells, anti-apoptotic proteins prevent MOMP.

The Bcl-2 class of proteins is all nuclear-encoded and different members have different cellular locations (12 – 14). For example, Bax is normally cytosolic as a soluble monomer but becomes membrane-integrated at the MOM during apoptosis. On the contrary, Bak is always resident in the MOM. The pro-apoptotic activity of Bak is kept in check by its engagement with VDAC2, an integral MOM protein and this interaction is disrupted by tBid during apoptosis (15).

Similar to Bax, Bid shows a cytosolic localization under normal conditions. During apoptosis, Bid undergoes proteolytic cleavage by caspase - 8 into a p15 and p7 fragment. The p15 fragment, called the tBid (truncated Bid) now has an exposed transmembrane region and integrates with the MOM (12). Other BH3 only proteins like Puma, Noxa and Bik show only cytosolic localization irrespective of the physiological status of the cell (12).

The anti-apoptotic proteins Bcl-xL, Mcl-1 and A1 are cytosolic but during apoptosis Bcl-xL migrates to the MOM to inhibit permeabilization. Bcl-2, another anti-apoptotic protein is an integral membrane protein of the MOM but has been found to localize to the ER membrane also (12).

The members of the Bcl-2 family show specificity in their interaction with other members of the family. For example, Bcl-xL interacts with Bax, Bak, tBid and most other BH3 only proteins. But Bcl-2 interacts with Bax and tBid but not with Bak. Similarly Mcl-1 interacts with Bak, Bim and tBid but not Bax (16). The spectrum of interaction of one Bcl-2 family member with another is determined by the sequence of the BH3 domain of each of the proteins. Independent of their role in apoptosis, the multi-domain Bcl-2

family proteins have pivotal roles in regulating mitochondrial fission/fusion dynamics. (17).

Bax

Bax is a 21 kDa monomeric cytosolic pro-apoptotic Bcl-2 family protein that translocates to mitochondria during apoptosis. This translocation is associated with conformational changes (termed Bax activation) and homo-oligomerization or hetero-oligomerization with Bak that eventually lead to MOMP. *In vitro*, activation of Bax can be induced by certain non-ionic detergents like octyl-glucoside at their **C**ritical **M**icellar **C**oncentration (CMC: the concentration at which the detergent molecules form micelles) (18, 19) or by BH3 only proteins like tBid or BIM in the presence of MOM or MOM-like membranes (20, 21).

Ceramide

Another crucial molecule, whose involvement in MOMP is increasingly being appreciated, is a sphingolipid called ceramide (22 - 24). Mitochondrial ceramide levels increase prior to MOMP (24 - 27). Mitochondrial ceramide is capable of causing translocation of Bax from the cytosol to the MOM and its subsequent activation (25, 28, 29). We have found that ceramide can form large protein-permeable channels in the MOM (30, 31). Unlike other common membrane lipids namely the phospholipids, sphingolipids are not based on esterification of glycerol but on sphingosine and its amide linkage to fatty acids. The amide linkage is planar as in α-helices of proteins and along with the two hydroxyls at the C1 and C3 positions has a great potential for hydrogen bonding. This is perfect for generating assemblies and ceramide channels are proposed to

be formed by a ring of columns each consisting of 6 ceramides interconnected by the hydrogen bonds of the amide linkage (Fig. 1.2). The columns of ceramide have a net dipole in one direction that can destabilize the column. In ceramide channels, adjacent columns are thought to have anti-parallel configuration and hence the dipoles would have opposite directions, hence canceling each other (32). These pairs of columns align themselves in the membrane forming a cylinder through which proteins can pass. The proposed ceramide channel model envisions that, with the addition of more ceramide, the channels expand in size with the incorporation of more ceramide into the channel structure. Studies with planar phospholipid membrane suggest that ceramide forms single channels in membranes that vary from being weakly cation-selective to non-selective. In the mitochondrial outer membrane, size measurements based on gel filtration of proteins released from the IMS suggest that the channels can be big enough to cause release of proteins up to 60kDa (31). These measurements were made under denaturing conditions and thus the actual size of the channels could be even greater.

Channel formation in the MOM can be measured in two ways. First, protein release from the IMS can be measured by assaying for the IMS enzymes or western blotting on the IMS proteins from the extra-mitochondrial medium. Alternatively, any protein-permeable pore in the membrane must allow the bi-directional diffusion of proteins across the membrane. The cytochrome *c* oxidation assay measures the rate of flux of exogenous cytochrome *c* across the MOM (31).This assay defines the status of the pore at any given time. One can follow both an increasing permeability as channels form and a decreasing one as they are disassembled (33).

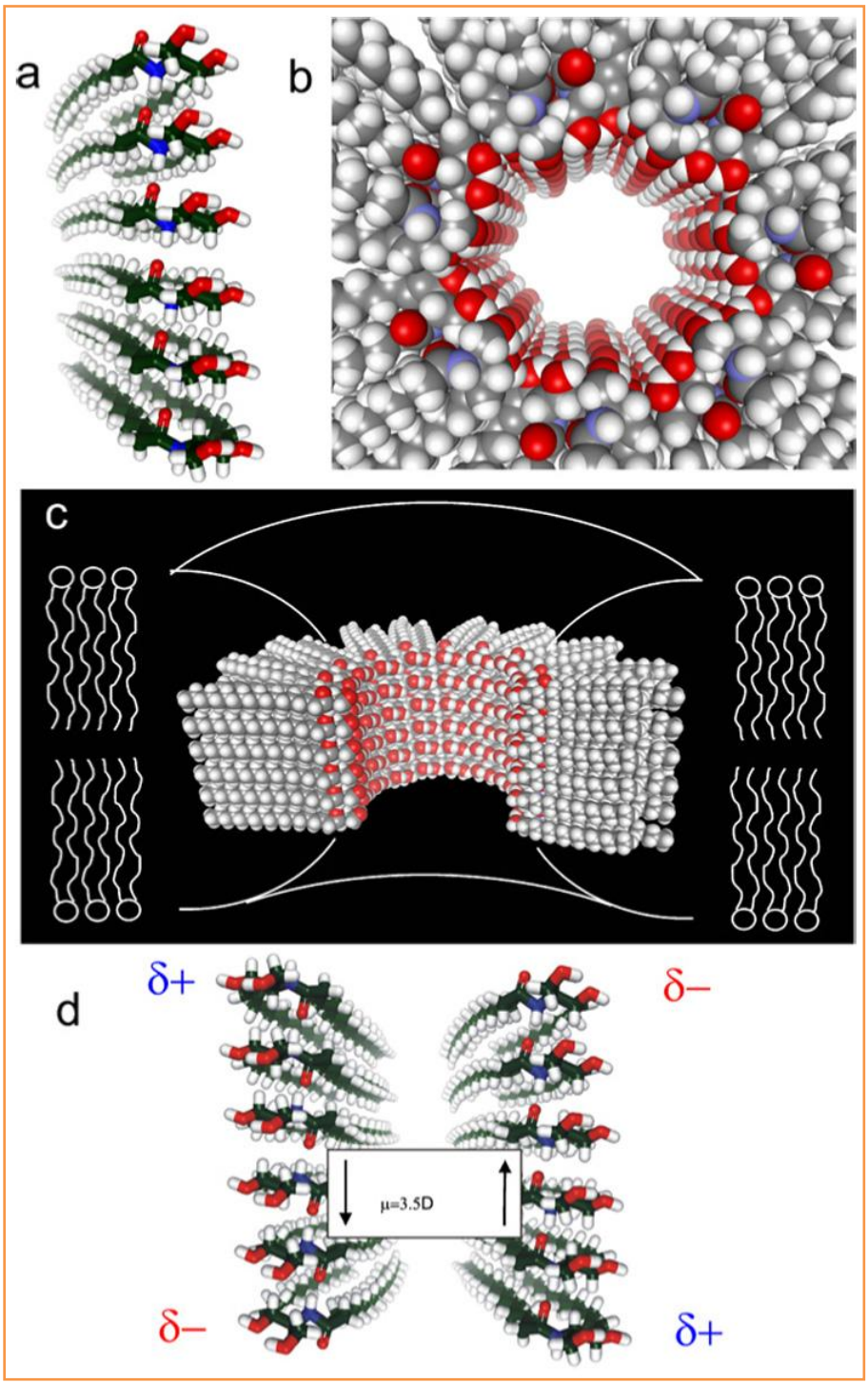

Fig 1.2: (reproduced from L.J. Siskind 2005(24)): a) A column of 6 ceramides can span the membrane. B & c) Many such columns align beside one another to form a ceramide channel. d) Each column is directional and has a net dipole. Adjacent columns have an anti-parallel orientation canceling the dipoles.

The concentration of ceramide in the membrane determines the ability of channel formation. This is determined by the metabolism of ceramide. In the mitochondrial outer membrane, there are enzymes capable of both ceramide synthesis and hydrolysis (34, 35, 36). The tight interaction between the MOM and ER membranes also provides an opportunity for ceramide exchange (37) between the site of ceramide de novo synthesis (the ER) and the MOM. However, ceramide metabolism can also produce other intermediates that influence ceramide channel formation. For example, both dihydroceramide and sphingosine interfere with ceramide channel formation (38, 39). Finally, and most importantly, Bcl-2-family proteins can also influence the stability of ceramide channels (33).

Ceramide metabolism

The synthesis and consumption of ceramide by multiple routes on different membranes presents an interesting and complex maze of that strongly defines the availability of ceramide at different locations to accomplish different functions. As already pointed out, ceramide metabolism determines the concentration of not only ceramide but also other sphingolipid metabolites in the MOM that can interfere with ceramide channel formation. Hence ceramide metabolism naturally factors itself into the study of ceramide channel formation especially in *in vivo* conditions.

Ceramide can be synthesized by anabolism from simpler molecules by the *de novo* pathway (22, 24) that begins with the condensation of serine and palmitoyl coA in the ER by the enzyme Serine Palmitoyl coA transferase. Since the palmitoyl group is saturated, the resulting molecule is 3-keto dihydrosphingosine which has only one acyl chain, that

of sphingosine. This molecule is acylated by another ER resident enzyme dihydroceramide synthase to generate dihydroceramide. There are different ceramide synthases that differ in their specificity of the acyl chain length that they add to the sphingosine (22). Finally Dihydroceramide desaturase converts dihydroceramide to ceramide in the ER. The ceramide can be further converted to sphingomyelin to by sphingomyelin synthases. Otherwise, the ceramide can be transported to the Golgi by a ceramide transfer protein called CERT (22). Different CERT isoforms show different acyl chain length specificities to the ceramide. Transport of ceramide from the ER to the mitochondria seems to occur through direct exchange of ceramide between mitochondria associated ER membranes and the MOM (37).

The salvage pathway of ceramide synthesis (22, 24) involves breakdown of sphingomyelin to ceramide by the enzymes sphingomyelinases. These sphingomyelinases are classified as acidic or neutral based on the optimal pH for their activity. They are present in different locations and hence constitute the major source of ceramide in different membranes like the plasma membrane and the lysosomes. During apoptosis, an acid sphingomyelinase from an unknown location has been found to localize in the mitochondria, presenting another source of ceramide generation in the MOM (27).

Ceramides are broken down by ceramidases which are also classified as acid, neutral or alkaline based on the optimal pH for their activity. These enzymes are also present in different locations including the mitochondria. Ceramidases convert the ceramide to sphingosine. Further breakdown of sphingosine after its phosphorylation to S1P in the ER occurs by an enzyme called S1P lyase which breaks down S1P to ethanolamine and hexadecanal (22, 24).

Physiological relevance of ceramide channels

Ceramide is a vital sphingolipid that participates in a slew of cellular events including cell senescence, apoptosis, differentiation, cell cycle arrest and raft formation during cell signaling (22). Focusing on apoptosis, exogenously-added ceramide has been found to be able to induce apoptosis in a variety of cell types. Moreover, cellular ceramide levels rise in response to various apoptotic stimuli (40 - 44). Since ceramide is virtually insoluble in water, it can be isolated in different membrane compartments. The mitochondrion is a particularly important site where an increase in the ceramide level is associated with apoptosis. While mitochondria are equipped with their own ceramide synthesizing machinery (34, 39) migration of acid sphingomyelinase to mitochondria has been observed in response to UV irradiation (27) resulting in elevation of mitochondrial ceramide. The localization of ceramide to the MOM during apoptosis is also correlated with MOMP (24). Several studies have found that isolated mitochondria can be permeabilized by adding ceramide (24, 28, 45, 46). Targeted elevation of mitochondrial ceramide can also lead to mitochondrial permeabilization and the subsequent steps of apoptosis (46). Anti-apoptotic Bcl-2 proteins, namely Bcl-2 and Bcl-xL have been found to negatively regulate ceramide synthesis during apoptosis (47 - 49) and to favor the disassembly of ceramide channels (33). Thus the case for ceramide's importance in causing apoptosis in cells is very strong.

Bax channels

Bax translocation to the MOM precedes MOMP in cells. *In vitro,* addition of Bax and tBid causes IMS protein release (50 - 54). Thus, Bax is thought to form channels in the

MOM to allow IMS protein efflux into cytosol during apoptosis. This notion is further substantiated by the observation that Bax is structurally similar to bacterial toxins particularly, diphtheria toxin (13). Also, Bax forms ion-conducting channels in planar membranes (55, 56). But the dynamics of Bax activation and subsequent channel formation are only partially understood. *In vivo*, a long time gap of a few hours exists between Bax translocation to mitochondria and MOMP (57, 58). This implies that additional activation signals are necessary to stimulate membrane-bound Bax to form channels (58). The stoichiometry of Bax channels, size, nature of open and closed states are also unknown.

Aim of the research

The goal of this dissertation is to study the mechanism of structural regulation of ceramide and Bax channel formation. While the role of anti-apoptotic proteins in regulating ceramide channels has been well established (33), the mechanism by which Bax, a pro-apoptotic Bcl-2 protein regulates ceramide mediated permeabilization is investigated here. The question of how the different functional groups of the ceramide molecule contribute to its ability to form channels was also investigated. Finally we have investigated the dynamics of Bax channel formation using ionic strength as a tool to dissect the different steps in the growth of Bax channels.

CHAPTER 2 COMMON MATERIALS AND METHODS

Isolation of rat liver mitochondria

The isolation of mitochondria from rat liver was done as described (31, 59). Briefly, male Sprague-Dawley rats were fasted overnight. On the next day, they were euthanized by exposure to high levels of CO_2 and decapitation. The liver was removed by surgery and minced and kept cold in ice-cold mitochondrial isolation buffer (70mM sucrose, 210mM mannitol, 1mM EGTA and 5mM HEPES-KOH pH 7.5) supplemented with 1% BSA. Then the tissue was homogenized. The homogenate was subjected to alternate cycles of centrifugation in low speed (700 RCF) and high speed (5600 RCF) twice each for 10 minutes at 4^oC to enrich the mitochondrial fraction. The resulting pellet was resuspended in BSA-free mitochondrial isolation buffer and centrifuged at high speed for 10 minutes at 4^oC to remove BSA. The final pellet was resuspended in ice-cold sucrose-free isosmotic buffer called FH (280mM mannitol, 1mM EGTA and 5mM HEPES-KOH pH 7.4). The concentration of mitochondrial protein was determined as previously described (4).

Preparation of cytochrome *c*

Horse heart cytochrome *c* (44mg) was dissolved in 1mL of 0.2M Tris-HCl pH 7.5 and then 11mg of ascorbate was added to reduce all the cytochrome *c*. The reduced cytochrome *c* was separated from the ascorbate in a sephadex G-10 column equilibrated with 0.2M Tris-HCl pH 7.5.

Cytochrome *c* oxidation assay

The cytochrome *c* oxidation or complex IV accessibility assay measured the ability of exogenously added cytochrome *c* to diffuse across the MOM to access the cytochrome oxidase complex (complex IV) in the MIM and be oxidized by it. The MOM is normally impermeable to proteins unless the outer membrane is permeabilized. Thus, the rate of oxidation of exogenous cytochrome *c* is directly proportional to the extent of outer membrane permeabilization. In this assay, mitochondria were treated with suitable permeabilizing agents (ceramide or Bax/tBid) and incubated. At the end of incubation, all or fraction of the mitochondria were resuspended in cytochrome *c* oxidation assay buffer (buffer isosmotic to FH supplemented with 5mM DNP and 5µM antimycin A). Cytochrome *c* (~25nM final) was added to the suspension and the change is absorbance was quickly measured for 2 minutes at 550nm. Reduced cytochrome *c* absorbs at 550nm but this absorbance declines as it gets oxidized. Thus, the rate of decline of absorbance at 550nm is a direct measure of rate of cytochrome *c* oxidation. And the initial rate of cytochrome *c* oxidation is a measure of the extent of MOMP permeabilization. Please refer to specific materials and methods in each chapter for details of the amount of mitochondrial protein used for assay, type and concentrations of permeabilizing agents used.

Measurement of mitochondrial intactness

The intactness of the mitochondrial preparation must be > 80% for reliable experimentation. For each mitochondrial preparation, the intactness was determined using the cytochrome *c* accessibility assay. The rate of oxidation of cytochrome *c* by

control mitochondria that were not treated with any permeabilizing agent must be very low. This rate was compared to the rate of cytochrome *c* oxidation by an equivalent amount of hypotonically shocked mitochondria that would allow complete access of exogenous cytochrome *c* to cytochrome oxidase complex. The ratio of control rate to hypotonically shocked rate multiplied by 100 gives % intactness of mitochondria.

Purification of Bcl-2 family proteins

All Bcl-2 proteins were expressed and purified in *E.coli.* Bax was purified as described (18, 60) with slight modifications. The final elute from the chitin column was dialyzed in microporous membrane of 12000MW cutoff for 24 hr at 4^{o}C in 3L buffer (1mM EDTA, 20mM Tris-HCl pH8). The dialysis was repeated in 5L of buffer of same composition to remove residual DTT. tBid (61) and Bcl-xL (60, 62) were purified as published earlier. All purified proteins were filter-sterilized through 0.2µm filter and glycerol was added to a final concentration of 10% v/v. small aliquots were flash-frozen with dry ice and ethanol in thin-walled glass tubes and stored at -80^{o}C until use. Once a tube was thawed for use, it was not re-frozen or re-stored.

Adenylate kinase (AK) assay

Adenylate kinase (AK) is a 24KDa IMS protein that is released into the cytosol from mitochondria during apoptosis. This enzyme converts 2 molecules of ADP into ATP and AMP. AK can be assayed using a coupled enzyme system that utilizes ATP (31). In this assay, ATP produced by the AK reaction is consumed by hexokinase to convert glucose to glucose – 6 – phosphate which is oxidized by G3P dehydrogenase and electrons transferred to NADP which forms NADPH. NADPH absorbs at 340nm while NADP

does not. Thus, when other reaction components are in excess and the amount of AK is the only rate-limiting factor, the rate of increase in absorbance at 340nm is a direct measure of AK activity. Mitochondria (final concentration 160µg/mL) were treated with suitable concentrations of the permeabilizing agents (exact quantities are mentioned in the methods of corresponding chapters or figure legends) and incubated. At the end of the incubation, the mitochondria were centrifuged at 14000 RCF and supernatant collected and kept cold. The 2.5µL enzyme mixture of hexokinase and G6P dehydrogenase (final concentration – 5 units each) was added to 350µL of AK reaction mixture (50mM Tris, 5mM $MgSO_4$, 10mM glucose, 5mM ADP, 0.2mM NADP pH 7.5) 5 minutes prior to assay to remove residual ATP from the mixture. Then 150µL of the mitochondrial supernatant was added to the reaction mixture and the initial increase in absorbance measured at 340nm for 5 minutes. Maximal release of AK corresponding to 100% was measured by osmotically lysing equivalent amount of mitochondria and measuring the activity of that supernatant.

CHAPTER 3 CERAMIDE AND ACTIVATED BAX ACT SYNERGISTICALLY TO ENHANCE MITOCHONDRIAL OUTER MEMBRANE PERMEABILIZATION

ABSTRACT

A critical step in apoptosis is mitochondrial outer membrane permeabilization (MOMP), releasing proteins critical to downstream events. While the regulation of this process by Bcl-2 family proteins is known, the role of ceramide, which is known to be involved at the mitochondrial level, is not well-understood. Here, we demonstrated that Bax and ceramide induce MOMP synergistically. Using a release assay and the real-time measurement of MOMP, the effect of activated Bax and ceramide together in inducing MOMP in isolated rat liver and yeast (lack mammalian apoptotic machinery) mitochondria was studied. The interaction between activated Bax and ceramide was also studied in the defined isolated system of planar phospholipid membranes. At concentrations where ceramide and activated Bax have little effects on their own, the combination induces substantial MOMP. Direct interaction between ceramide and activated Bax was demonstrated both by using yeast mitochondria and phospholipid membranes. The apparent affinity of activated Bax for ceramide increases with ceramide content indicating that activated Bax shows enhanced propensity to permeabilize in the presence of ceramide. An agent that inhibits ceramide-induced but not activated Bax induced permeabilization blocked the enhanced MOMP, suggesting that ceramide is the key permeabilizing entity, at least when ceramide is present. These and previous findings that anti-apoptotic proteins disassemble ceramide channels suggest that ceramide

channels, regulated by Bcl-2-family proteins, may be responsible for the MOMP during apoptosis.

INTRODUCTION

Apoptosis, a type of programmed cell death, is a regulated process where unwanted or damaged cells are eliminated. The permeabilization of the mitochondrial outer membrane (MOM) to key intermembrane space (IMS) proteins such as cytochrome *c*, Smac/Diablo, and apoptosis-inducing factor, is an irreversible and decision-making step in apoptosis, which leads to the execution phase involving effector caspase activation. Ceramide, a pro-apoptotic sphingolipid, has been reported (22) to act as a second messenger in several cellular processes, including apoptosis. It can also form channels and thus can directly permeabilize the MOM without the aid of ancillary proteins (24, 30 - 33). Physiological studies show that ceramide is both an extracellular stimulus and intracellular mediator (22) of mitochondrial apoptosis. Several lines of evidence indicate that cellular levels of ceramide become elevated (22, 24) most importantly in mitochondria (24). We have shown that Bcl-xL and Bcl-2 can inhibit permeabilization induced by ceramide in isolated rat liver mitochondria (33). This is achieved by the anti-apoptotic proteins inhibiting ceramide channel formation and disassembling pre-formed ceramide channels.

The mechanism by which Bax increases MOMP is cause for much debate (51. 63 – 67). Bax is located in the cytosol or loosely associated with the MOM in the monomeric form. Upon an apoptotic signal, Bax inserts into the MOM and becomes activated and oligomerized. Activated Bax and/or Bak are proposed to be directly

responsible for the release of intermembrane space proteins by forming channels in cells and indeed, in phospholipid membranes, Bax treated with β-octyl glucoside (activated Bax) is capable of forming channels (61). Yet whether these channels are large enough to allow for the release of all the IMS proteins is unclear (68). In yeast cells that lack the mammalian apoptotic machinery, expression of Bax still leads to leads to cytochrome *c* release and cell death indicating that Bax channels may suffice despite the presence of ceramide. However the effect of Bax is inhibited by co-expression of sphingomyelin synthase, which consumes ceramide (69). In mammalian cells, ceramide-induced cytochrome *c* release does not require Bax (24, 70) but Bax enhances apoptosis induced by ceramide (24, 71). Also, ceramide has been found to activate monomeric Bax in the presence of the MOM (25, 28). When combined, these publications can be interpreted to indicate that Bax and ceramide may interact cooperatively to generate the MOMP. This is clearly not the view of most investigators in the field but it is a logical conclusion from published experiments. The present work provides direct evidence of a synergistic interaction between activated Bax and ceramide resulting in enhanced MOMP to proteins. We also provide mechanistic insights into this interaction.

MATERIALS AND METHODS

Reagents

C_{16}-ceramide were bought from Avanti Polar Lipids. Antimycin A, 2, 4-dinitrophenol [DNP], horse heart cytochrome *c*, fatty acid-depleted Bovine Serum Albumin (BSA), and sodium ascorbate were bought from Sigma Chemical Co. Other chemicals were reagent grade.

Isolation of yeast mitochondria

Yeast mitochondria were prepared and isolated as previous described (72) until the washed spheroplast pellet was obtained. Twice, the pellet was resuspended in H-medium (0.6 M mannitol, 0.1 mM EGTA, 10 mM HEPES, pH 7.2) and spun at 700 RCF for 5 min to yield the mitochondrion-containing supernatants. The supernatants were spun at 5600 RCF for 10 min and the pellets were retained. The pellets were resuspended in H-Medium, combined and spun at 700 RCF for 5 min. The supernatant was spun at 5600 RCF for 10 minutes yielding the final mitochondrial pellet which was resuspended in H-medium. The intactness of the mitochondria, as measured by comparing their rate of cytochrome *c* oxidation with that of osmotically shocked mitochondria (18) was more than 93% for yeast mitochondria.

Bax activation

Bax was purified as described in the common materials and methods section. The native Bax was oligomerized by adding 10% β-octyl glucoside to a final concentration of 0.7% and incubated for 30 min on ice. The proper folding of the detergent treated Bax was confirmed by its partial resistance to trypsin as published elsewhere (73). Note that the concentrations of activated Bax reported here were based on the molecular weight of monomeric Bax because the activated form is heterogeneous.

Cytochrome *c* accessibility assay

Shortly before use, mitochondria were diluted in the isolation buffer to 0.5 mg protein/mL and stored on ice. Once diluted, mitochondria lose function more rapidly and so the diluted suspension is used within an hour. In a typical experiment, 50µL of this

dilution was dispersed in 650µL of room temperature incubation buffer [the sucrose-free buffer supplemented with 5mM DNP and 5µM antimycin A and pH 7.25 (31) to final protein content of 25 µg in 700µL. Unless otherwise stated, this was done for all experiments. In most experiments, when Bax was added, it was added immediately. Then the mitochondria were incubated for 10 min at room temperature to allow them to acclimate and interact with Bax. Ceramide was generally added at this point from a 1 mg/mL solution in isopropanol. In experiments where tBid and monomeric Bax were used, the mitochondria were incubated with the permeabilizing agents for 30 minutes at 30^{o}C. In experiments where activated Bax was used, the mitochondria were incubated with activated Bax for 20 minutes at room temperature. It was added while simultaneously vortexing the microfuge tube vigorously so as to achieve rapid and effective dispersal of the sphingolipid (controls show that this does not damage the outer membrane). After dispersal, the mixture was incubated for 10 min followed by measurement of the outer membrane permeability. Reduced cytochrome *c* was added to the mitochondrial suspension (10µL; final concentration approx 25µM) and the absorbance at 550nm was measured immediately for 2 min. The initial rate was used to assess the permeability of the MOM to cytochrome c. The extinction coefficient of 18.5 $mM^{-1} \cdot cm^{-1}$ [$\Delta \in_{Red.-Ox.}$] was used to convert absorbance units to µM units.

Assessment of apparent dissociation constant of ceramide channels for activated Bax

The oxidation rate was used as the functional parameter to evaluate the apparent dissociation constant of ceramide channels for activated Bax. The data was plotted using the Hill formalism for cooperative binding.

$$\log \frac{rate_{Bax}}{rate_{\max}} = \log(K) + n \log[Bax]$$

where the rates are the initial activated Bax-stimulated rates of oxidation at a specific ceramide concentration, above the rate observed with ceramide alone. $rate_{Bax}$ is the rate at any [activated Bax] and $rate_{max}$ is the maximal rate. K and n are the parameters of the Hill formalism. The inherent variability in the experiments forced us to combine these parameters into one. Since K and n increased simultaneously with amount of ceramide used, we found it more informative to combine these two parameters into one term:

$K_{0.5} = [1/K]^{1/n}$

$K_{0.5}$ is the Bax concentration at which the extent of permeabilization (as measured by the rate of cytochrome *c* oxidation] is half-maximal. It is a measure of the apparent dissociation constant, the reciprocal of the apparent affinity.

Electrophysiological experiments

The monolayer method was used as described previously (74) to make planar phospholipid membranes. Calomel electrodes were used to interface with the aqueous solutions (1.0 M KCl, 1mM $MgCl_2$, 5mM PIPES pH 6.95) on either side of the membrane. The voltage was clamped and the current recorded. The lipid solution contains 0.5% (w/v) 1,2-diphytanoyl-*sn*-glycero-3-phosphocholine, 0.5% (w/v) asolectin, and 0.05% (w/v) cholesterol dissolved in hexane. To form a ceramide channel, a stock solution of 0.05 mg/ml C_{16}- ceramide was made in isopropanol and 10-20μL amounts were added to the cis side of the membrane while stirring for 15 seconds to induce an initial conductance. The channel was then allowed to enlarge and stabilize before the

addition of proteins or other compounds. To obtain an activated Bax conductance, activated Bax was added to the cis side of the membrane only.

Adenylate Kinase (AK) assay

As described earlier (31), mitochondria were resuspended in the incubation buffer (50mM potassium lactobionate, 180mM mannitol, 0.1mM EGTA and 2mM HEPES and pH 7.4) to a final mitochondrial protein concentration of 160µg/mL. After adding ceramide and Bax, as done for cytochrome c oxidation assay, mitochondria were incubated at 30^{o}C for 30 min. The mitochondria were sedimented at 14,000 RCF for 5 min at 4^{o}C and 300µL of the supernatant was combined with 700µL adenylate kinase reaction buffer (50mM Tris, 5mM $MgSO_4$, 10mM glucose, 5mM ADP, 0.2mM NADP pH 7.5) that had been preincubated for 2 min with 5µL of enzyme mixture (2.5 units of hexokinase and 8.7 units of glucose-6-phosphate dehydrogenase). The absorbance of the mixture at 340nm was recorded immediately and the initial rate used as a measure of the adenylate kinase activity. Maximal release of adenylate kinase was achieved by exposing the mitochondria to an osmotic shock. An aliquot of the mitochondrial suspension (usually 10-20 µL containing 160 µg mitochondrial protein) was added to in 1mL distilled H_2O (50 to 100 fold shock) and incubated on ice for 10 min.

RESULTS

Activated Bax enhances ceramide-induced MOMP

To evaluate the influence of Bax on ceramide permeabilization of the MOM, we used a dynamic cytochrome *c* accessibility assay, as previously described (31). This is a dynamic measurement of permeability and permeability changes in the MOM to

cytochrome *c* in real-time. While treatment of isolated mitochondria with low levels of ceramide or tBid-monomeric Bax induced a small amount of membrane permeabilization, when the same amounts were added together, there was a synergistic increase in MOMP (Fig. 3.1A). This synergistic induction of permeabilization was also observed using the adenylate kinase release assay that evaluates release of proteins from the intermembrane space. (Fig 3.1B). tBid alone did not have any effect on ceramide-induced MOMP at these levels. Bax activated chemically with detergent has been found to permeabilize the MOM in similar manner to physiologically activated Bax (61, 75) and shows similar restricted accessibility to trypsin (73). A similar synergistic enhancement of permeabilization was also observed with ceramide and chemically activated Bax (Fig 3.1C). Under these conditions, there was no swelling of the mitochondria and thus the permeabilization was not secondary to inner-membrane swelling.

One possible interpretation for the synergistic interaction between ceramide and activated Bax is that activated Bax could be binding to anti-apoptotic proteins thus removing any inhibitory effect on ceramide induced MOMP. To test if the anti-apoptotic Bcl-2 proteins are involved in this interaction, ceramide induced MOMP enhancement by activated Bax was tested using yeast mitochondria, which are devoid of Bcl-2 family proteins. We found that activated Bax and ceramide interact synergistically to induce MOMP in yeast mitochondria also, suggesting that their interaction could be direct and not indirectly mediated by elimination of inhibition by anti-apoptotic members (Fig. 3.1D). This also suggests that the interaction between activated Bax and ceramide does not require processed Bid or Bak.

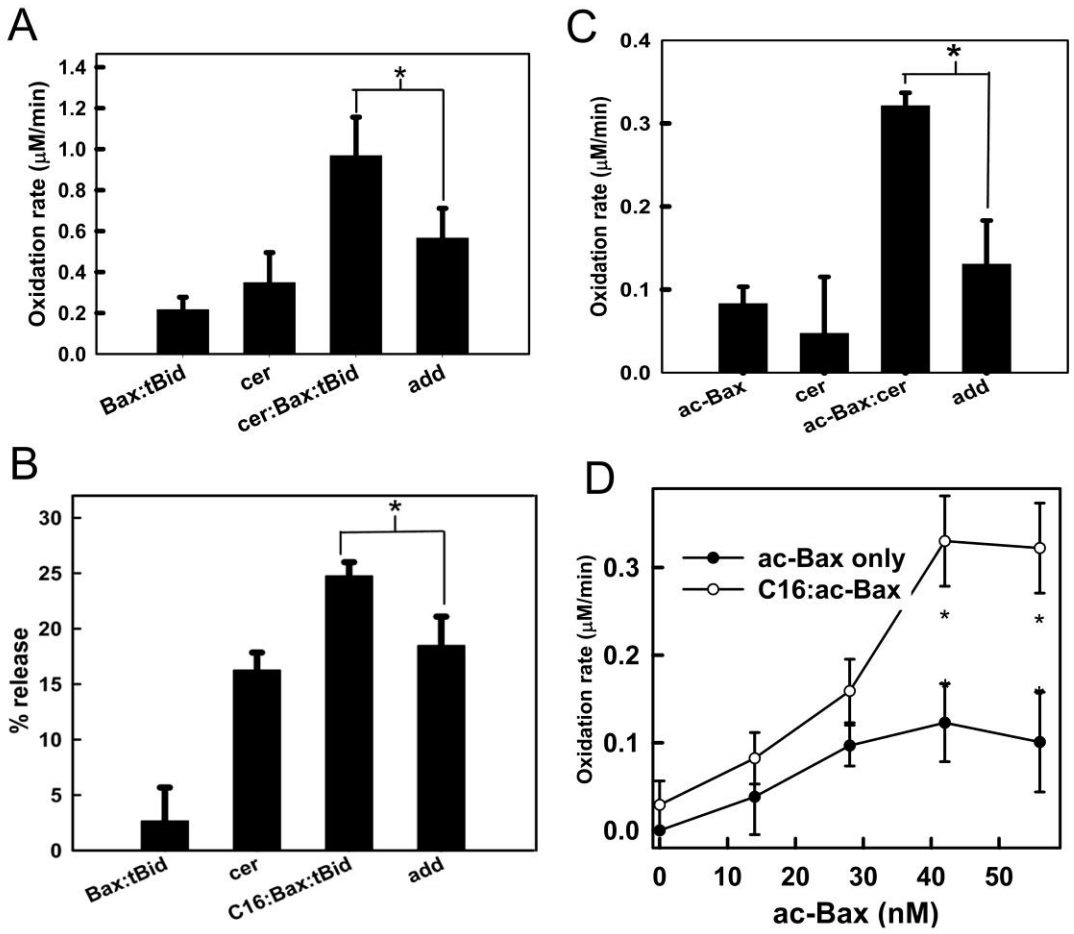

Fig 3.1 Ceramide (cer) and activated Bax increase the MOMP in a cooperative fashion assessed by the cytochrome *c* accessibility assay (A, C, D) or adenylate kinase release (B). A. Isolated rat liver mitochondria diluted to 250 µg protein/ml were pre-treated with both 45 nM N/C Bid and 40 nM monomeric Bax. Sub-aliquots containing 25 µg of mitochondria were either treated with 5 µl isopropanol (as a vehicle control) or 5 µl of 1 mg/ml ceramide (in isopropanol) and incubated at room temperature for 10 min before assaying for cytochrome *c* accessibility. Respective vehicle controls were subtracted from the data shown. The "add" bar is the sum of the rates measured with ceramide alone and Bid/Bax alone. The results are the means ± SD of three experiments. The respiration rate of the combined treatment differed from the sum of the individual rates with P < .01. B. Rat liver mitochondria were treated either with 10 µg ceramide or a combination of 40 nM monomeric Bax and 245 nM N/C Bid or both and the released adenylate kinase activity was measured. The "add" bar is the sum of the results of individual treatments minus their product divided by the maximal

possible release (to correct for both agents acting on the same mitochondrion). The combined treatment exceeded the sum of individual treatments, "add", with P < .05. C. Isolated rat liver mitochondria were treated with either 1 µg ceramide, 15 nM detergent activated Bax (ac-Bax), or both. The results are mean ± SE of three experiments. The combined treatment exceeded the sum of individual treatments, "add", with P < .05. D. Mitochondria isolated from wild-type S. *cerevisiae* were used and treated with 2 µg of ceramide and activated Bax as shown. The results are means ± SE of three to five experiments. Statistical tests yielding P < .05 compared the results of the combined treatment of ceramide and ac-Bax with the numerical addition of the results of treatments with ceramide alone and ac-Bax alone

Bax mediated enhancement of ceramide induced permeabilization can be inhibited by trehalose, a disaccharide that disassembles ceramide channels

Since both Bax and ceramide are channel formers and each of them is capable of permeabilizing the MOM in the absence of the other, we wanted to test whether, in this synergistic interaction, Bax is enhancing ceramide channels or vice versa. Some insight was gained by using trehalose, a disaccharide that inhibits ceramide channels causing partial disassembly. The same dose of trehalose inhibited both the ceramide induced MOM permeabilization and the enhancement of this permeabilization induced by activated Bax (Fig. 3.2). In this experiment, activated Bax alone had essentially no effect. Using a higher concentration of activated Bax (inset) a significant MOMP was achieved and trehalose had no effect on this MOMP induced by activated Bax alone. The simplest interpretation is that the enhanced MOMP has the properties of ceramide channels. Activated Bax could be acting by enhancing the permeabilization induced by ceramide, perhaps by favoring the growth of ceramide channels. This observation can also be explained by a complex structural assembly of ceramide and activated Bax that is sensitive to trehalose. However, this observation is inconsistent with the possibility that ceramide is simply enhancing Bax activation. In addition, if the enhanced MOMP were

the result of ceramide monomers enhancing channels formed by activated Bax then it is hard to see how trehalose could interfere with this process because trehalose cannot remove ceramide from the membrane. The amount of trehalose needed to inhibit ceramide induced permeabilization seems to be 10^5 to 10^6 orders of magnitude more than ceramide stoichiometrically. This could be because the affinity of trehalose for ceramide channel might be much lower than with water or between trehalose molecules. And unlike ceramide molecules in channel which have much lower entropy in the membrane, soluble trehalose has much higher entropy.

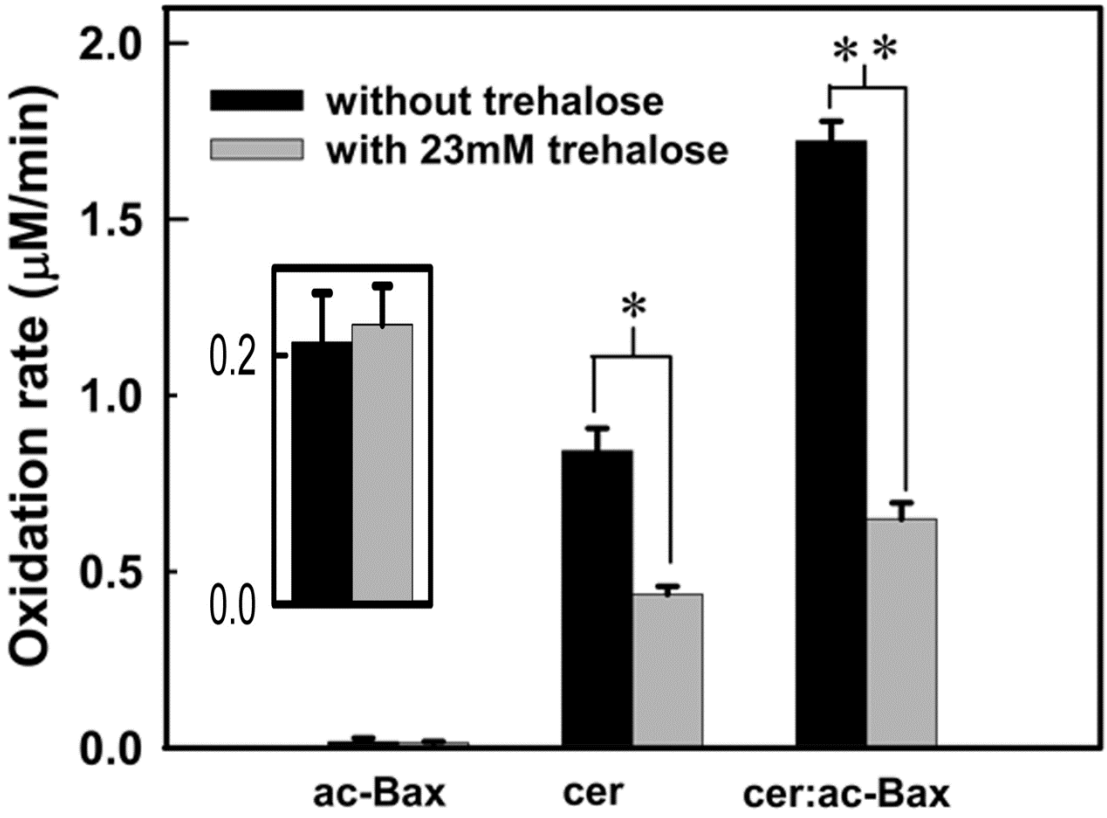

Fig 3.2 Trehalose (23 mM final) inhibits MOMP induced by ceramide alone and that induced by the combination of ac-Bax and ceramide. In the main figure, samples were treated with 30 μg of

ceramide and 10 nM ac-Bax as indicated. In the *inset* 43 nM ac-Bax was used to obtain a high enough MOMP. The cytochrome *c* oxidation rates are means ± SE of three to four experiments.
**** Represents *P* < .01 and *** represents *P* < .001**

Bax expands ceramide induced conductance in planar phospholipid membranes

Planar phospholipid membranes are membranes consisting only of phospholipids and cholesterol. Being a defined system, one can clearly demonstrate interactions without the influence of other constituents found in natural membranes. The ability of ceramide to form channels in planar membranes has been established (30). To assess the effect of activated Bax on ceramide channels in an environment free of other membrane components, ceramide channels were formed in the planar membranes and then activated Bax was added. Activated Bax caused a large increase in conductance while monomeric Bax (m-Bax) did not significantly affect the channel (Fig. 3.3A). This is typical of many experiments. These show that the interaction between activated Bax and ceramide is a direct one and does not require other proteins.

Trehalose also inhibited the conductance of a ceramide channel formed in a phospholipid membrane (data not shown). In Fig. 3.3B, a small ceramide conductance was greatly increased by the addition of activated Bax. At the reduced scale used to show the experiment, the initial ceramide conductance is barely visible. Once the conductance stabilized, trehalose was added resulting in an immediate decline in conductance. Thus the activated Bax-enhanced conductance was reduced by trehalose (Fig. 3.3B). Trehalose has no effect on the conductance produced by activated Bax alone (Fig. 3.3C). Thus, trehalose is useful to effectively distinguish between a permeability formed by activated Bax and one formed by ceramide. When the conductance was inhibited using lanthanum ions, there was stochastic delay in channel disassembly,

suggesting that a singular structure is responsible for the conductance observed. Ceramide and activated Bax may be forming a unified structure or activated Bax might enhance the size of the ceramide channel (3.3D) These experiments also suggest that metabolism of ceramide to other sphingolipids like sphingosine is not necessary for interaction with activated Bax and the consequent changes in permeability.

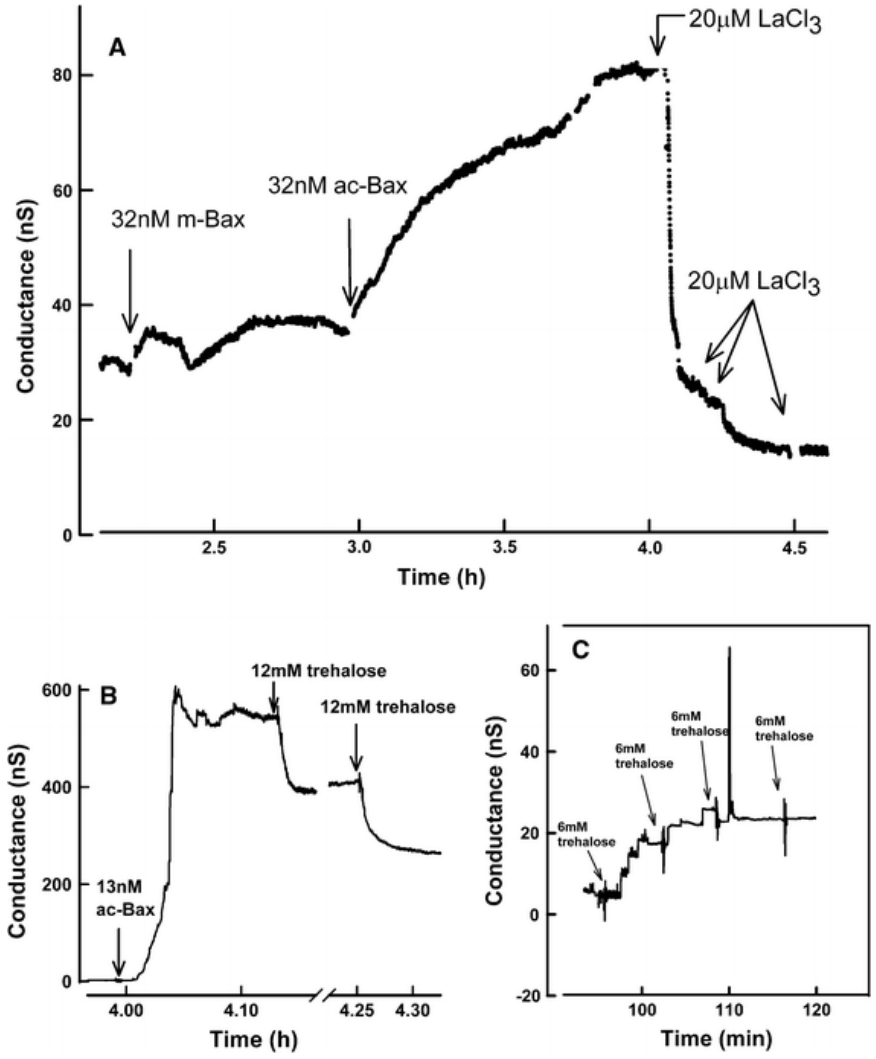

Fig 3.3: Addition of activated Bax to a ceramide channel in a planar phospholipid membrane causes it to enlarge. A. The initial conductance was formed by the addition of 16 µg ceramide to a high-resistance phospholipid membrane. Once the conductance had stabilized first monomeric Bax then activated Bax were added to both sides of the membrane. Once the conductance rise had restabilized at a higher level $LaCl_3$ was added to the final concentrations indicated in the figure. The

$LaCl_3$ additions were added to one side in the sequence: *cis, cis, trans, trans*. The experiment shown is representative of more than eight experiments. Amounts of added ceramide and ac-Bax were different between experiments. Bax enhancement of a ceramide channel was seen in over 50 experiments. B. A small ceramide channel was formed followed by the addition of ac-Bax at the indicated final concentration. Trehalose was added as indicated. C. Activated Bax conductances were induced in a planar phospholipid membrane in the experiment illustrated in the figure. The total amount of activated Bax added was equivalent to 42 nM. Trehalose was added as indicated stepping up the final concentration by 6 mM at each addition. This is typical of more than three experiments.

The influence of activated Bax on MOMP depends on the amount of added ceramide

At a low level of added ceramide 1.4 µg/mL, the amount of activated Bax needed to enhance the MOMP to half maximal was 30 nM. At a higher dose of 2.8 µg ceramide, less activated Bax was needed to achieve a half-maximal effect (12nM) (Fig. 3.4A). Both of these results were obtained on the same mitochondrial preparation, eliminating variability between mitochondrial isolations. This difference can be interpreted as a change in apparent affinity between activated Bax and a ceramide channel as the size of the ceramide channel increases. In a separate set of experiments (Fig. 3.4B) low levels of ceramide still show a dose-dependence but at high levels (10 µg), the enhancement by activated Bax was not observed (Fig. 3.4B). The lack of further stimulation was not due to the achievement of maximal cytochrome *c* accessibility to cytochrome oxidase because higher levels of ceramide did produce still higher rates of cytochrome *c* oxidation, closer to those observed with hypotonically-shocked mitochondria. This indicates that the effect of activated Bax on ceramide induced-MOMP is a saturable function of the amount of ceramide. This saturation could be interpreted as activated Bax favoring an optimal size of the ceramide channel and if the channel is already at the optimal size there is no

further change in MOMP. A Hill plot revealed changes in both the measure of cooperativity, n, and the constant, K. The Hill parameters were combined [see methods] to evaluate the apparent dissociation constant, $K_{0.5}$ (the Bax concentration at which half-

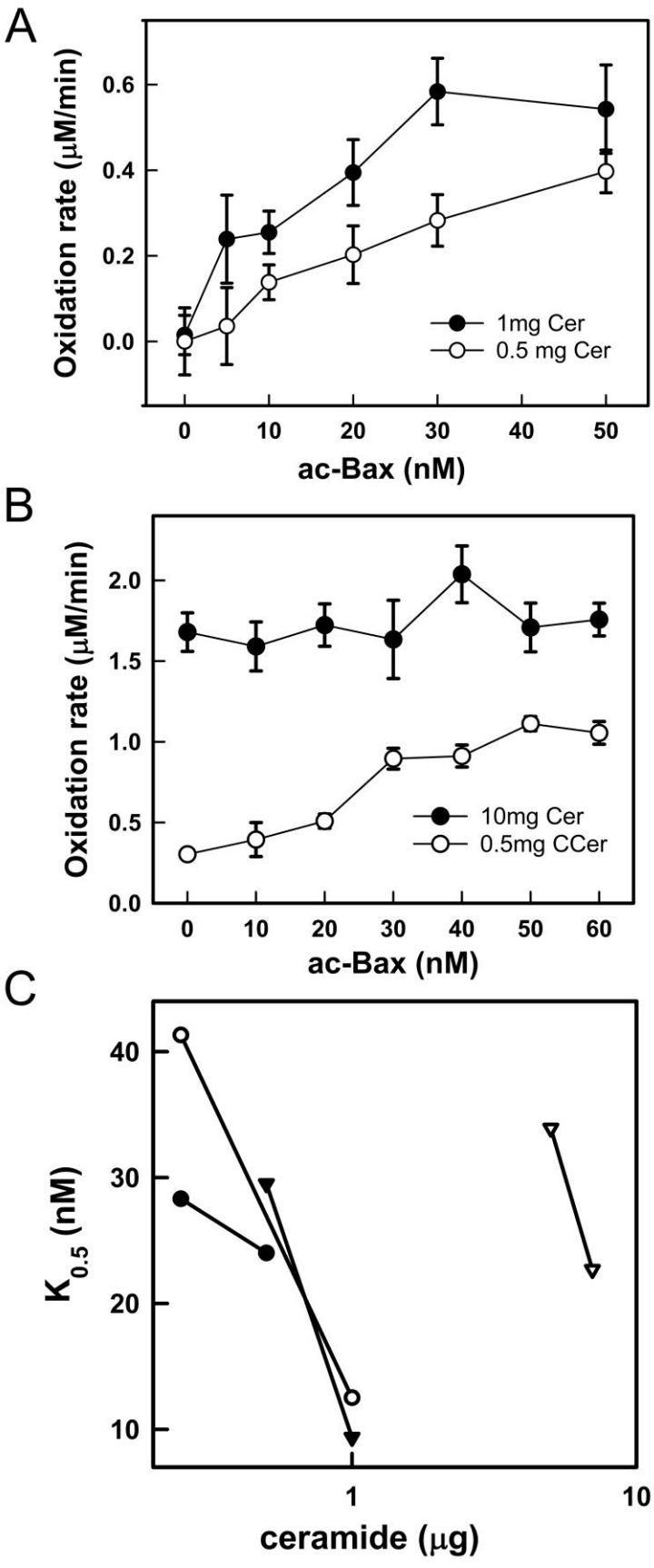

Fig 3.4: Dose–response curves of the enhancement of ceramide mediated MOMP by the addition of activated Bax to rat liver mitochondria.

A and B: Experiments were performed by pre-incubating the mitochondria with the indicated amount of activated Bax for 10 min followed by addition of the indicated amount of ceramide.

A. 0.5 and 1 µg of ceramide were used. These results are mean ± SE of four experiments.

B. 0.5 and 10 µg of ceramide were used. These results are mean ± SE of three to four experiments. Experiments within one panel were performed on the same batch of mitochondria.

C. Summary of the results of four independent experiments. Each set of data points defining each line was determined from a set of experiments performed on the same mitochondrial isolation. The figure shows the increase in apparent affinity of activated Bax for ceramide channels with increase in ceramide content.

K 0.5 is defined in the "Materials and Methods" section of this chapter in the sub-section "Assessment of apparent dissociation constant of ceramide channels for activated Bax".

maximal enhanced permeabilization is achieved). The resulting apparent dissociation constant of activated Bax for ceramide channels in the MOM decreases as the ceramide concentration increases (Fig. 3.4C). This is highly reproducible, despite the variation in intrinsic sensitivity of isolated mitochondria to added ceramide. Each line represents the results of sets of experiments performed on one isolated batch of mitochondria. These results indicate a relationship between the structure of activated Bax and the structure formed in the presence of ceramide. An increase in affinity indicates a better fit. The increase in MOMP may result from an increase in diameter of the Bax-ceramide assembly resulting is a better match to the structure of activated Bax. In this way activated Bax could result in the formation of a channel of a particular size.

DISCUSSION

The release of proteins from mitochondria is a critical, decision-making step in apoptosis and thus the identification of the structure responsible for this release has many important implications. A favorite candidate for the release pathway is activated Bax since Bax is pro-apoptotic, can form channels and its activation on the MOM leads to protein release. Interestingly, ceramide is also pro-apoptotic, can self-assemble to form channels (22, 24) and its delivery to the MOM leads to protein release (24, 25, 28, 46). Here we show that activated Bax and ceramide act synergistically to permeabilize the MOM.

The nature of the channels formed in the presence of both ceramide and activated Bax is not known and could be a structure fundamentally different from that formed by either substance alone. Some findings in this work, however, are easily interpreted in terms of activated Bax controlling the structure of ceramide channels. The apparent

affinity of activated Bax for ceramide-induced MOM permeability increases with the amount of ceramide added. In other words, as the amount of added ceramide was increased, lesser amounts of Bax were required to achieve half-maximal permeabilization. This could be due to more ceramide increasing the degree of Bax activation but at high levels of ceramide, where ceramide by itself produced a large permeability, there was no further stimulation by activated Bax (even though additional amounts of ceramide would have increased MOMP). This observation is not easily compatible with ceramide activating Bax or the two channels mutually enhancing each other. It is more naturally explained by activated Bax favoring the growth of a ceramide channel up to a size designated by the structure of activated Bax.

Activated Bax seems to enhance the size of ceramide channels up to some critical level, probably an optimum channel size. The increased radius of curvature may offer a better fit for activated Bax. Regardless of the site of interaction, if the interaction energy increases with channel size, then the binding of activated Bax to a smaller channel could generate stress on the channel that would be relieved by the channel growing in size. The dynamic equilibrium between ceramides in the channel and non-conducting ceramide in the membrane would be shifted toward ceramide insertion into the channel and thus growth of the channel size (Fig 3.5). Once the optimal size is achieved, activated Bax would have no further effect and this was observed. It is possible that the physical shape of the activated Bax in the membrane might act as a molecular mold to drive the ceramide channel to an optimum size.

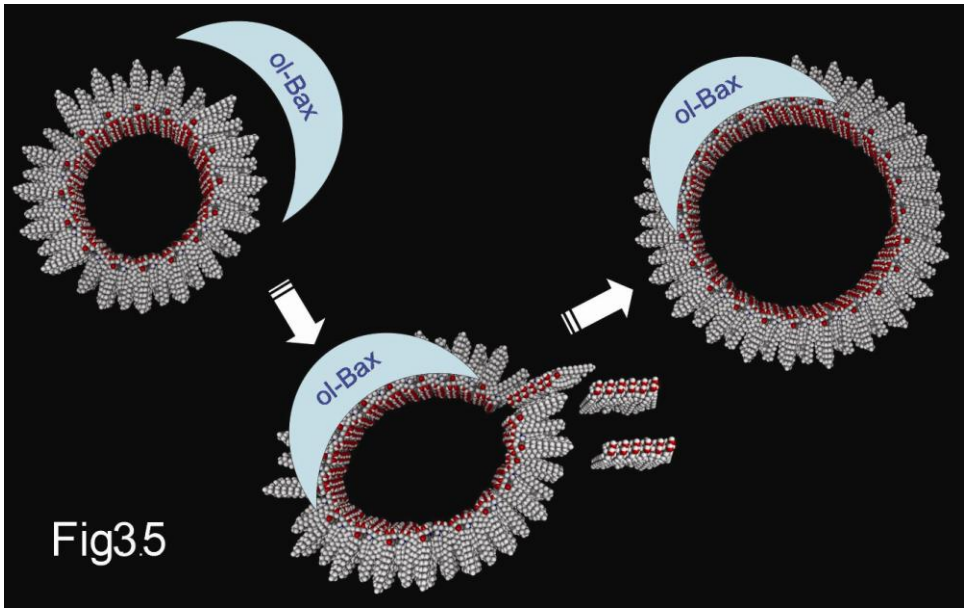

Fig 3.5: Illustration of how activated Bax might increase the size of the ceramide channel. On the *left,* a 32-column ceramide channel has a small radius of curvature than ac-Bax. When ac-Bax binds (*center*) it distorts the channel, disturbing the equilibrium between ceramide aggregates on the monolayer and ceramides forming the channel. The insertion of more ceramide columns increases the channel size until its curvature matches that of activated Bax (*right*), forming a 48-column channel.

The results obtained with phospholipid membranes argue that the interaction between activated Bax and ceramide must be direct. Furthermore, these demonstrate that activated Bax increases the size of the single existing ceramide channel because the disassembly of the resulting enhanced permeability shows stochastic properties consistent with a unified structure. If the added Bax were to form a separate structure then the disassembly would show two separate processes rather than just one. This is in harmony with the natural interpretation of the mitochondrial experiments that measured the apparent affinity of activated Bax as described above.

Experiments on isolated mitochondria raise the possibility of indirect effects. Ceramide could act on another mitochondrial component and thus indirectly influence the ability of activated Bax to permeabilize the outer membrane. Indeed, a product of ceramide metabolism could be the active species. Mitochondria have ceramidases that could convert ceramide to sphingosine (35, 39). Although the conversion rate was shown to be minimal under the conditions of our experiments (39), even a small conversion might be important. Sphingosine was shown to be capable of interacting with and influencing the formation of ceramide channels (39) and thus might influence the channel-forming ability of activated Bax. Although this possibility cannot be excluded, the experiments performed in planar membranes demonstrate a direct functional synergism between ceramide and activated Bax in terms of channel formation. The close parallelism between the results obtained with the two experimental approaches provides strong confidence that both are reporting the same synergistic permeabilization.

Our work shows that activated Bax could alternatively function by acting on ceramide channels to increase their size or form large hybrid channels with ceramide. Indeed, the channel formed in Fig. 3.3B has a calculated diameter of 50 nm, certainly large enough to allow the passage of all proteins known to be released from mitochondria early in apoptosis.

Upton et al. (57) show that Bax inserts into the MOM through a C-terminal targeting signal but that Bax can insert into the MOM even in the absence of this targeting signal once the mitochondria have been permeabilized, in a caspase independent manner. These authors and others (76) have concluded that activated Bax is a receptor for cytosolic Bax. However, it is also likely that cytosolic Bax binds to ceramide

channels downstream or concomitant with MOMP in a target-signal-independent fashion, especially because a constitutively membrane localized Bax mutant that cannot induce permeabilization does not recruit cytosolic Bax to membranes. Mutant Bcl-xL that cannot interact with either Bax or tBid still prevents membrane permeabilization (50), suggesting that additional levels of regulation exist beyond Bax through which Bcl-xL inhibits MOMP. One of these is direct inhibition of ceramide channels by Bcl-xL (33). Cell death induced in yeast by the over-expression of Bax, was inhibited when ceramide levels were reduced by co-expression with sphingomyelin synthase (69). While either Bax or Bak has been found to be mandatory in inducing apoptosis to various stimuli, ASMase knockout cells are resistant to UV induced apoptosis even in the presence of both Bax and Bak (77). The multiple routes and organelles of ceramide generation, stimulation of alternative routes of ceramide synthesis by different stimuli and Pleiotropic roles of ceramide in different membranes under different circumstances make appropriate knockouts for ceramide impossible.

It is not clear whether the release of IMS proteins is due to transient openings or sustained permeability. Many publications (51, 54) have reported a Bax-induced release of cytochrome *c* from isolated mitochondria over a period of hours without significant increases in the MOM permeability to cytochrome *c*. Transient channel openings are a likely explanation. Does this mean that the Bax/ceramide sustained permeabilization of the MOM and thus rapid release of protein is unnecessary or unphysiological? It seems unlikely that the Bax/ceramide synergism is an interaction that is not specific and not maintained by natural selection, especially since anti-apoptotic proteins act precisely in the opposite manner (33). Further, Kluck et. al (51), have shown that, in the presence of

a putative apoptotic component of the cytosol (which would be expected to be available to apoptotic mitochondria *in vivo)*, Bax induces sustained enhancement of permeability. Munoz-Piendo et al (78) report that a non-specific pore showing prolonged permeability is responsible for protein release during apoptosis. Thus the sustained permeability observed in the presence of activated Bax and ceramide is not an aberration.

It must be emphasized that the experiments were performed with physiologically relevant doses of ceramide and Bax. The ceramide used in this study is C_{16}-ceramide which is one of the common, naturally occurring, long-chain ceramides. The amounts of ceramide used seem high but, only about 5% of the ceramide added to isolated mitochondria inserts into mitochondrial membranes (79) requiring the addition of larger amounts of ceramide to the mitochondrial suspension to achieve MOMP. Nevertheless, as shown previously (24, 79), we are working at mole fractions of ceramide typically found in mitochondria early in apoptosis. The amount of activated Bax used in these experiments is also at physiological levels. Enhancement of ceramide induced MOMP was achieved with levels of activated Bax in the low nM range. At these levels, activated Bax often has little or no effect on MOMP, indicating that its action on ceramide channels may be more important.

Activation of Bax in cells is thought to be mediated by tBid in cells. Apart from tBid, non-ionic detergents, at their CMC, have also been found to activate Bax (18, 61). This detergent-activated Bax shows similar reactivity to conformation specific antibody (18) and restricted accessibility to trypsin digestion (73). Historically, it was believed that the detergent-activated Bax oligomerizes in solution, while recent work (75) shows that activated Bax is still a monomer in solution. We have used detergent activated Bax

for most of our experiments to circumvent complicating interactions arising from variations in effect of various concentrations of tBid on Bax, effect of high concentrations of tBid itself on ceramide. The results presented here and earlier work showing inhibition of ceramide induced MOMP by Bcl-xL evince structural regulation of MOMP by ceramide and Bcl-2 family proteins. The Bcl-2 family proteins have been shown to regulate the formation of ceramide also during apoptosis.

These and earlier studies with the anti-apoptotic Bcl-2 family proteins underscore that natural selection has favored mechanistic interactions between some Bcl-2 family proteins and ceramide resulting in functional outcomes. These functional interactions could be pivotal in regulating MOMP under circumstances where both ceramide and the Bcl-2 family proteins are present.

CONCLUSION

Experiments with isolated mitochondria and phospholipid membranes show that low levels activated Bax and ceramide interact to enhance the membrane permeability to a level greater that each agent alone. The results are best interpreted as activated Bax enhancing ceramide channels but other interpretations are not excluded. These results are in harmony with published results showing that anti-apoptotic proteins disassemble ceramide channels. These show that the Bcl-2 family of proteins that regulate protein release from mitochondria early in apoptosis also interact with ceramide and ceramide channels to influence MOMP. This result is consistent with an emerging picture that ceramide channels may be a pathway by which proteins are released from mitochondria, initiating the execution phase of apoptosis.

Note: This line of research was accomplished in collaboration with Meenu Perera who is an equal contributor. I was responsible for the purification of the mitochondria from rat liver. Meenu was responsible for the purification of the recombinant proteins. The experiments to test ceramide and Bax on the MOMP was done by me and Meenu. The experiments with planar membranes reported here were performed by David Colombini, Debra Datovskiy and Kirti Chada.

CHAPTER 4 CERAMIDE CHANNELS: INFLUENCE OF MOLECULAR STRUCTURE ON CHANNEL FORMATION IN MEMBRANES

ABSTRACT

The sphingolipid, ceramide, has been demonstrated to self-assemble in the mitochondrial outer membrane (MOM), forming large channels capable of translocating proteins. These channels are believed to be involved in protein release from mitochondria, a key decision-making step in apoptosis. Synthetic analogs of ceramide, bearing modifications in each of the major structural features of ceramide were used to probe the molecular basis for the stability of ceramide channels. Channel stability and mitochondrial permeabilization were disrupted by methylation of the C1-hydroxyl group whereas modifications of the C3 allylic hydroxyl group were well tolerated. A change in chirality at C2 that would influence the orientation of the C1-hydroxyl group resulted in a strong reduction of channel-forming ability. Similarly, methylation of the amide nitrogen is also detrimental to channel formation. Many changes in the degree, location and nature of the unsaturation of ceramide had little effect on mitochondrial permeabilization. Competition experiments between ceramide and analogs resulted in synergy with structures compatible with the ceramide channel model and antagonism with incompatible structures. The results are consistent with ceramide channels being highly organized structures, stabilized by specific inter-molecular interactions, similar to the interactions responsible for protein folding.

INTRODUCTION

The sphingolipid, ceramide, has been shown to be able to form channels in planar membranes (30, 32), liposomes (38) and the mitochondrial outer membrane (31, 33). In mammalian mitochondria, channel formation occurs at physiologically relevant ceramide levels; levels measured in mitochondria from cells early in the apoptotic process (24, 79 - 81). In addition, the propensity to form channels and their size is influenced by Bcl-2 family proteins (33, 82). These channels are large, stable and capable of allowing proteins to cross membranes. The size was determined from the molecular weight of proteins released from mitochondria (31), from the conductance of single channels formed in planar membranes (32), and from visualization of the pores by electron microscopy (83). A range of sizes was reported with a typical channel having an estimated pore diameter of 10 nm (32, 83). Thus hundreds of ceramide molecules must spontaneously self-assemble in the 2-dimensional liquid phase of the membrane. Unlike the fluid and transient toroidal pores or lipidic pores formed when lamellar lipids are disturbed by amphipathic molecules such as peptides or synthetic structures (84 – 86) whole proteins (87, 88), or at the phase transition (89), the channels formed by ceramide seem to be highly structured and rigid. The disassembly of channels formed by short-chain ceramide shows a quantization of conductance with a strong preference for large conductance drops to be multiples of 4 nS (30). This finding not only supports the notion that ceramide channels are highly-organized cylindrical structures, but is also consistent with a modification of the originally-proposed barrel-stave structure (30). Each stave of the barrel is proposed to consist of a stack of ceramide molecules held together

by intermolecular hydrogen-bonding through the amide and carbonyl groups of the amide linkage. These span the membrane forming a cylinder when arranged in an anti-parallel fashion (Fig. 4.1) (32). Molecular dynamic simulations indicate that this structure is stable (90).

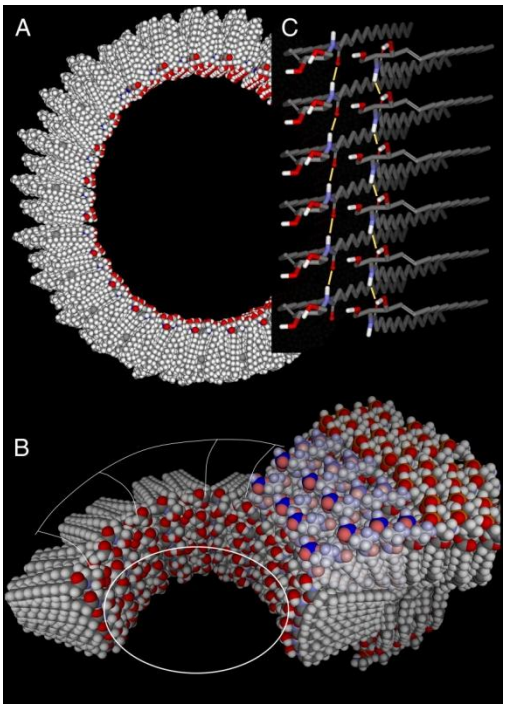

Fig 4.1: Model of the structure of the C16-ceramide channel. A. Model of a 48-column channel forming a 10 nm diameter pore. The columns are anti-parallel and so every other column has a red dot, the oxygen of the carbonyl group at the end of the column. The hydroxyl groups are facing the channel lumen and are proposed to hydrogen bond with water within the lumen (not shown). The phospholipid bilayer, not shown, would be in the plane of the image. B. A portion of a small ceramide channel showing how the channel might interface with the phospholipid bilayer. Note how the channel is proposed to take on a slightly hourglass shape and the interfacing phospholipids are proposed to tilt (alternate colored molecules) in order to the cover the apolar portion of the end of the ceramide channel. C. An expanded view of two ceramide columns in antiparallel orientation. Each column consists of a stack of 6 ceramide molecules. The figure shows the hydroxyl groups that would face the channel lumen and the hydrocarbon chains extending into the background, toward the lipid bilayer. The yellow bars indicate the hydrogen-bonding between the amide group of one ceramide and the carbonyl group of the adjacent ceramide.

The working structure of the ceramide channel is fundamentally a barrel-stave structure similar to the structure, both proposed and solved, for many channels. The main difference is that for all other channels described to date, there is a strong preference for a fixed number of monomers forming a channel. Forming channels with one stave more or less is highly unfavored. If the ceramide channel has such a preference, it is not a strong preference. Perhaps this unexpected feature is due to the large size of pore needed to allow the translocation of proteins resulting in a large radius of curvature. Thus relatively small changes in this radius of curvature, as more staves are added to the barrel, may be accommodated by relatively small changes in the conformation of the polar headgroup. Alternatively, the structure of the polar region may allow enough flexibility to adapt to changes in the radius of curvature. The difficulty observed in initially forming a ceramide channel and the rapid growth following initial formation (83) may indicate that a small radius of curvature is energetically unfavorable.

The ability of ceramide to form channels must, at least in part, be attributed to the structural features of the ceramide molecule. The polar head group of ceramide (Fig. 4.2), with its amide linkage and two hydroxyl groups located in close proximity, constitutes a tridentate hydrogen-bonding donor/acceptor center and is capable of generating an effective network of directed hydrogen bonding interactions. These structural features may partly explain its ability to form large, stable channels in membranes. However, it is not known if the location and orientation of the interacting groups are critical to achieve a stable structure. In addition, other structural features (such as the length of the hydrocarbon chains and the number and configuration of the double bonds) may be important.

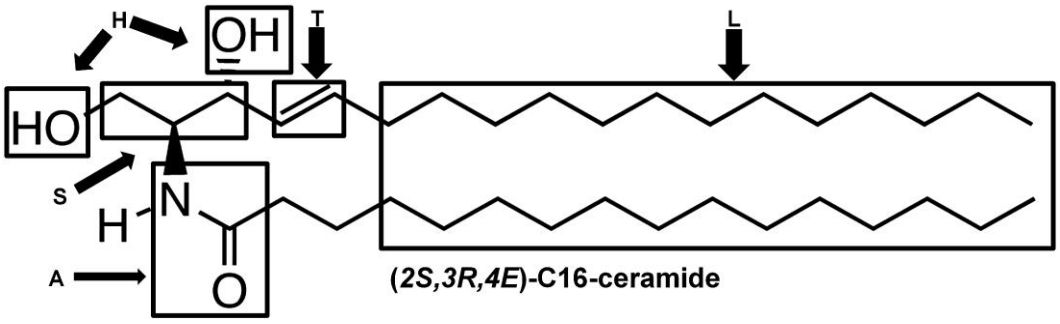

Fig 4.2: Structure of N-palmitoyl-D-erythro-sphingosine (D-e-C16-ceramide or C16-Cer) showing the major features of the molecule and the codes used for the synthetic analogs: H for changes to the hydroxyl groups, S for changes in stereochemistry, A for changes to the amide group, T for changes to the trans double bond and L for changes to the chain length.

Therefore, we have undertaken a study of synthetic ceramide analogs (Table 4.1 and Fig. 4.3) to determine (a) if naturally occurring ceramides are uniquely suited to form large aqueous pores and (b) the structural and stereochemical features in ceramide that are necessary for the formation of large channels.

Code	Structural Change	Type/Location of Change
S1	enantiomer: 2*S*,3*R* to 2*R*,3*S*	Stereochemical
S2	diastereomer: 3*R* to 3*S*	
A1	C_{16}-ceramine (conversion of amide chain to amine-linked chain)	amide linkage
A2	C_8-ceramine	
A3	*N*-methylation of amide chain	
A4	urea-ceramide	
A5	α-methoxy group in amide chain of C_8-ceramide	
H1	*O*-methylation of C1-hydroxyl group	hydroxyl group
H2	*O*-methylation of C3-hydroxyl group	
H3	oxidation of C3-OH to keto group; no double bond	
T1	translocation of double bond on sphingoid base	
T2	phytoceramide: double bond replaced by OH at C4	
T3	double bond converted to triple bond	
T4	allene: adjacent double bonds	
T5	4,6-diene: conjugated *trans* double bonds in C_8-ceramide	
T6	*trans* double bond converted to *cis* in C_8-ceramide	
T7	translocation of double bond and C3-OH in C_8-ceramide	
L1	C_{10}-ceramide	hydrocarbon chains
L2	truncation of sphingoid base	
L3	C_8-ceramide	
L4	NBD-ceramide	
L5	*N*-palmitoyl-serinol	
L6	*N*-oleoyl-ceramide ($C_{18:1}$)	

Table 4.1 Ceramide analogs.

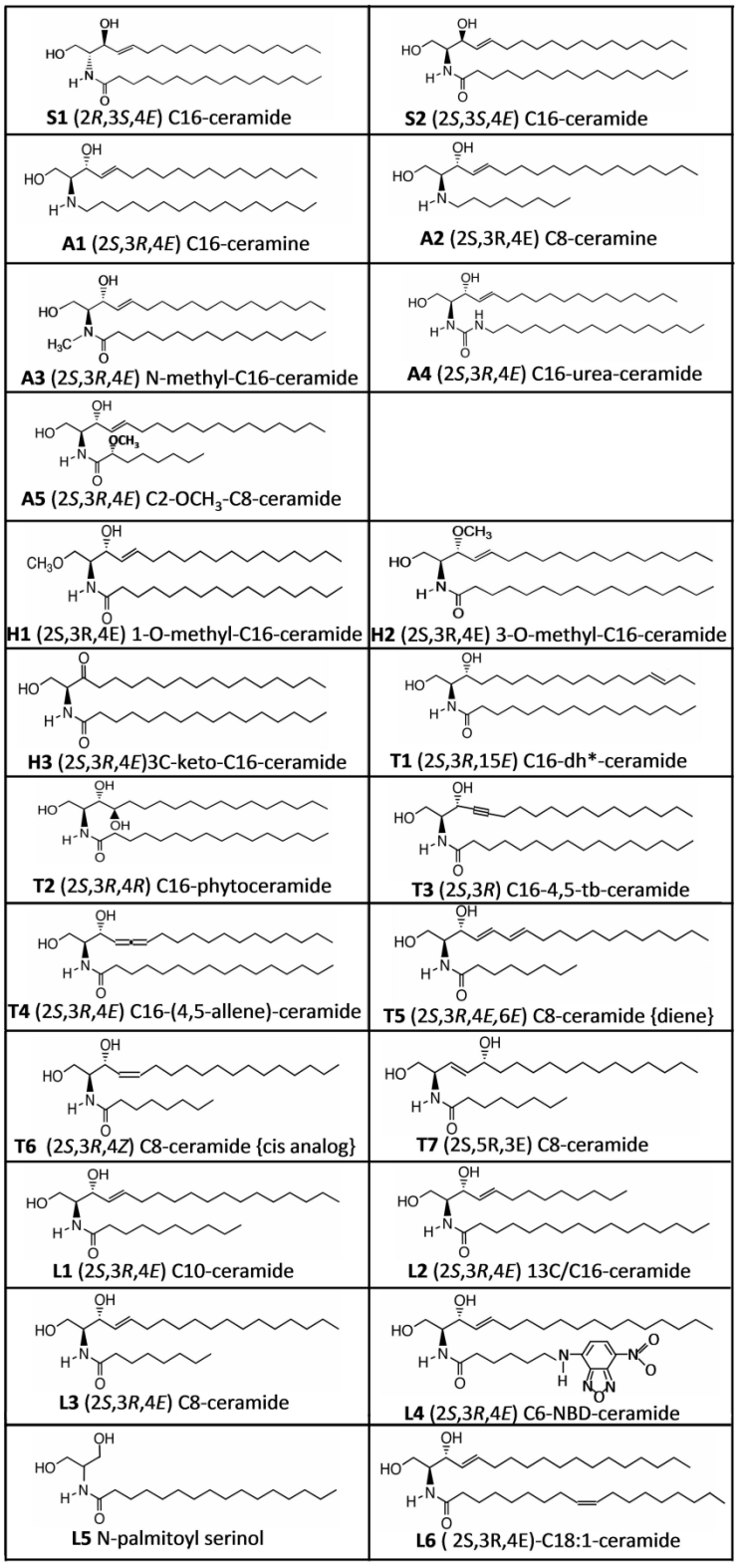

Fig 4.3: Chemical structures of the analogs used

MATERIALS AND METHODS

Reagents

N-Palmitoyl-D-*erythro*-sphingosine (D-e-C_{16}-ceramide or C_{16}-Cer) and *N*-oleoyl-D-*erythro*-sphingosine (D-e-$C_{18:1}$-ceramide or $C_{18:1}$-Cer) were obtained from Avanti Polar Lipids (Alabaster, AL). The analogs of C_{16}-Cer and D-e-C_8-ceramide (C_8-Cer), **T1** and **T4** (Fig. 4.3) were synthesized as described previously (91 – 98). Antimycin A, 2,4-dinitrophenol (DNP), horse heart cytochrome *c*, and fatty acid depleted bovine serum albumin (BSA) were purchased from Sigma (St. Louis, MO). DPX (p-xylene-bis-pyridinium bromide) was purchased from Molecular Probes (Invitrogen). 5(6)-carboxyfluorescein was purchased from Acros Organics.

Cytochrome *c* oxidation assay as a measure of mitochondrial outer membrane permeability

The rate of oxidation of exogenously-added reduced cytochrome *c* by cytochrome oxidase in isolated mitochondria is a measure of the permeability of the outer membrane to cytochrome *c* because translocation of cytochrome *c* through the outer membrane is a rate limiting step. The procedure previously described (31) was modified to improve reproducibility. As the mitochondria were found to be more stable at higher concentrations, mitochondria were diluted in H buffer at 4 ^{o}C to a concentration of 0.2 mg/mL, in small batches just before the assay. Then, 50 µL aliquots were dispersed in 650 µL of room temperature H buffer supplemented with 5 mM DNP and 5 µM antimycin A. The final protein concentration was 14.3 µg/mL. The mitochondria were allowed to acclimate at room temperature (10 min) in a microfuge tube. Then ceramide

or one of the analogs (dissolved in 2-propanol at 1 mg/mL) was delivered to the mitochondria while the suspension was vortexed for 30 s to achieve effective dispersal of the sphingolipid. After dispersal, the mixture was incubated for 10 min at room temperature followed by addition of cytochrome *c* (20 µL; final concentration, approx. 25 µM) and immediate measurement of the absorbance at 550 nm for a period of 2 min. The initial rate of decline of absorbance of reduced cytochrome *c* was used as a measure of the permeability of the outer membrane to cytochrome *c*; ε_{550} (red-ox) = 18.5 mM^{-1} cm^{-1}. Vehicle controls were treated in an identical way. The percent of mitochondria with intact MOMs in these experiments was greater than 85%. Rates were corrected for the rate of oxidation observed with vehicle alone and this was very close to the untreated rate arising from a small number of damaged mitochondria.

The sensitivity of isolated mitochondria to permeabilization by added ceramide or analogs varied from one preparation to another. Therefore experiments with analogs were always performed in parallel with experiments with C_{16}-Cer. In this way the permeabilization produced by the analog (measures as the rate of cytochrome *c* oxidation) could be compared to that of C_{16}-Cer, either directly by reporting both rates or by expressing the result as a percent of that observed with C_{16}-Cer (Table 4.2).

Compound	Code	% of C_{16}-Cer permeabilization at 0.5-1nmol/µg protein	P Value	% of C_{16}-Cer permeabilization at 3nmol/µg protein	P value	% of C_{16}-Cer partitioning from Table 4.3
(2*R*,3*S*,4*E*) C_{16}-ceramide	S1	No effect (P = 0.32 relative to vehicle control)	<0.01	16 ± 4	<0.01	40
(2*S*,3*S*,4*E*) C_{16}-ceramide	S2	40 ± 60	N/S	80 ± 9	<0.05	--
(2*S*,3*R*,4*E*) *N*-methyl-C_{16}-ceramide	A3	No effect (P = 0.41 relative to vehicle control)	<0.02	21 ± 4	<0.01	75
(2*S*,3*R*,4*E*) C16-urea-ceramide	A4	236 ± 35	N/S	229 ± 7	<0.005	--
(2*S*,3*R*,4*E*) 3-*O*-methyl-C_{16}-ceramide	H2	125 ± 3	N/S	107 ± 15	N/S	60
(2*S*)-3-keto-C_{16}-dh-ceramide	H3	N/D		320 ± 82	<0.01	--
(2S,3R,15*E*) C_{16}-dh-ceramide	T1	76 ± 4	<0.03	385 ± 59	<0.001	30
(2*S*,3*R*,4*R*) C_{16}-phytoceramide	T2	429 ± 27	<0.03	230 ± 50	<0.05	460
(2*S*,3*R*) C_{16}-4,5-tb-ceramide	T3	N/D		120 ± 20*	N/S	--
(2*S*,3*R*,4*E*) C_{16}-(4,5-allene)-ceramide	T4	N/D		303 ± 26	<0.02	--
(2*S*,3*R*,4*E*) C_{10}-ceramide	L1	46 ± 17	<0.02	662 ± 26	<0.005	90
(2*S*,3*R*,4*E*) 13C/C_{16}-ceramide	L2	1310 ± 104	<0.005	606 ± 27	<0.005	--
N-palmitoyl-serinol	L5	N/D		306 ± 92	<0.01	--
(2*S*,3*R*,4*E*)$C_{18:1}$-ceramide	L6	100 ± 19	N/S	113 ± 4	N/S	--

Table 4.2: Relative potency of analogs to permeabilize the mitochondrial outer membrane. MOM was permeabilized by the addition of the indicated amount of analog (nmoles of analog per µg of mitochondrial protein) and the degree of permeabilization, as measured by the rate of cytochrome *c* oxidation is expressed as a percent (± S.E. of at least 3 trials) of the permeabilization measured in parallel experiments with C_{16}-Cer. The P values indicate the statistical significance of the permeabilization compared to that observed with C_{16}-Cer using the Student's T test. N/D means not done. N/S means not significantly different at the 95% confidence level.

The degree of cooperativity between an analog and C_{16}-Cer was determined by averaging the rate of cytochrome *c* oxidation achieved with a specific amount of each agent alone (called the "expected average") and comparing this with the rate observed with half the amount of each agent added combined (called the "combined effect"). The degree of cooperativity is expressed as the ratio of the combined effect to the expected average. A result not significantly different from "1" means no cooperativity; greater than "1" is synergy; less than "1" is antagonism.

Measurement of lipid insertion into mitochondria

C_{16}-Cer, one of the analogs, or a combination of both was added to a 0.7 mL mitochondrial suspension containing 160 μg of mitochondrial protein in H buffer. In each experiment 30 μL of a 1 mg/mL 2-propanol solution of the lipid(s) was added while vortexing as described above. The suspension was then layered on 0.7 mL of ice-cold solution of 15% (w/v) sucrose, 5mM HEPES pH 7.5 and centrifuged at 18,000 g for 5 min at 4 ^{o}C. (Beckman Coulter Microfuge 22R Centrifuge). The mitochondria sedimented and the uninserted lipid remained out of the sucrose layer (prior experiments showed that dispersed ceramide floats at this density (79). Most of the supernatant was aspirated gradually and the tube inverted and any liquid wiped off with paper wipe. The pellets were used for lipid extraction and measurement of the mitochondria incorporated ceramide and analogs by LC-MS/MS as previously described (99, 100).

Liposome permeabilization

Single-walled liposomes (93% asolectin and 7% cholesterol, by weight) were prepared by the extrusion method as previously described (38). In summary, lipids (total

mass, 5 mg) were hydrated in a buffer containing 1.5 mM carboxyfluorescein (CF), 6 mM DPX, 38.8 mM NaCl, 10 mM HEPES, and 1 mM EDTA, pH 7.0. The mixture was vortexed and subjected to 4 cycles of freeze-thaw-sonication followed by freeze-thawing and extrusion through a polycarbonate membrane (13 times) to form uniform single walled vesicles (100 nm diameter). A Sephacryl S200 gel filtration column (1.5 cm×30 cm) was used to separate the liposomes from untrapped fluorophore using an isoosmotic elution buffer lacking carboxyfluorescein and DPX (50 mM NaCl, 10 mM HEPES, 1 mM EDTA, pH 7.0). Aliquots (100 µL; containing approximately 0.1 mg of lipid) of the liposome suspension were diluted into 2 mL of the eluting buffer. CF was excited at 495 nm and the emitted light was detected at 520 nm in a Deltascan spectrofluorometer (Photon Technology Instruments). The fluorescence intensity was measured as a function of time under constant stirring and the test compound was added. The increase in fluorescence intensity was the result of the release of CF from the liposomes and its dilution from the quenching agent, DPX. The maximal increase in fluorescence intensity was measured after the addition of 150 µL of 5% Triton-X 100. The liposome permeabilization was plotted as % release of CF relative to maximal release.

Channel formation in planar membranes

Electrophysiological studies were conducted on some of the analogs to determine whether they were able to permeabilize planar phospholipid membranes devoid of proteins or other mitochondrial factors. Planar phospholipid membranes were generated using the monolayer method as previously described (101) and modified (74). The lipids comprising the monolayers were 1,2-diphytanoyl-sn-glycero-3-phosphocholine, asolectin, and cholesterol at a 1:1:0.1 ratio by weight. The aqueous solutions were 1.0 M

KCl, 1mM $MgCl_2$, 5mM PIPES pH 6.9 on both sides of the chamber. The bilayer was formed across a 100μm diameter hole in a Saran (polyvinylidene chloride) partition Calomel electrodes were used to interface with the aqueous solution, the voltage was clamped at 10 mV and the current recorded using a Digidata 1322A digitizer by Axon Instruments and Clampex 9.0 software by Axon Laboratories. To form a channel, successive additions of 5-20 μL of 0.05 mg/mL of the analog in 2-propyl alcohol were stirred into the aqueous solution (5 mL) on one side of the membrane. The vehicle has no effect and its final concentration was less that 1% (v/v).

RESULTS

The analogs were tested for their ability to permeabilize the outer membrane of isolated rat liver mitochondria to proteins, using the cytochrome *c* oxidation assay. Permeation through the MOM limits the rate of oxidation of exogenously-added cytochrome *c* by cytochrome oxidase in the inner membrane and thus the initial rate of oxidation of cytochrome *c* was utilized as a measure of the permeabilization of the MOM to proteins. Sample dose-response curves are shown in Fig. 4.4. Note that the shapes of these curves vary from rectangular hyperbola to sigmoid, making rigorous comparisons difficult. Generally a dose of 30 nmoles per 10 μg of mitochondrial protein was chosen as the common dose for comparison because it was low enough to avoid pronounced saturation by some analogs but high enough to detect permeabilization by the less-effective analogs. Results with lower doses are also reported. The sensitivity of mitochondria to MOM permeabilization varied from one isolation to the next so the permeabilization results summarized in Table 4.2 are expressed as a percentage of the

permeabilization achieved by ceramide in the same mitochondrial preparation, either C_{16}-Cer or C_8-Cer, as appropriate.

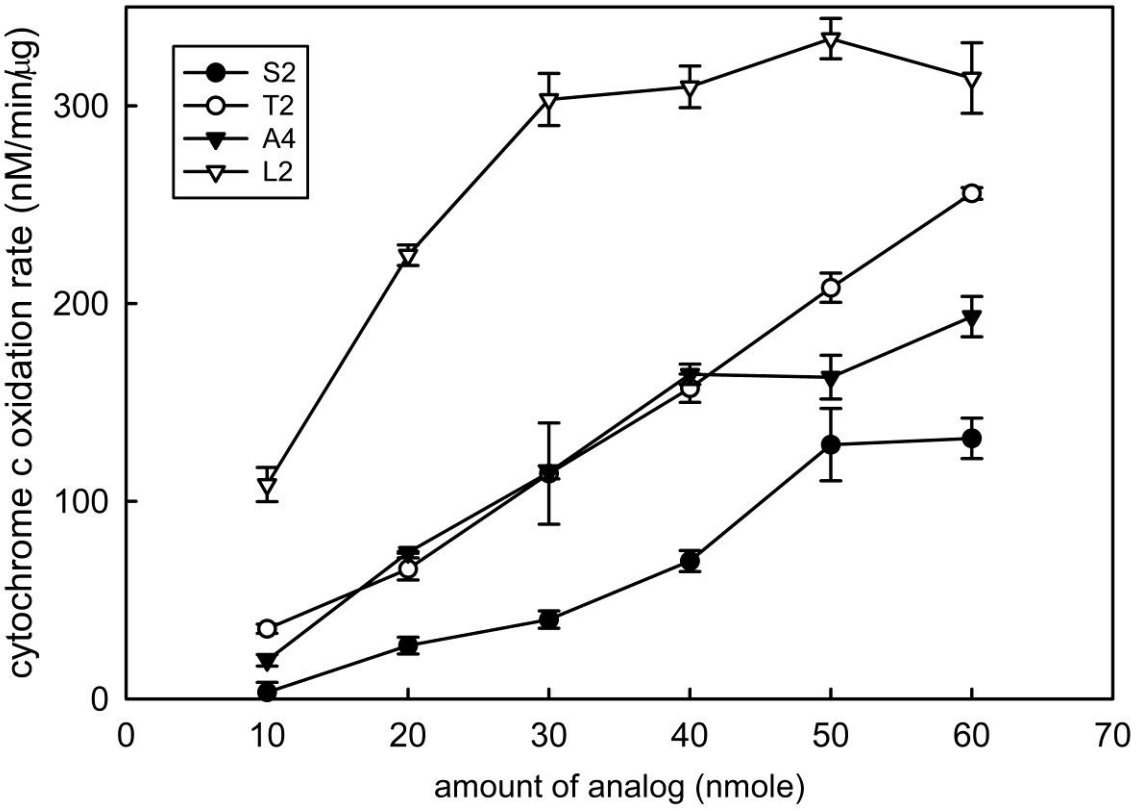

Figure 4.4: Examples of dose–response curves of the analogs used. The cytochrome *c* oxidation rate was used to assess the permeability of the MOM to proteins. The indicated amount of analog was added to 0.7 mL of a mitochondrial suspension.

An indication of MOM permeabilization was also obtained by measuring the extent of release of adenylate kinase. This is not a measure of MOM permeabilization but rather an indication of the fraction of mitochondria that have been permeabilized. With one notable outlier (vide infra) the MOM permeabilization assay and the adenylate kinase release assay yielded similar results for the analogs when compared to the effect of ceramide (Fig. 4.5). The permeabilizing ability of the analog is expressed as a fraction of

the ability of the corresponding ceramide, either C_{16}-Cer or C_8-Cer. The line drawn is not fit to the data but is a theoretical line for a 1:1 correlation between the two experimental results.

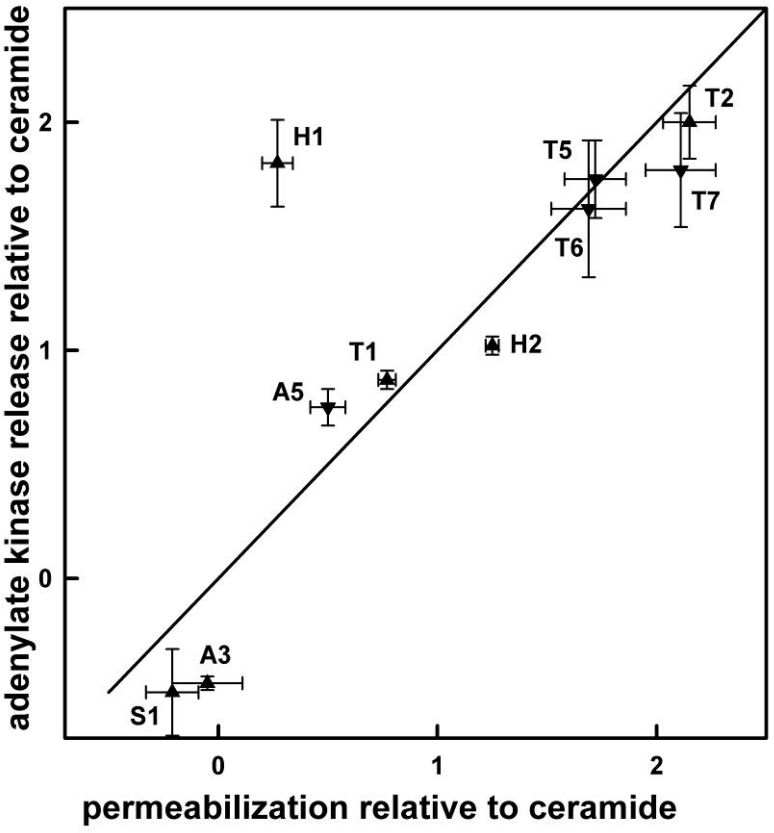

Figure 4.5: Correlation between changes in MOM permeability and adenylate kinase release by analogs. The "permeabilization relative to ceramide" is the rate of cytochrome *c* oxidation induced by the analog divided by that induced by ceramide (C16-Cer for triangles and C8-Cer for inverted triangles) under the same conditions. "adenylate kinase release relative to ceramide" is the activity of adenylate kinase released from mitochondria by analog addition divided by that released by ceramide. The error bars are standard error of at least three experiments.

The MOM permeabilization is dependent on the extent of insertion of the analog into the mitochondria, the propensity for channel formation, and the stability of the channels. Typically, only 0.3 to 1% of the added analog actually inserted into the mitochondrial membranes (Table 4.3). Phytoceramide was the exception with nearly 5% insertion. The extent of insertion helped to interpret the observed ability of an analog to permeabilize the MOM.

Compound	nmoles added	% incorporation	% incorporation in the presence of C_{16}-Cer	P value
D-C_{16}-Cer	56	1.04 ± 0.23		
L-C_{16}-Cer {S1}	56	0.41 ± 0.06		
C_{10}-Cer {L1}	66	0.95 ± 0.07	2.45 ± 0.34	0.01
Phytoceramide {T2}	54	4.78 ± 0.80	1.64 ± 0.36	0.004
N-Me-C_{16}-Cer {A3}	54	0.74, 0.85		
1-O-Me-C_{16}-Cer {H1}	54	1.00, 1.25		
3-O-Me-C_{16}-Cer {H2}	54	0.35, 0.95		
15E-C_{16}-Cer {T1}	56	0.23, 0.42		

Table 4.3 Extent of delivery of ceramide and its analogs to mitochondrial membranes. The indicated amount of lipid was added to a mitochondrial suspension (160 µg protein). The percent of the added lipid that incorporated into mitochondria is shown as mean ± S.E. of 4 trials or the values of individual trials. Column 4 shows the extent of analog insertion when added with equal amounts of C16-Cer. The insertion of C16-Cer was not affected by the presence of the analog. Column 5 is the T-test probability value obtained when comparing results in column 3 and 4.

Ability of analogs to permeabilize the MOM to proteins

Changes in the non-polar portions of ceramide did not interfere with channel formation. The analogs of ceramide having a shorter *N*-acyl chain **{L1}** or a shorter sphingosine backbone **{L2, L5}** were more potent in permeabilizing the MOM than C_{16}-Cer (Table 4.2). For C_2-ceramide (79) the additional potency was attributed to an enhanced ability to incorporate into the mitochondrial membrane. That is not the case for C_{10}-ceramide **{L1}** (Table 4.2, column 5) as the permeabilization was increased 6 fold despite no difference in the degree of incorporation into the MOM**.** Increasing the effective bulk of the hydrocarbon chain by using fluorescently labeled C_6-NBD-ceramide **{L4}**, or $C_{18:1}$-Cer **{L6}** with a *cis* double bond in the middle of the acyl chain, inhibited cytochrome oxidase activity. After correction for the inhibition, channel formation by $C_{18:1}$-Cer **{L6}** was indistinguishable from that of C_{16}-Cer (Table 4.2).

Major alterations in ceramide's *trans* double bond were also well tolerated (Table 4.2 and table 4.4).

Compound	Code	Liposome % release	MOM % perm.	Adenylate Kinase % release
(2*S*,3*R*,4*E*) C_8-ceramide	L3	17 ± 2 22 ± 3	36 ± 4	24 ± 2
(2*S*,3*R*,4*E*) C_8-ceramine[a]	A2	100	N/D	none
(2*S*,3*R*,4*E*) C2 - OCH_3 - C_8-ceramide	A5	18 ± 2 24 ± 3	18 ± 3	18 ± 2
(2*S*,3*R*,4*E*,6*E*)C_8-ceramide {diene}	T5	32 ± 3 40 ± 3	62 ± 5	42 ± 4
(2*S*,3*R*,4*Z*) C_8-ceramide {*cis* analog}	T6	37 ± 3 47 ± 4	61 ± 6	39 ± 7
(2*S*,5*R*,3*E*) C_8-ceramide	T7	36 ± 3 46 ± 4	76 ± 6	43 ± 6

Table 4.4: Comparison of channel-forming activity in mitochondria and liposomes. Liposomes and mitochondria were treated with ceramide analogs to assess the latter's ability to permeabilize membranes. For the liposomes (column 3) the % release of contents was performed at 2 different doses: 87 and 147 nmol per 2.5 mL of liposome suspension. For the MOM permeabilization (column 4) results are expressed as a % permeabilization achieved by hypotonic shock. The dose used was 0.19 nmol/µg protein. Measurements of adenylate kinase release (column 5) are expressed as percent of the kinase activity released following treatment with 0.25 nmol/µg protein. Release from liposomes was complete with as little as 15 nmol per 2.5 mL of liposome suspension. MOM permeabilization could not be done (N/D) because of strong inhibition of cytochrome oxidase.

Some of these were analogs of C_8-ceramide. Under identical treatments, C_8-Cer **{L3}** permeabilized the MOM to cytochrome *c* 36% of the maximal permeabilization, whereas the *cis* isomer **{T6}** resulted in a 61% of maximal permeabilization (Table 4.4). An analog with an extra double bond (6*E*) in conjugation with the first **{T5}** permeabilized the outer membrane to the same extent as the *cis* isomer **{T6}**. Moving the 4*E* double bond to a position between the two hydroxyl groups by putting it at the C3 position and moving the C3-hydroxyl group to the C5 position **{T7}** did not prevent MOM permeabilization. Similar results were obtained with analogs of C_{16}-Cer. C_{16}-

phytoceramide **{T2}**, where the 4*E*-double bond is replaced by a C4-hydroxyl group, had a 2-fold higher ability to permeabilize the MOM as compared to C_{16}-Cer but this can be more than accounted for by an enhanced ability to insert into the MOM (Table 4.3). Replacing the 4*E*-double bond by a C4, C5-triple bond **{T3}** also did not significantly affect the ability of the molecule to permeabilize the MOM. Moving the double bond farther down the chain **{T1}** to a position that does not form an allylic system results in an enhanced MOM permeabilization, despite a substantial reduction in its ability to insert into mitochondria. Hence the location, conformation, and degree of unsaturation do not have significant effect on channel forming ability.

The amide linkage in ceramide is proposed to have similar organizing effects as the amide linkages in proteins (102). The hydrogen-bonding ability of this linkage was proposed to organize ceramide monomers into columns. We found that increasing the hydrogen-bonding ability of this region by introducing a "urea" linkage **{A4}** resulted in an enhanced ability to permeabilize the MOM (Table 4.2). Moreover, reducing the hydrogen-bonding capacity by using C_8- and C_{16}-ceramines **{A1, A2},** which differ from ceramide by having an amino instead of an amide group, eliminated the molecule's ability to permeabilize MOM to proteins. Since both of these ceramines strongly inhibit cytochrome oxidase activity, release of adenylate kinase from the mitochondrial intermembrane space was measured. The ceramines caused no significant release of adenylate kinase. For C_{16}-ceramine, kinase release was -0.6 ± 7% for the highest dose tested (8 nmol/µg mitochondrial protein). C_8-ceramine was much more effective at releasing carboxyfluorescein from liposomes than C_8-Cer (Table 4.4) showing that it readily forms channels but these are very small. Methylation of the amide nitrogen,

affording *N*-methyl-C_{16}-Cer **{A3}**, drastically reduced but did not completely eliminate the ability of the molecule to permeabilize the MOM to cytochrome *c* (Table 4.2). The partitioning of **{A3}** into mitochondria was slightly reduced, however the reduced insertion into the membrane of this analog could not account for the extent of its loss of function.

Compound	Code	Combined effect / Expected average	P value	Nature of interaction
(2*R*,3*S*,4*E*) C_{16}-ceramide	S1	0.33	0.0005	Antagonistic
(2*S*,3*S*,4*E*) C_{16}-ceramide	S2	1[a]	0.36	Neutral
(2*S*,3*R*,4*E*) *N*-methyl-C_{16}-ceramide	A3	0.21	0.003	Antagonistic
(2*S*,3*R*,4*E*) C_{16}-urea-ceramide	A4	1.5[a]	0.015	Synergistic
(2*S*,3*R*,4*E*) 3-O-methyl-C16-ceramide	H2	1.0	0.25	Neutral
(2*S*)-3-keto-C_{16}-dh-ceramide	H3	1.0	0.41	Neutral
(2S,3R,15E) C_{16}-dh-ceramide	T1	1.3	0.15	Neutral
(2*S*,3*R*,4*R*) C_{16}-phytoceramide	T2	0.52[a]	0.009	Antagonistic
(2*S*,3*R*) C_{16}-4,5-tb-ceramide	T3	0.95[a]	0.33	Neutral
(2*S*,3*R*,4*E*) C_{16}-(4,5-allene)-ceramide	T4	1.3	0.06	Neutral
(2*S*,3*R*,4*E*) C_{10}-ceramide	L1	1.5[a]	0.04	Synergistic
(2*S*,3*R*,4*E*) 13C/C_{16}-ceramide	L2	1.4[a]	0.02	Synergistic
N-palmitoyl-serinol	L5	1.4	0.002	Synergistic

Table 4.5: Cooperativity between C16-ceramide and its analogs. The analog was mixed in equimolar quantities with C16-Cer and the permeabilization of the MOM was compared to the average permeabilization observed with equal total amounts of either C16-Cer or the analog alone. At least 3

experiments were performed for each condition and P values for the t-tests are listed. Using 95% confidence, ratios significantly greater than 1 are labeled synergistic; significantly less than 1, antagonistic; not significantly different, neutral. [a] The increase in MOMP resulting from the addition of a total of 3.6 nmoles/μg protein of an equimolar mixture of C_{16}-Cer and the specified analog was compared to 3.6 nmoles/μg protein of either C_{16}-Cer or the analog alone. In the other experiments, 5.6 nmoles/μg protein were used.

The ability of **{A3}** to form channels, even at a much reduced potency raises a severe problem with the working model of the ceramide channel where the hydrogen bonding from the amide nitrogen is essential to the overall structure. In the model, the amide nitrogen of one ceramide molecule forms a hydrogen bond with the carbonyl group of another to form ceramide columns. Methylation of the amide nitrogen as in **{A3}** would effectively prevent such interactions. However, in molecular dynamic simulations performed by Andriy Anishkin (90), whereas the working model of the ceramide channel is the predominant form arising from such simulations, other, minor forms were also detected. In some of these the carbonyl oxygen is not hydrogen bonding with the amide hydrogen of the adjacent ceramide but hydrogen bonding with a C1-hydroxyl through a water bridge . Thus it may be possible for **{A3}** to form a similar structure.

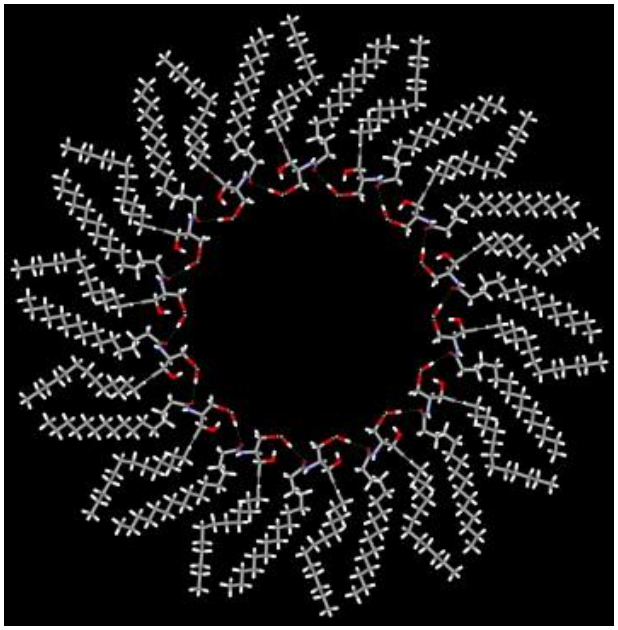

Figure 4.6 showing the top view of a ceramide channel structure. This figure, which was obtained by Andriy Anishkin as part of the structures formed by simulated annealing, is one of a few structures in which the carbonyl oxygen forms a hydrogen bond with one of the hydroxyl groups rather than forming a hydrogen bond with the amide group of an adjacent ceramide molecule. In this structure, the ceramide columns are arranged in parallel rather than anti-parallel.

The C1 and C3 hydroxyl groups have been proposed to stabilize channel structure via hydrogen bonds with the corresponding functional groups on adjacent ceramide molecules. Analogs of these functional groups were utilized to determine the contribution of these groups to the channel structure. *O*-Methylation of the C1-hydroxyl group **{H1}** was chosen because the methyl group should prevent this hydroxyl group from participating in a hydrogen bond. The methylation of the C1 hydroxyl resulted in an almost complete loss of any stable MOM permeabilization despite no change in ability to insert into mitochondria (Table 4.5). When the ability of **{H1}** to release adenylate kinase was tested, it was almost double that observed with C_{16}-Cer indicating that twice as many mitochondria were permeabilized, if only transiently, by **{H1}**. When reconstituted into planar membranes, **{H1}** produced conductances that were transient

(vide infra) as opposed to the growing conductances observed with C_{16}-Cer. These were similar to those published for sphingosine (36) except that these are large enough to allow the release of adenylate kinase (Fig. 4.5).

Unlike **{H1},** methylation at the C3-hydroxyl **{H2}** produced functional properties very similar to those of C_{16}-Cer (Table 4.2). Both the cytochrome *c* oxidation assay and the adenylate kinase release assay produced results indistinguishable from those of C_{16}-Cer. The importance of the location of the C3-hydroxyl group and the stereochemistry of the adjacent chiral center were tested by relocating the hydroxyl to the C5 position **{T7}** and by changing configuration from (2*S*,3*R*)-C_{16}-Cer to (2*S*,3*S*)-C_{16}-Cer **{S2}**, respectively. Neither of these alterations had a large effect on the ability of these molecules to permeabilize MOMs of isolated mitochondria (Table 4.2). Thus the location and orientation of the C3-hydroxyl can be changed with minimal consequences. By sharp contrast, converting the (2*S*,3*R*)-C_{16}-Cer to (2*R*,3*S*)-C_{16}-Cer **{S1}** (i.e. an additional change in the chirality at C2) greatly reduced its ability to permeabilize MOMs, consistent with the importance of the C1-hydroxyl group (Table 4.2). Unlike the results with **{H1}**, **{S1}** was unable to permeabilize the MOM or release adenylate kinase at 1 nmole/µg protein and produced only 16% of the permeabilization of C_{16}-Cer at 3 nmoles/µg protein. The amount of insertion was reduced by a little over half but not enough to account for the large reduction in ability to permeabilize the MOM. Thus, the stereochemistry of ceramide that limits the possible and preferred positions of its polar groups (94), can also influence the propensity for channel formation in the MOM.

Interactions between D-e-C_{16}-ceramide and its analogs

Isolated mitochondria were treated with either C_{16}-Cer alone or the analog alone, or an equimolar mixture of C_{16}-Cer and the analog at half the dose. Thus, the total amount of sphingolipid added was kept constant. The ability of each of the three treatments to permeabilize the MOM to cytochrome *c* was measured. Examples of the results are shown in Fig. 4.7. For **{A4}** and **{L2}** the simultaneous presence of both lipids (designated as both) yielded a higher rate of cytochrome *c* oxidation (and therefore a higher permeability) than the average of the individual treatments (avg), thus indicating synergy. The converse was true for **{T4}**, indicating antagonism. For **{S2}** there was no significant difference, indicating neutrality or no cooperativity. Depending on the experimental set, 40 nmol or 60 nmol of lipids were utilized (as indicated in Table 4.4). The permeability resulting from the combined treatment ("combined effect" in Table 4.4) was compared to the "expected average" which is the average of the permeabilities observed with the individual sphingolipid treatments. The ratio is reported in Table 4.5 along with the P values of statistical significance and the interpretation of the results. Ratios significantly greater than 1 indicate synergy and ratios significantly less show antagonism.

A subtle change, such as the replacement of the 4*E* double bond of ceramide with a C4,C5-triple bond **{T3},** resulted in a neutral effect when combined with C_{16}-Cer (Table 4.5). Experiments with the diastereomer **{S2}** (2*S*,3*S* as opposed to 2*S*,3*R* for C_{16}-Cer) were also consistent with simple neutrality (Fig. 4.7 and Table 4.5).

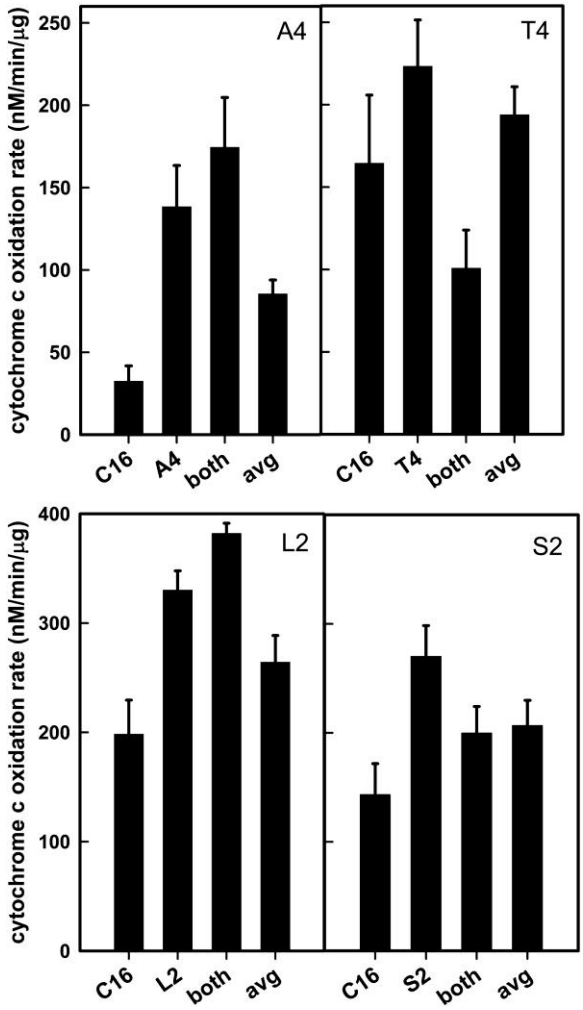

Figure 4.7: Cooperativity between analogs and C16-Cer. For an individual addition, a total of 40 nmol was used. For combined additions (both), 20 nmol of each was used. The average bar (avg) shows the average of the results obtained with each lipid alone. The statistics are shown in Table 4.5. The individual and combined additions for each analog were performed with the same batch of mitochondria under the same conditions to avoid the variability in sensitivity to ceramide found among mitochondrial preparations.

Treating mitochondria with a mixture of C_{16}-Cer and the shorter chain analog, $13C/C_{16:0}$ **{L2}** resulted in a permeabilization that was greater than the average of treatments with individual compounds (Fig. 4.7). Similar results were obtained with other short-chain analogs **{L1, L5}** (Table 4.4) and with urea-ceramide **{A4}.**

Mitochondria treated with an equimolar mixture of ceramide and phytoceramide **{T2}** achieved a much reduced level of permeabilization than expected from averaging the individual treatments (Fig. 4.7, Table 4.4). This inhibition was also found between phytoceramide **{T2}** and L-e-C_{16}-Cer **{S1}** (data not shown). A similar antagonistic interaction was found between C_{16}-Cer and either *N*-methyl-C_{16}–Cer **{A3}** or the enantiomer, (2*R*,3*S*) **{S1}**.

The type and degree of cooperativity correlates with the channel-forming ability of the analog. A plot of the channel-forming potency relative to that of C_{16}-Cer versus the cooperativity ratio from Table 4.5 shows the strong correlation (Fig. 4.8). The upper right quadrant contains data from the analogs showing synergy and higher propensity for channel formation whereas the lower right quadrant contains data from those displaying antagonism and lower channel-forming propensity. Analogs showing no cooperativity and essentially similar channel-forming propensity to C_{16}-Cer tend to cluster at the "origin". The other two quadrants are essentially vacant.

The permeabilization of the MOM following the dispersal of ceramide or an analog must involve at least two processes: insertion and self-assembly. The cooperativity could take place at one or both of these. The influence of combined delivery on the insertion of the sphingolipids was assessed for one analog showing synergy **{L1}** and one showing antagonism **{T2}** (Table 4.3). The presence of C_{16}-Cer influenced the ability of the analogs to insert into the MOM in harmony with the observed cooperativity. The amount of **{T2}** that inserted when combined with C_{16}-Cer was one third of that measured following its individual addition whereas the insertion of

{L1} doubled. The insertion of C_{16}-Cer was not significantly affected by the presence of the analog.

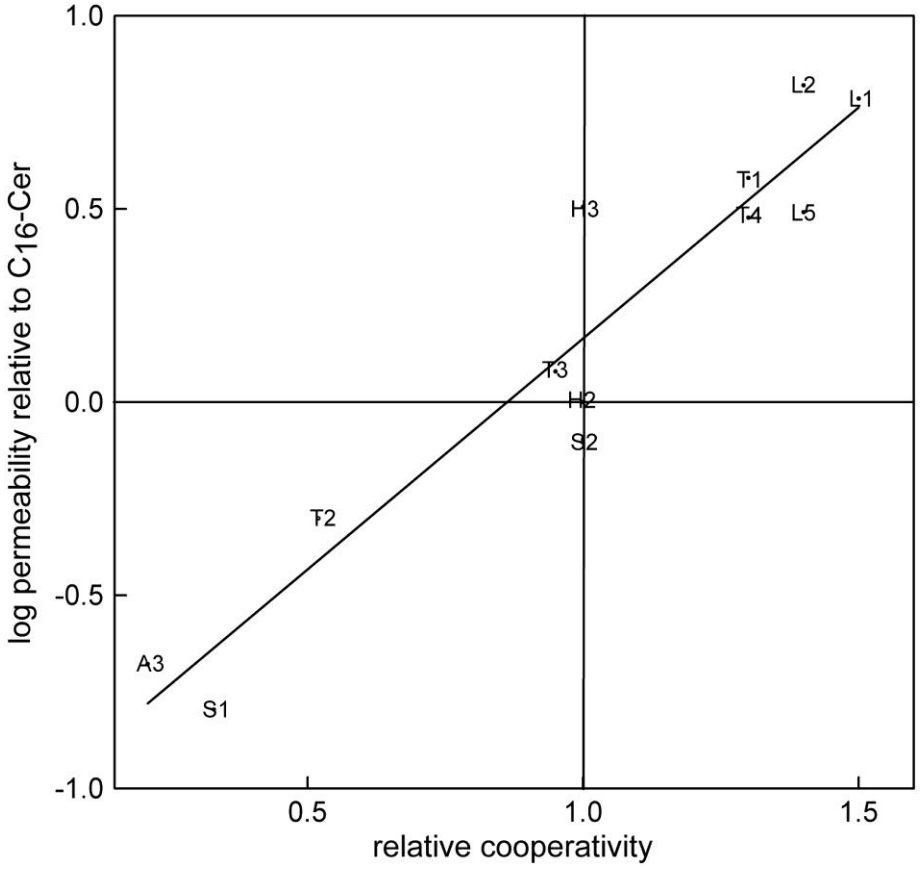

Figure 4.8: Correlation between degree of cooperativity and ability of an analog to permeabilize the MOM. Relative cooperativity is from column 3 of Table4.5. The permeability relative to C16-Cer is from Table 4.2 column 3 after dividing by 100 and taking the log.

The antagonism observed in mitochondrial experiments was also evident in experiments with liposomes, showing a direct interaction between these lipids. Premixing C_{16}-Cer and C_{16}-phytoceramide {T2} resulted in a much smaller permeabilization of liposome membranes than phytoceramide {T2} alone (Fig. 4.9).

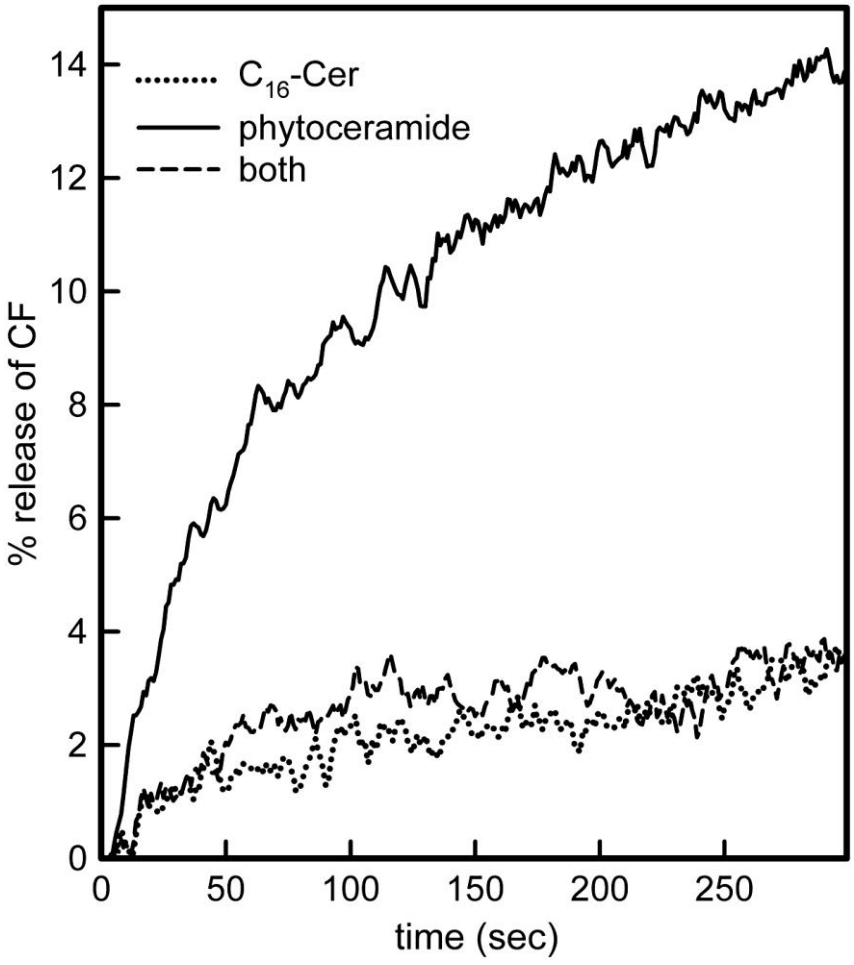

Figure 4.9: Permeabilization of liposomes by C16-Cer, C16-phytoceramide {T2}, or the two together.

Channel formation in phospholipid membranes

To directly observe channel formation by ceramide analogs and to gain insight into their stability and dynamics, experiments were performed in defined systems consisting of phospholipid membranes: planar membranes and liposomes. In planar membranes, channel formation was monitored as changes in conductance to K^+ and Cl^- ions. In liposomes, the release of carboxyfluorescein and the quenching agent, DPX, was used to assess the permeabilization of single-walled liposomes by the analogs. In both of these experimental systems, the analogs that were able to permeabilize the MOM were

also able to permeabilize phospholipid membranes that were free of proteins, demonstrating that the analogs form channels rather than inducing MOM proteins to form channels.

Most of the analogs that could permeabilize the MOM produced conductances in planar membranes with similar characteristics to those of C_{16}-Cer. Examples for phytoceramide **{T2}** and urea-ceramide **{A4}** are shown in Fig. 4.10. Channel formation occurred after a lag phase and usually required a few separate additions. Fig. 4.10A shows how a sustained conductance developed after a final addition of 1 nmole of **{A4}**. The conductance increased in steps of varying size until it reached a plateau. Sometimes the increase was rapid, reaching a high conductance (Fig. 4.10B). At the reduced gain required to observe the total conductance the increase appears to be very smooth. Addition of La^{+3} resulted in channel disassembly after a variable delay (Fig. 4.10B), which is similar to the effect of La^{+3} on a C_{16}-ceramide channels as previously reported (30). The variable delay is characteristic of a stochastic process (30) and is also consistent with the formation of a single channel that enlarges in size. Most of the analogs appear to form a single large channel in the planar membrane (data not shown), as was demonstrated for ceramide (30).

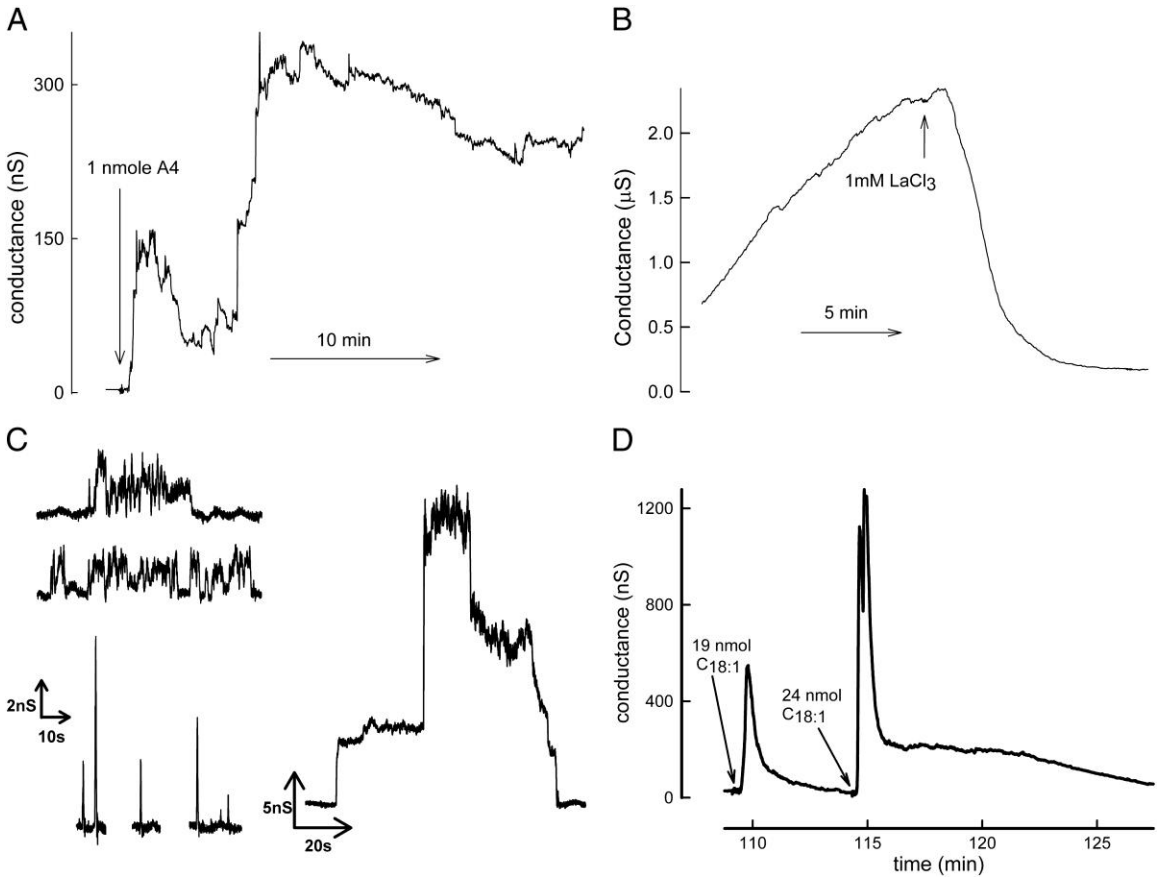

Figure 4.10: Electrophysiological recording of conductances formed by ceramide analogs in planar phospholipid membranes. A. The formation of a channel by urea ceramide {A4}. Equal amounts of the analog were added at intervals (for a total of 4.6 nanomoles) with the last shown in the figure. B. The formation of a C16-phytoceramide {T2} channel and its partial disassembly by the addition of LaCl3. Channel formation followed the addition of 0.46 nmol of C16-phytoceramide {T2}. C. Segments of conductance transients observed after addition of 1 nmol of ceramide methylated at the C1-hydroxyl {H1}. The bursts shown were observed over a 40 min time period. D. Transient channels formed by {L6} C18:1-ceramide. A total of 25 nmol of C18:1 was added at intervals and similar patterns of channel growth and disassembly were seen after each addition. In all cases the transmembrane voltage was clamped at 10 mV.

Marked exceptions were the behaviors of the conductances produced by 1-O-methyl-C_{16}-ceramide **{H1}**, *N*-methyl-C_{16}-ceramide **{A3}** and $C_{18:1}$-Cer **{L6}**. With these compounds, the conductance rose rapidly but was transient, declining and returning to the baseline shortly thereafter. This behavior was often observed multiple times in the same

membrane. Only occasionally would a prolonged conductance form. The analog with the shortest conductance bursts was **{H1}** (Fig. 4.10C). The figure shows samples of conductance burst recorded within a 40 min period of activity. **{L6}** was at the other end of the spectrum, producing greater conductances but these also tended to decay (Fig. 4.10D). The addition of more sample produced a second transient conductance. **{A3}** was intermediate between these (data not shown). The behavior of these analogs is consistent with a less stable structure and in agreement with the observations made with isolated mitochondria. **{H1}** produced virtually no permeability; **{A3}** had a much diminished permeabilizing ability (21% of that induced by C_{16}-cer, Table 4.2); **{L6}** produced an effective permeabilization similar to C_{16}-Cer. Clearly the channel dynamics are not detectable in mitochondrial experiments and only the average permeability to cytochrome *c* is assessed.

In general, liposome permeabilization experiments and adenylate kinase release experiments produced results in agreement with mitochondrial permeability measurements (Table 4.4 and Fig. 4.8). **{H1}** and the ceramines **{A1}** and **{A2}** were the exception. **{A2}** induced the maximal release of liposomal contents, but did not facilitate the release of adenylate kinase from the mitochondrial intermembrane space (Table 4.4). The fact that ceramine can permeabilize liposomes to carboxyfluorescein, but did not permeabilize the MOM to adenylate kinase is consistent with its formation of small channels capable of allowing small molecules to cross membranes, but not large enough to allow the passage of proteins. These conductances resemble those published for sphingosine (36), Like **{H1}**, these conductances did not grow in size but returned to the baseline and were likely the result of the formation of small pathways such as the toroidal

structures induced by amphipathic structures (85 – 87). Unlike **{H1}** the transient conductances did not become large enough to release adenylate kinase from mitochondria.

DISCUSSION

The data presented show that the structure of ceramide can be altered in a number of ways without losing the ability of the molecule to permeabilize membranes in a manner that is consistent with self-assembly into large channels capable of translocating proteins through membranes. The mitochondrial and planar membrane experiments suggest that many of the analogs form large, stable channels. The results indicate the relative importance of specific structural features of ceramide for channel formation, namely the differential importance of the hydroxyl groups, the role of the *trans* double bond, and the importance of the stereochemistry.

Ceramide channel formation is minimally affected by apolar chain length

Physiologically, the length of the *N*-acyl chain of ceramide is clearly very important (103, 104). For example, the ceramide synthases show strong specificity for different acyl-CoA substrates (105 - 108). Some preferentially produce long-chain ceramides such as C_{16}-Cer, whilst others preferentially produce very long-chain ceramides such as C_{24}-Cer (107, 108). Many enzymes that metabolize ceramide do not recognize C_2-Cer (109, 110). Yet, with regard to the ability to form channels, the length of the *N*-acyl chain was found to be relatively unimportant. After compensating for the difference in delivery to the mitochondrial membranes, the potency of C_{16}-Cer and C_2-Cer were found to be indistinguishable (79). Here we tested analogs having shorter *N*-

acyl chains **{L1, L3}** and shorter sphingoid base backbones **{L2, L5}**. The results indicate that these can also form permeability pathways in membranes in a manner consistent with channels and interact synergistically with ceramide. For **{L1}**, the synergy arises from the ability of C_{16}-Cer to aid in the insertion of **{L1}** into mitochondria.

It is important to note that the minimal ceramide analog, N-palmitoyl-serinol **{L5}**, functions very well with only one aliphatic chain. Thus, one might ask why natural ceramides have such a large amount of apolar mass. The simplest answer would be that the extra bulk anchors the lipid in the membrane, limiting spontaneous, uncatalyzed motion between membranes of different organelles.

C1- hydroxyl group is critical to stable ceramide channel formation; modifications to the *trans* double bond are well tolerated

An important feature in the ceramide structure is the C4,C5-*trans* double bond in the sphingoid base backbone (93, 103, 111) For permeabilization of the MOM, many changes were well tolerated, namely conversion of *trans* to *cis*, displacement of the double bond relative to the adjacent hydroxyl, and replacement of the double bond by a third hydroxyl. Thus, a variety of structures are capable of permeabilizing membranes in a manner consistent with the channels formed by C_{16}-ceramide.

The ability to form stable channels was lost by *O*-methylation of the C1-hydroxyl group **{H1}**. It forms transient pores capable of allowing adenylate kinase release but too short-lived to significantly increase the overall MOM permeability to proteins. The transient conductances were evident in planar membrane experiments. By contrast, *O*-

methylation of the C3-hydroxyl group **{H2}** was well tolerated. Similar results with the C3-keto **{H3}** analog provide additional evidence that C3-hydroxyl modifications are well tolerated. Further evidence for a difference in the importance of these two hydroxyl groups comes from results obtained with stereochemical isomers. The diastereomer studied in which "3R" was changed to "3S" **{S2}** showed no change in MOM permeabilizing properties despite a change in orientation of the C3-hydroxyl. However, the enantiomer, with the same change at the C3 position and an additional change from "S" to "R" at the C2 position **{S1}**, was much weaker in its capacity to permeabilize mitochondria. Thus the presence and orientation of the free hydroxyl at C1 is critical to the stability of the channels, indicating that this hydroxyl forms part of a highly organized structure.

Amide linkage provides stabilizing structural support for the ceramide channel

The importance of the amide linkage as an organizing unit is supported by the finding that the conversion of an amide chain to an amine-linked chain in ceramine **{A1, A2}** prevents the permeabilization of the MOM to proteins. If the ceramides are arranged in the channel as proposed by the structural model (18, 80) then the conversion of the amide linkage to an amine would indeed destabilize the structure by eliminating the hydrogen bonding that has been proposed to be the basis for the columns that make up the channel. By contrast, the greater hydrogen-bonding and ordering ability of a urea linkage according to the structural model would be expected to stabilize the channel, and indeed this analog **{A4}** forms channels. The introduction of a methoxy group in the amide region **{A5}** still allowed channel formation, indicating that the modification is tolerated.

N-methyl C_{16}-Cer **{A3}** can still form channels, which is in apparent contradiction to the structural model because the methyl group that replaces the C3 hydroxyl cannot participate in hydrogen bonding. Whilst its ability to permeabilize the MOM is much reduced as compared to C_{16}-Cer and in planar membranes it forms unstable channels, the ability to form channels at all seems to invalidate the structural model of the ceramide channel. However, channel formation by **{A3}** is antagonistic with that of C_{16}-Cer, indicating that structural incompatibilities were introduced by *N*-methylation. Molecular modeling studies show that a channel can be formed with the carbonyl group hydrogen-bonding with the C1-hydroxyl group through a water bridge as shown by the example structure. This structure is quite different from the working model of the ceramide channel (30).

Cooperativity between ceramide and analogs

Combined addition of C_{16}-Cer and an analog showed cooperativity in membrane permeabilization in certain cases: either synergy or antagonism. The cooperativity correlates well with the ability of individual lipids to permeabilize the MOM. Surprisingly, the cooperativity seems to involve the insertion into the MOM. Insertion may be catalyzed by structures formed by sphingolipids in the membrane. Perhaps ceramide forms phases or domains in the membrane that could engage or exclude other analogs depending on the compatibility or incompatibility of the molecular structures (i.e. their ability to bind to each other). Organized structures composed of many sphingolipids would require that each component fit well sterically and in bonding interactions. Thus very similar structures would be interchangeable, complementary structures would show

synergy and poorly compatible structures would show antagonism. Without structural information it will be difficult to understand the molecular basis for the cooperativity.

Influence of structural changes on channel function

The ability of ceramide to self-assemble and form membrane channels is remarkably resistant to changes in molecular structure. However, structural changes in specific regions such as the C1-hydroxyl and the amide linkage do decrease channel stability or form channels too small to release proteins. These changes would reduce or eliminate the ability of the channel to release proteins from mitochondria. A reduction in the rate of release and amount of protein release does result in a failure to initiate apoptosis. The use of lasers to damage mitochondria in live cells failed to induce apoptosis presumably because of insufficient protein release and thus failure to achieve a critical cytosolic concentration of pro-apoptotic proteins such as cytochrome *c*. Thus natural selection pressure maintains the structure of ceramide and the ability to form large and stable channels.

CONCLUSIONS

The results of previously published work on ceramide channels strongly suggests that these channels have a highly organized structure, one in which an altered configuration of the polar lipid head region would disrupt the structure. The results presented here identify key functional groups important for ceramide channel formation and structural aspects where changes are tolerated. The C1-hydroxyl is indispensable for channel stability whereas C3-hydroxyl is not critical for channel formation. It is interesting that further elaborations of ceramide in cells involve additions to the C1-

hydroxyl rather than the C3-hydroxyl, thus interfering with the propensity to form channels. The amide linkage is also highly important for channel stability. Reducing the length of the hydrocarbon chains favors channel formation and indeed a single chain is sufficient. The allylic system is not necessary and the *trans* double bond does not seem important to the ability to form channels. The sensitivity of channel stability to the stereochemistry at C2 further supports the notion of ceramide channels being highly-organized structures.

Note: This body of research was accomplished in collaboration with Meenu Perera who is an equal contributor to this work. The experiments with planar membranes reported here were performed by various undergraduate students. Leah J. Siskind did the experiments with C8 ceramide. I and Meenu shared the responsibility of testing various analogs of ceramide for their ability to induce MOMP. Drs. Szulc, Bielawska, Bielawski, and Bittman provided us with the various analogs.

CHAPTER 5 MECHANISTIC INSIGHTS INTO BAX MEDIATED MOMP USING IONIC STRENGTH

ABSTRACT

Mitochondrial outer membrane permeabilization (MOMP) is a complex multi-step process. Studies of MOMP *in vivo* are limited by the stochastic variability of MOMP between cells and rapid completion of IMS protein release within single cells. *In vitro* models have provided useful insights into MOMP. We have investigated the dynamics of Bax mediated MOMP in isolated mitochondria using ionic strength as a tool to control the rate of MOMP. We find that Bax can induce both transient permeabilization, detected by protein release and more substantial long-lasting permeabilization measured by the rate of oxidation of added cytochrome *c*. We found that higher ionic strength causes Bax to form small channels quickly but the expansion of these early channels is impeded. This inhibitory effect of ionic strength is independent of tBid. Channels formed under low ionic strength are not destabilized by raising the ionic strength. Increase in ionic strength also increases the ability of Bcl-xL to inhibit Bax mediated MOMP. Ionic strength does not affect Bax insertion into mitochondria. Thus ionic strength influences the assembly of Bax molecules already in membrane into channels. Ionic strength can be used as an effective biophysical tool to study Bax mediated channel formation.

INTRODUCTION

Apoptosis is a form of programmed cell death that is crucial to the elimination of damaged or unwanted cells. Its proper execution is vital for appropriate development. A key event in the apoptotic pathway is increased permeability of the mitochondrial outer membrane (MOM[†]), which leads to the release of intermembrane space (IMS) proteins.

These proteins trigger the activation of downstream caspases, which carry out the repackaging of the cell into apoptotic bodies. The rate-limiting increase in MOMP leading to the release of IMS proteins is well known to be modulated by Bcl-2 family of proteins (13, 20, 112, 113). The Bcl-2 proteins can be categorized broadly on the basis of their mode of action into pro-apoptotic and anti-apoptotic proteins. Pro-apoptotic BH1-3 proteins act directly to enhance MOMP by forming protein –permeable pores. BH3-only proteins increase MOMP indirectly by activating BH1-3 proteins or inhibiting anti-apoptotic Bcl-2 proteins (or both). Anti-apoptotic BH1-4 type proteins inhibit the action of the pro-apoptotic proteins (112 - 115).

The control of MOMP by the Bcl-2 proteins has been studied extensively. Bax, normally cytosolic, upon activation by the BH3 only protein, tBid, targets the MOM, inserts, and forms oligomeric pores (40, 116 - 119)**.** Bcl-xL inhibits MOMP by either out-competing Bax for tBid and/or interacting directly with Bax to inhibit its insertion into the MOM (40). The molecular roles of different domains of Bax in membrane insertion are well known (54, 57, 119 - 121). Some amino acids have also been identified that either enhance or eliminate the pro-apoptotic function of Bax (57, 121) but the properties of the oligomeric channel such as size, stoichiometry, and kinetics of channel assembly are only partially understood. We sought to study the dynamics of Bax induced permeabilization of the MOM to proteins in isolated mitochondria using ionic strength as a modulating tool.

Since MOMP is a rapid, irreversible, essentially all-or none process where most IMS proteins are released almost simultaneously within a few minutes (78, 122 - 124), *in vitro* models have been very useful in studying the regulation of MOMP by Bcl-2 family

proteins (50 - 56, 125, 126). We use ionic strength as a diagnostic tool to provide mechanistic insights into the dynamics of Bax mediated permeabilization.

MATERIALS AND METHODS

Preparation of cytochrome *c*

Horse heart cytochrome *c* (44mg) was reduced with 11mg ascorbate in 1mL of 0.2M Tris-HCl pH 7.5. The reduced cytochrome *c* was separated from the ascorbate by gel filtration through a Sephadex G-10 column equilibrated with 0.2M Tris-HCl pH 7.5.

Isolation of rat liver mitochondria

Fresh mitochondria were purified from rat liver as described (31). The BSA was removed by sedimenting mitochondria in BSA free isolation buffer and the final pellet resuspended in 300mM mannitol, 5mM HEPES and 0.1mM EGTA pH 7.4 (FH-buffer) to a final concentration of 10-20mg mitochondrial protein/mL. The mitochondrial stock was always kept cold and dilutions were made periodically from the stock for experiments.

Purification of recombinant proteins

Recombinant human Bax was produced as described (18) but the purification procedure was modified. The Bax eluted from the chitin column was dialyzed (12000 MW cutoff) at 4ºC for 24hrs against 3L of 1mM EDTA, 20mM Tris-HCl, pH 8. Then it was dialyzed again for 48hrs against 5L of 20mM Tris-HCl pH 8 to remove all remaining DTT. Recombinant tBid was purified as described (51). Bcl-xL was purified as described (60, 62). All proteins were filter-sterilized (0.2μm filter), glycerol added (10% final), rapidly

flash-frozen with ethanol and dry-ice, and stored at -80^{o}C. Protein concentration was determined after dialysis by the BCA method.

Preparation of mitochondrial samples for cytochrome *c* oxidation and IMS protein release assays

Isolated rat liver mitochondria were incubated in buffers of varying salt concentrations with the total osmotic pressure kept constant at 300 mOs by addition of the appropriate amount of mannitol. To this mitochondrial suspension, a combination of Bcl-2 family proteins (Bax, tBid, and Bcl-xL) was added as needed. Prior to each experiment, the mitochondria were diluted to a protein concentration of 160μg/ml in FH (300mM mannitol, 0.1mM EGTA and 5mM HEPES pH 7.4) buffer. Since mitochondrial function degrades once diluted, the mitochondria were used within 10 minutes of dilution. In all experiments 600μL of this mitochondrial dilution was added to 400μL of isosmotic buffer (with either 25.1mM KCl or 150mM KCl) pre-mixed with appropriate amounts of Bcl-2 family proteins to achieve a final mitochondrial concentration of 96μg/mL (and final [KCl] of either 10mM or 60mM respectively). These isosmotic solutions are referred to as "KCl buffer" prefixed with the [KCl]. The same methodology was followed when NaCl or potassium lactobionate was tested. For 90mM buffer, the mitochondrial stock was diluted 50-100 fold in 150mM KCl buffer to a protein concentration of 160μg/ml. 600μL of this suspension was then diluted with 400μL of FH buffer containing the Bcl-2 family proteins to achieve a final ionic strength of 90mM. The mitochondria were preincubated at 30^{o}C with the Bcl-2 family proteins for 30 minutes except for time course experiments. For all experiments using Bcl-xL, the Bcl-2 proteins were incubated together for 10 minutes prior to the addition of mitochondria. Once the

incubation period was over, 100μL of the mitochondrial suspension was used for the cytochrome *c* accessibility assay, while the rest was centrifuged and the supernatant used for adenylate kinase and sulfite oxidase assays. In corresponding experiments, 50μL of cyclosporin A (dissolved in DMSO to a stock concentration of 1mg/mL) was added to 1mL of mitochondrial suspension to a final concentration of 50μM just prior to the preincubation process.

Western blot analysis

For all western blotting experiments, three 1mL mitochondrial suspensions (960μg/mL) were incubated at 30^{o}C under the conditions and for the times indicated in the figure legends. The triplicates were centrifuged (10,000 RCF for 5 min) and each resuspended into 200μL of FH buffer. These were pooled together, mitochondria repelleted and subjected to sodium carbonate treatment as described (127). The pellet was resuspended in 50μL of 2% SDS and incubated for 1 hr on ice. Then, the detergent solubilized fraction was separated from the detergent-insoluble fraction by centrifugation and 30 μL used for PAGE/blotting analysis. VDAC served as loading control. Bax was probed with rabbit anti-Bax (Ab7977: 1:1000) and VDAC was probed with rabbit anti-VDAC anti-serum (1:1,000,000). Both the primary antibodies were probed with HRP tagged anti-rabbit secondary antibodies (1:2500 for Bax and 1:5000 for VDAC). Blots were developed with DAB as described in (128).

Cytochrome *c* accessibility assay

The cytochrome *c* oxidation or accessibility assay was performed as described previously (31). After appropriate treatment of 96μg/mL mitochondria with Bcl-2 family proteins,

100μL of this suspension was dispersed in 600μL of cytochrome *c* oxidation assay buffer (equivalent to FH buffer (mannitol + KCl (total 300mOs), 0.1mM EGTA, 5mM HEPES pH 7.5) of appropriate ionic strength supplemented with 5mM DNP and 5μM antimycin A) and quickly assayed for cytochrome *c* oxidation by adding 10μL of reduced cytochrome *c* to a final concentration of ~25μM. Cytochrome *c* oxidation was measured as decline in absorbance at 550nm. The rate of oxidation was calculated from the slope of the linear region of the absorbance change measured for 2 minutes. Maximal rate of cytochrome *c* oxidation (corresponding to 100% permeabilization) was determined by the rate of cytochrome *c* oxidation by equivalent amount of hypotonically shocked mitochondria (at least 1 volume of mitochondrial suspension to 50 volumes of double distilled H_2O). Hypotonic lysis breaks the MOM and exposes all the cytochrome oxidase to exogenous cytochrome *c*. The % oxidation rate was calculated with maximal oxidation rate as 100% and rate of oxidation by control mitochondria (no treatment) as 0%. Cytochrome oxidase activity was strongly sensitive to ionic strength, so control and maximal oxidation rates were determined for each salt concentration tested. The actual numerical values of control, Bax-tBid treated and maximal cytochrome *c* oxidation rates at 10 and 90mM KCl are presented (Fig 5.1A) for comparison.

Adenylate kinase (AK) assay

The assay was performed as described previously (31). This assay measures the release of the 24kDa protein, adenylate kinase, from the IMS of mitochondria. In this coupled enzyme assay, NADP is reduced to form NADPH which has a strong absorbance at 340nm. (The oxidized form NADP does not have this absorbance). Prior to assaying,

2.5μL of a mix of Hexokinase/Glucose-6-Phosphate Dehydrogenase (5 units each) was incubated in 350μL AK buffer (5mM $MgSO_4$, 10mM glucose, 5mM ADP, 0.2mM NADP, 50mM Tris, and pH 7.5) to remove residual ATP. After 2-3 minute incubation, 150μL of mitochondrial supernatant was added to the AK buffer/enzyme mix, and absorption was measured for 5 minutes at 340nm. The initial linear slope of increase in absorption was taken as the rate of AK reaction. Since all other reaction components are in excess, the concentration of AK is the rate-limiting factor. Hence the rate of NADPH formation is a direct measure of amount of AK released from mitochondria. Maximal rate of NADPH formation, corresponding to 100% release of AK from mitochondria, was measured from the activity of supernatant from equivalent amount of hypotonically shocked mitochondria. The actual numerical values of AK activity used as control (0% AK activity or no release of AK), Bax-tBid treated and lysed (100% AK activity or complete release of AK) are presented in Fig 5.1B for comparison.

Sulfite oxidase (SOX) assay

SOX is a 120kDa IMS protein and its release from mitochondria was assayed as described (129). SOX reduces cytochrome *c* using sulfite as the electron donor. Prior to the assay, a one-to-one solution of 40mM Na_2SO_3 and 50mg/ml oxidized cytochrome *c* was made. Then 10μL of this solution (0.4mM Na_2SO_3 and 0.5mg oxidized cytochrome *c* final) was added to 500μL mitochondrial supernatant and the absorbance was quickly measured at 550nm for 5 minutes. Maximal release was measured from the activity of supernatant from equivalent amount of hypotonically shocked mitochondria. SOX activity was strongly sensitive to ionic strength. Hence, the supernatant was

supplemented with suitable amount of salt by dilution from stock salt solution to adjust the ionic strength. The actual numerical values of SOX activity used as control (0% SOX activity or no release of SOX), Bax-tBid treated and lysed (100% SOX activity or complete release of SOX) are presented in Fig 5.1C for comparison.

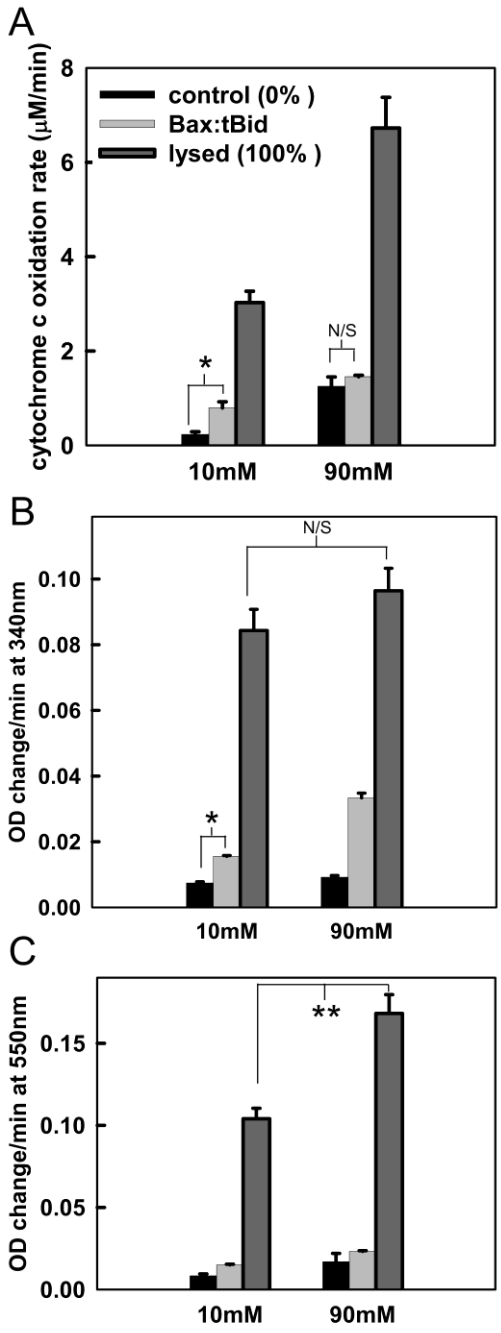

FIGURE 5.1: Measured rates of enzymatic activity in a set of experiments showing the rates prior to any treatment (control rates), the rates after tBid/Bax treatment, and the maximal rates after hypotonic shock. The influence of ionic strength on some of these rates is illustrated. By subtracting the control rates and expressing the results as a percentage of the maximal rates we correct for background rates and effects of ionic strength. The figure shows the rates of cytochrome *c* (25μM) oxidation (A), AK activity as measured by absorbance (OD) change at 340nm (B) and SOX activity as measured by absorbance change at 550nm (C) recorded from 96μg/mL mitochondrial suspensions

that were either untreated (control), or treated with 17nM Bax and 120nM tBid or osmotically lysed (lysed). Incubations (30 min) were in either 10 or 90mM KCl buffer. * represents P value < 0. 05 and ** represents P value < 0.01. n= 3.

Measurement of fumarase activity

Fumarase is a matrix enzyme that reversibly converts malate to fumarate. Fumarase release was measured by a standard procedure (130). Briefly 96μg/mL mitochondrial suspension in FH buffer was treated with varying concentrations of digitonin (from 0.0025% to 0.1% in multiples of 2) for 5 minutes at room temperature and centrifuged for 5 minutes at 14000 RCF and supernatant collected. 500μL of the supernatant was mixed with 500μL of fumarase assay buffer (50mM malate, 50mM Na_2HPO_4 pH 7.3) and change in absorbance measured for 5 minutes at 250nm in quartz cuvettes to measure formation of fumarate which shows strong absorbance at 250nm. Maximal fumarase release corresponding to 100% was obtained by treating equivalent amount of mitochondria with 0.2% Triton-X100.

Normalization of data

Normalization of data was performed for two reasons: 1) activity varied from one mitochondrial preparation to another; 2) the activity of some enzymes was sensitive to ionic strength. The latter was especially important because the relevant parameters sought were the degree of permeabilization of the outer membrane and the fractional release of a particular protein. By normalizing, the results obtained at different ionic strengths could be compared directly. Normalization involved subtracting the activity of untreated mitochondria (control) from the experimental value and dividing the difference

by the maximal activity after hypotonic shock (control subtracted) measured under the same conditions (e.g. the same ionic strength).

Statistics

The results are reported as means ± S.E. of at least 3 independent experiments. Significance was determined by Student's t-test. *, **, *** indicate significance with P values <0.05, <0.01, and <.001 resp. N/S indicates P values >0.05 and thus judged to be not significant.

RESULTS

Increase in ionic strength decreases real-time MOMP but the extent of IMS protein release increases

In isolated mitochondria, MOMP can be measured in 2 ways. Firstly, release of IMS proteins can be measured. This provides information on the minimum size of the MOMP pore and also the fraction of the population of mitochondria that have been permeabilized but does not define the status of the pore at any given time. The second method records the real-time flux of cytochrome *c* across the outer membrane by measuring the rate of oxidation of exogenously added cytochrome *c*. MOM is impermeable to cytochrome *c*. However, once the mitochondria are permeabilized with Bax, cytochrome *c* crosses the MOM, accesses the cytochrome oxidase complex in the inner membrane and becomes oxidized. The rate of oxidation is directly proportional to the extent of permeabilization i.e. the size of the MOMP pore and the number of pores in the mitochondrial population.

Both methods were used to observe the ability of Bax to permeabilize the outer membrane at different KCl concentrations. Protein release from the IMS was monitored by measuring the release of adenylate kinase (AK: 24kDa). Real-time permeabilization

was measured by measuring the rate of oxidation of exogenously added cytochrome *c*. Neither Bax alone (up to 50nM) nor tBid alone (up to 120nM) resulted in any significant MOMP by either assay method (Fig 5.2 A- B).

However, when mitochondria were incubated with Bax and tBid at either low salt (10mM KCl) or high salt (90mM KCl) buffer, permeabilization was achieved (Fig 5.3A and 5.2A – B). After treatment, a fraction of the mitochondrial suspension was assayed for cytochrome *c* oxidation; the remaining suspension was centrifuged and the supernatant was assayed for AK activity. At the lower KCl concentration (10mM) a substantial amount of both AK release and real-time permeabilization was observed. However, at the higher KCl concentration (90mM), the release of AK was comparable to (e.g. in Fig 5.3A) or sometimes more than that at low salt depending on the Bax concentration, but the extent of real-time permeabilization was always much lower (Fig 5.3A). The Real-time permeabilization decreased linearly with increase in [KCl]. (Fig 5.3B) This behavior is not specific to KCl but rather an ionic strength effect because substituting KCl with either NaCl or potassium lactobionate resulted in a similar decline in cytochrome *c* oxidation rate with increasing salt concentration during the Bax/tBid treatment (Fig 5.2C).

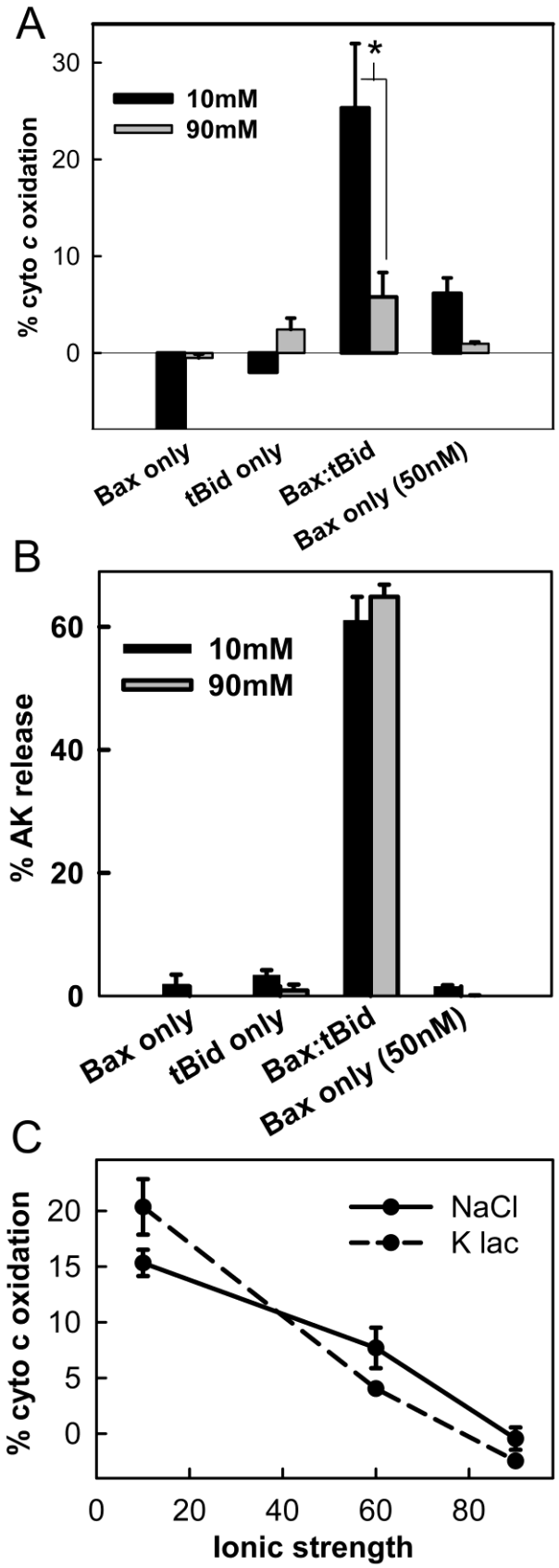

Figure 5.2: Control experiments and evidence of ionic strength dependence. A, B: Bax and tBid alone have little or no effect on MOMP. The rates of cytochrome *c* oxidation (A) or AK release (B) by 96μg/mL mitochondrial suspension are expressed as a percent of the maximal amount.Except as indicated, mitochondria were incubated for 30 min with 17nM Bax and/or 120nM tBid in the presence of either 10mM (black bars) or 90mM KCl (grey bars) buffer. C. The rates of cytochrome *c* oxidation (expressed as a % of the maximal values) induced by a 30 min incubation with 17nM Bax and 120nM tBid in the presence of varying concentrations of either NaCl (solid line) or potassium lactobionate (K lac, broken line). * represents P value < 0.05. n = 3.

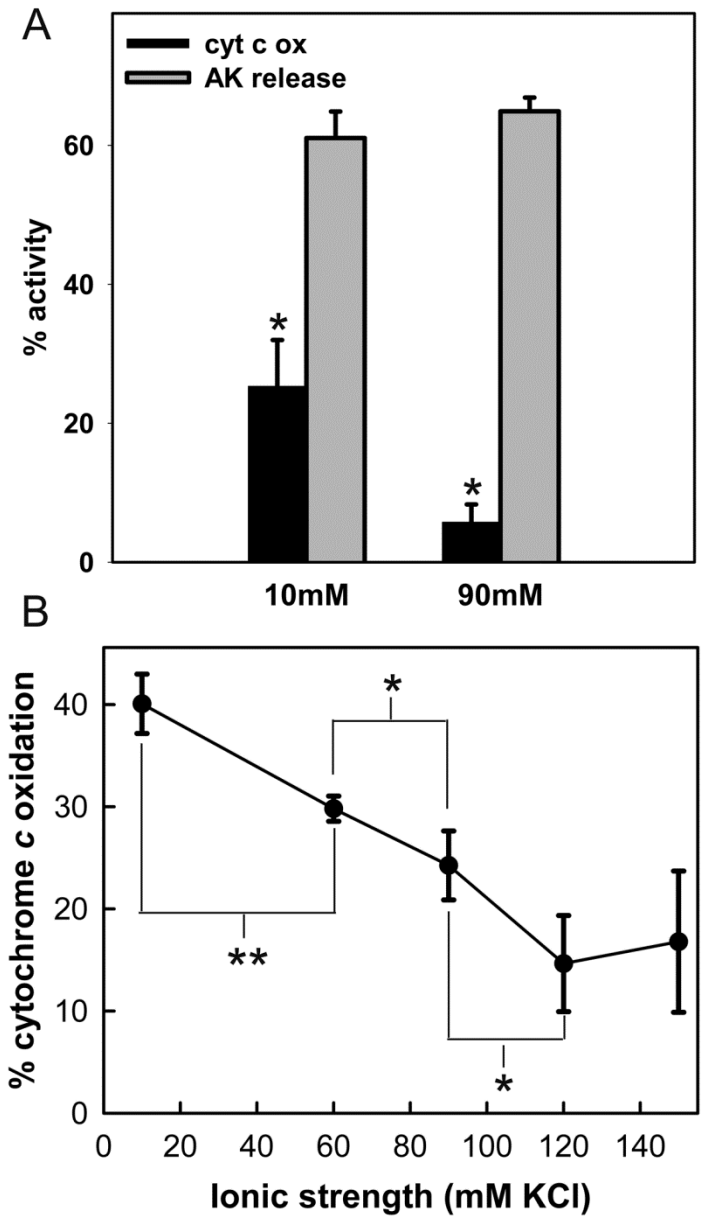

Figure 5.3: Increase in ionic strength inhibits real-time permeabilization by Bax without inhibiting IMS protein release. A. Mitochondrial suspension was treated with 17nM Bax and 120nM tBid at either 10mM or 90mM KCl buffer and rates of cytochrome *c* oxidation (black bar) and AK release (grey bar) were measured. The "*" refer to the statistically significant difference between the black bars. B. The measured rates of cytochrome *c* oxidation by mitochondria exposed to tBid/Bax at the indicated KCl concentrations. The results are means ± S.E. of 3 experiments.

In these experimental conditions, PTP did not influence MOMP as we found that CsA did not alter the rate of cytochrome *c* oxidation or AK release by Bax and tBid at either ionic strength (Fig 5.4).

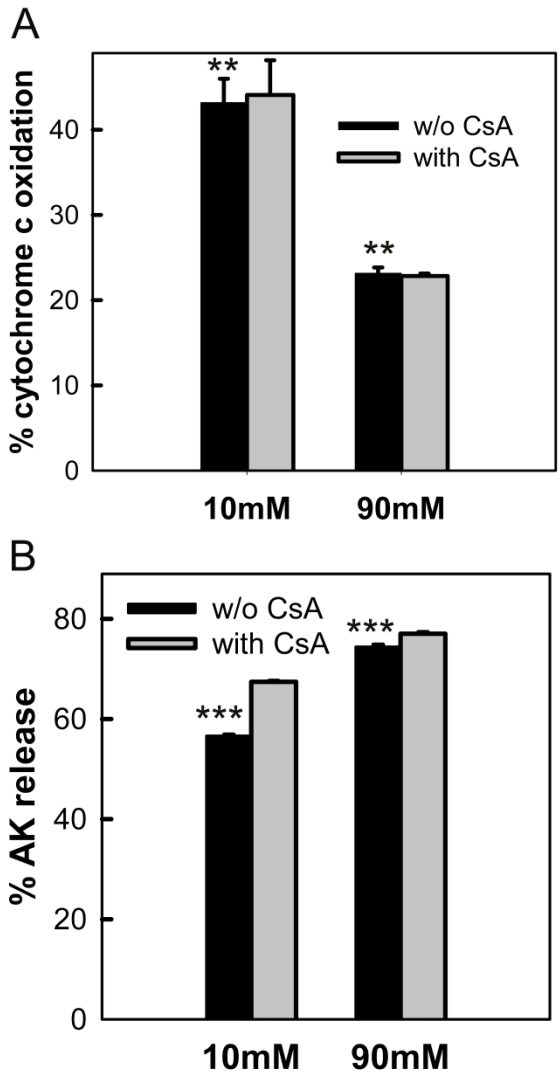

Figure 5.4: MOMP induced by Bax and tBid is independent of PTP. Mitochondria were incubated with 35nM Bax and 120nM tBid in the presence or absence of 50 μM CsA at either 10mM KCl or 90mM KCl for 30 minutes at 30°C. Then, the mitochondria from each treatment were assayed for real-time permeabilization using the cytochrome *c* oxidation assay and the supernatant analyzed for extent of AK release. The statistical tests are between the black bars in each panel. Both are significantly different ** P value < 0.01 and *** P value < 0.001. n = 3.

It was reported that tBid causes remodeling of the inner membrane and ionic strength could affect this process (131). This remodeling might explain the different rates of cytochrome *c* oxidation observed at different ionic strengths if restricted diffusion of cytochrome *c* between the cristae is rate limiting in our system and changed by the remodeling. To investigate if the cristae folds limit the cytochrome *c* oxidation rate, we compared the maximal rates of cytochrome *c* oxidation after osmotic lysis where swelling unfolds the cristae and MOM permeabilization with digitonin where the cristae structures remain intact at doses that do not permeabilize the inner membrane (131, 132). Under our conditions, 0.01% digitonin selectively permeabilized the MOM without releasing the matrix enzyme, fumarase (Fig 5.5A). Whether mitochondria were treated with digitonin or hypotonic shock, in the presence of 10 or 90mM KCl buffer, the rates of cytochrome *c* oxidation were not significantly different. In another set, mitochondria were pre-incubated for 30 minutes with tBid to allow remodeling of the inner membrane at either ionic strength and then treated with digitonin and similar oxidation rates were observed (Fig 5.5B). Thus any potential changes in the inner membrane due to changes in the ionic strength did not affect the rates of cytochrome *c* oxidation observed. The permeability of the outer membrane seems to be the rate-limiting factor in the oxidation of exogenous cytochrome *c* by mitochondria.

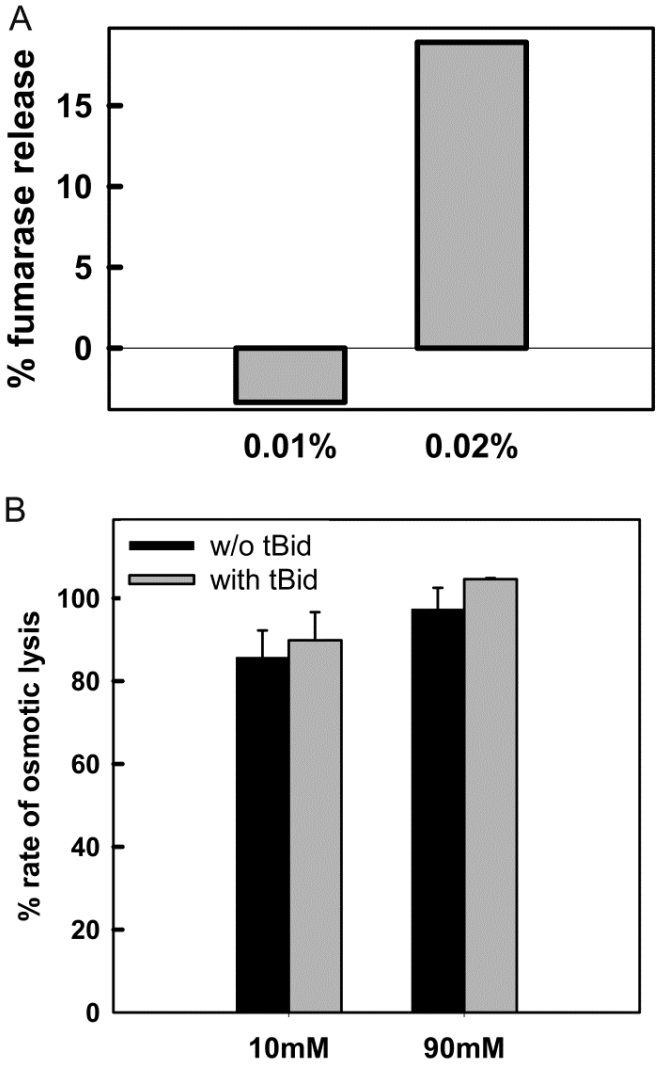

Figure 5.5: Comparison of maximal cytochrome *c* oxidation obtained under swelling and non-swelling conditions. A) At 0.01% digitonin, no activity of fumarase, a matrix enzyme, could be detected, but at 0.02% nearly 20% of fumarase was released from 96μg/mL mitochondrial suspension. B) 96μg/mL mitochondrial suspension was treated with 0.01% digitonin for 5 minutes either without tBid or after pre-incubation of the mitochondrial suspension with 120nM tBid for 30 minutes at 30oC at either ionic strength. Then, the mitochondrial suspension was assayed for the rate of cytochrome *c* oxidation. The mean values are the % of cytochrome *c* oxidation rate observed with an equivalent amount of osmotically lysed mitochondria at the corresponding ionic strengths. No

statistically significant difference was found between digitonin treated samples (with or without tBid) and osmotically lysed samples. (P values > 0.15). n = 3.

The different results obtained with the two methods of measurement of permeability (AK release and cytochrome *c* oxidation) could be explained in three ways:

1) Change in the energetics: The higher ionic strength makes the channels flicker, allowing release without much permeabilization.

2) Transient permeabilization: At the higher ionic strength the channels form for some time and then close resulting in restoration of a protein impermeable outer membrane.

3) Kinetic delay: Bax channel formation begins with small or flickering channels but with time these become larger and more stable. At high ionic strength this process is slow. Experiments were performed to distinguish among these possibilities.

MOMP induced at lower [KCl] is not reversed by increasing the salt concentration

One interpretation of the ionic strength effect is that Bax channels are in equilibrium between an open and a closed state and the ionic strength influences the position of the equilibrium. Perhaps the equilibrium favors the open state at low ionic strength and the closed at high ionic strength. To test this, Bax mediated MOMP was induced under low ionic strength (10mM KCl buffer) for 30 minutes by treating mitochondria with Bax and tBid. Under these conditions a significant level of MOMP was achieved. The permeabilized mitochondria were sedimented (14000RCF, 5min) and resuspended in higher ionic strength medium (90mM KCl buffer) and incubated for another 30 minutes. We found that after switching from low salt to high salt (90mM), the MOMP did not decrease but remained at the high value found at low salt (Fig 5.6). This demonstrates that the process is far from equilibrium. Thus ionic strength is not merely shifting a fast equilibrium between conducting states of Bax channels. Instead, once Bax channels

achieve a highly permeable state, that state is not reversible. Thus the first option is not correct. A time course of growth of real-time MOMP with Bax and tBid shows that the rate of permeabilization is monotonic. There is no indication of a transient permeabilization because at all times tested, the real-time permeability remained low at higher ionic strength. Thus the second option is incorrect. However, it is also clear that the permeabilization increases much faster at low salt than at high salt (Fig 5.7). Thus the difference between the two methods is partly explained by a difference in kinetics.

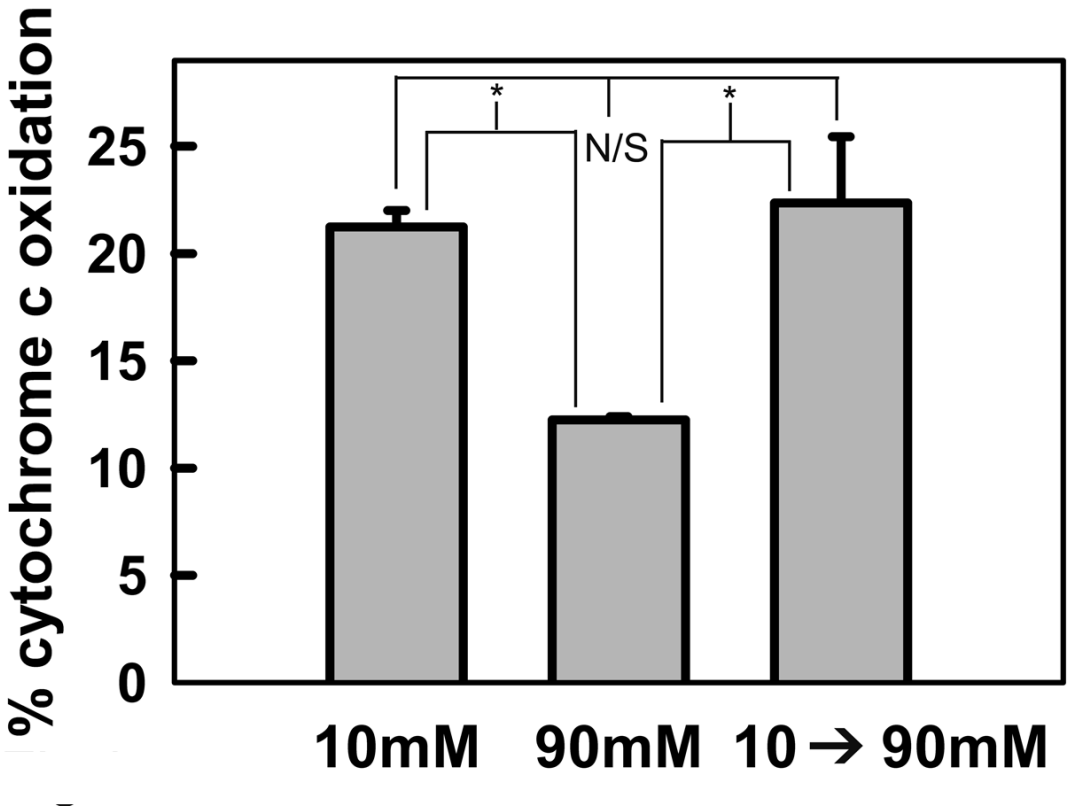

Figure 5.6: Bax permeability induced at lower ionic strength was not reversed by raising ionic strength. Mitochondrial suspensions were treated with 8nM Bax and 120nM tBid for 30 minutes at 30oC in either 10mM or 90mM KCl buffer. At the end of 30 minutes, the rate of cytochrome *c* oxidation by these mitochondria were determined. Simultaneously, the mitochondrial suspension incubated in 10mM KCl buffer was centrifuged and mitochondrial pellet resuspended in 90mM KCl buffer to raise the ionic strength. This suspension was incubated for 30 minutes at 30oC and at the end of the incubation, rate of cytochrome *c* oxidation measured. To correct for any loss of

mitochondria during centrifugation, control and lysed samples with equivalent amount of mitochondria were also treated in an identical manner and pellet resuspended in 90mM KCl buffer (control without Bax or tBid) or H2O (lysed) and rates measured. The results are means ± S.E. of 3 experiments.

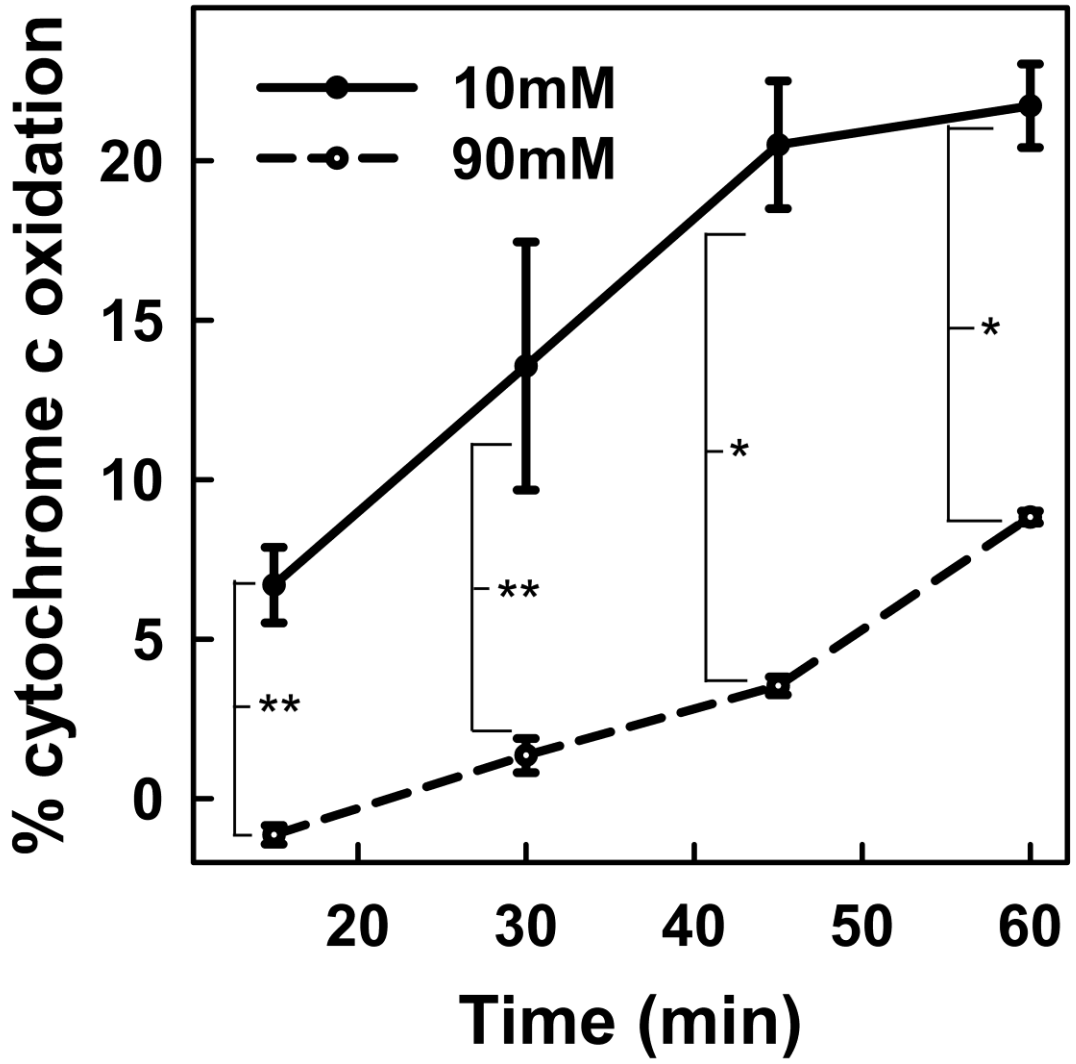

Figure 5.7: Bax induced MOMP increased at a faster rate at lower ionic strength. Mitochondrial suspensions were treated with 34nM monomeric Bax and 120nM tBid at 30°C at either 10mM KCl buffer (solid lines) or 90mM KCl buffer (dashed lines) and the rate of cytochrome *c* oxidation was determined at different time intervals. * represents P value < 0.05, ** - P value < 0.01. n = 3.

At high ionic strength, Bax forms smaller channels more rapidly

To better understand the kinetics of Bax channel formation, the Bax-induced release of AK (24kDa) and that of a larger protein sulfite oxidase (SOX: 120KDa) were measured as a function of time and ionic strength using different Bax concentrations (Fig. 5.8). At all Bax concentrations tested, the rate of release of AK was faster at 90mM than at 10mM KCl. At the smallest Bax concentration tested (8nM), the release of SOX lagged behind the release of AK at both salt concentrations (Fig 5.8A and B). Since the flux of proteins across the membrane through the Bax pore is not rate-limiting (see discussion), the increase in the amount of release corresponds to the formation of channels in more mitochondria. The kinetic delay between the release of AK and SOX suggests that the channels grow in size with time. At a higher Bax concentration (17nM), the rates of release of AK and SOX were identical for 10mM KCl but at 90mM, the release of AK was faster than release of SOX (Fig 5.8C and D). It must be noted again that the rate of AK release was higher with 90mM KCl than with 10mM KCl. At 34nM, with 90mM KCl, the amount of release of AK saturated at 30min indicating that essentially all the mitochondria were permeabilized but only about half of the channels were large enough to allow to flux of SOX. The release of SOX increased with time and by 60min 90% of the AK permeable mitochondria has channels large enough to release SOX, clearly indicating slow channel growth. In contrast, at 10mM KCl, the release of AK and SOX increased synchronously (Fig 5.8E and F) indicating slower channel formation but fast growth to a large size capable of releasing both proteins at the same time. Clearly both the initial permeabilization of mitochondria, as indicated by the AK release, and the growth of channels, as indicated by the % of permeabilized mitochondria that released

SOX, are augmented by increasing the Bax concentration. The extent of SOX release did not change very much comparing low and high salt but that can be explained by the conflicting effects of ionic strength: augmenting the formation of new channels and inhibiting their rate of growth.

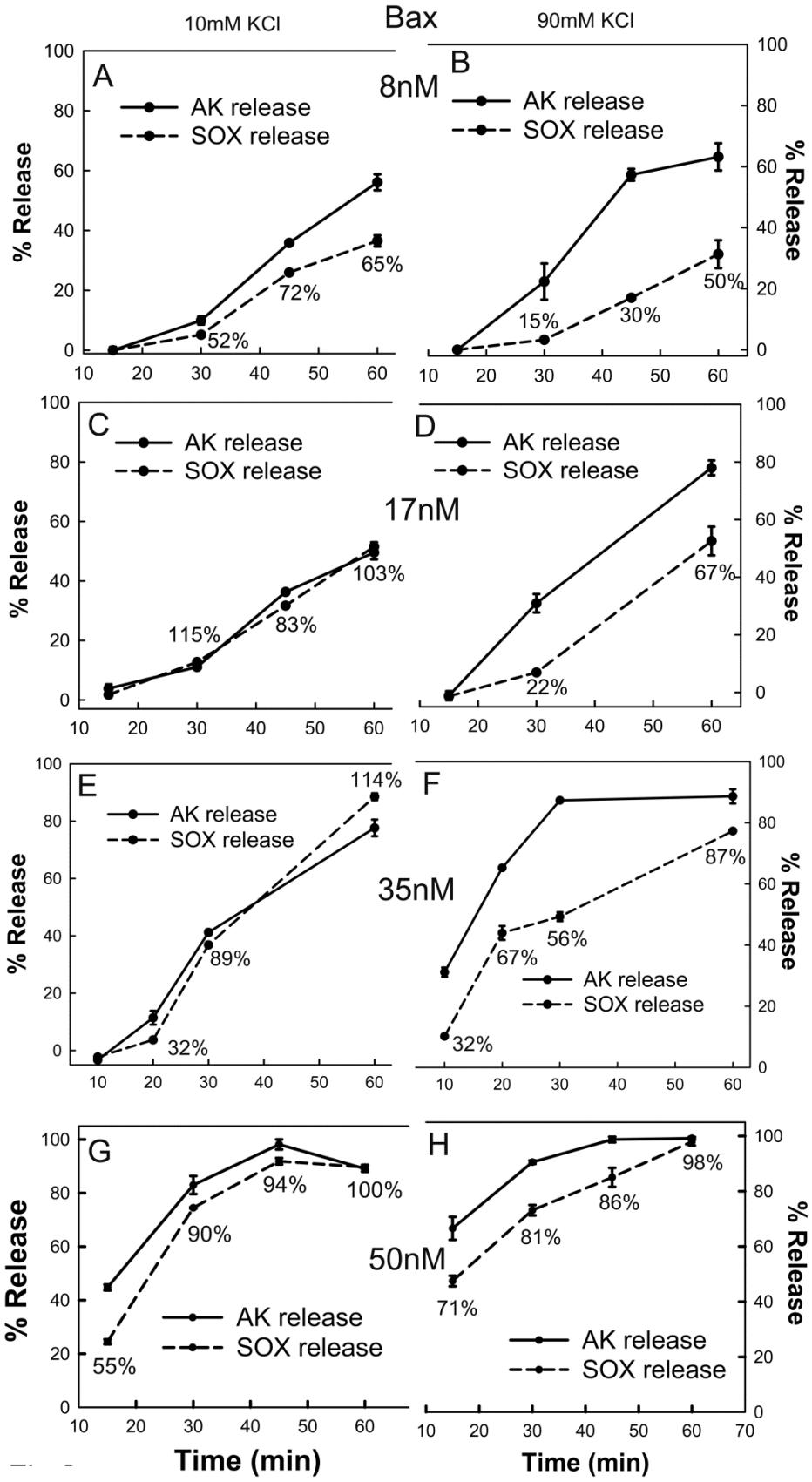

Figure 5.8: Bax channels expand in size with time but this expansion is slower at higher ionic strength. Mitochondrial suspensions were incubated in 10mM KCl buffer (A, C, E and G) or 90mM KCl buffer (B, D F and H) with 120nM tBid and either 8nM Bax (A and B) or 17nM Bax (C and D) or 34nM Bax (E and F) or 50nM Bax (G and H) for various time points at 30°C. Then the mitochondria were centrifuged and the supernatants were assayed for either AK release (solid lines) or SOX release (dashed lines). Percentage values next to SOX data indicate % of AK permeable mitochondria that have been permeabilized to SOX. Note that in some cases the error bars are smaller than the data point. The results are means ± S.E. of 3 experiments.

tBid does not alter the sensitivity of Bax induced MOMP to ionic strength

tBid is necessary for Bax to permeabilize the MOM. Thus, we hypothesized that the interaction between tBid and Bax may be sensitive to ionic strength i.e. changing the tBid concentration could change the sensitivity of Bax-induced MOMP to ionic strength. Increasing the level of tBid might enhance channel expansion at 90 mM. To test this, real-time MOMP induced by Bax was measured in either 10mM or 90mM KCl buffer at three different tBid concentrations (Fig 5.9)**.** The permeabilization did not change over a wide concentration range of tBid at either ionic strength. This is consistent with a catalytic function of tBid in initiating Bax mediated MOMP (20, 21) but not in the growth process. Thus the influence of ionic strength on MOMP is not due to an effect on tBid.

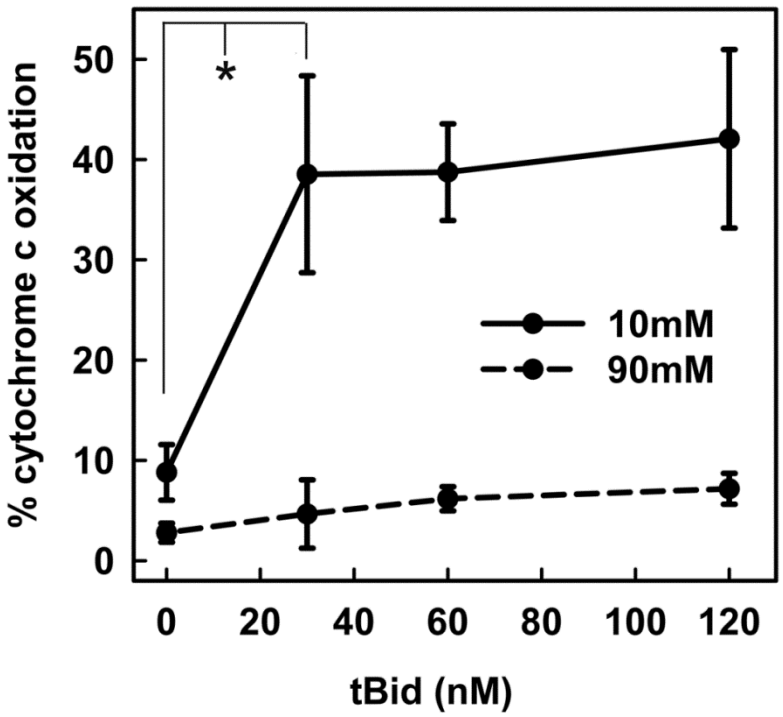

Figure 5.9: Ionic strength effect on Bax channel dynamics is not mediated by tBid. Mitochondrial suspensions were incubated in 10mM KCl buffer (solid line) or 90mM KCl buffer (dashed line) with 34nM Bax and varying concentrations of tBid (24, 60 and 120nM) for 30 minutes at 30°C. Then, the real-time permeability was determined by measuring the cytochrome *c* oxidation rate. There was no significant difference in cytochrome c oxidation rates between any treatments at 90mM KCl buffer. The results are means ± S.E. of 3 experiments.

Ionic strength affects Bcl-xL mediated inhibition of MOMP by Bax-tBid

Bcl-xL inhibits MOMP by multiple processes. We tested whether the inhibition of Bax mediated MOMP by Bcl-xL is also sensitive to ionic strength. We hypothesized that since decreasing the ionic strength resulted in more stable permeabilization (a pro-apoptotic effect), a higher ionic strength will facilitate Bcl-xL mediated MOMP inhibition. Consistent with this hypothesis, for a given amount of tBid and Bax, less Bcl-xL was needed to inhibit MOMP at 90mM KCl than at 10mM KCl (Fig 5.10). Unlike what was observed for the action of tBid on Bax, inhibition of MOMP by Bcl-xL changed with the tBid concentration (Fig 5.11). Presumably tBid reduced the amount of Bcl-xL available to interact with and inhibit Bax.

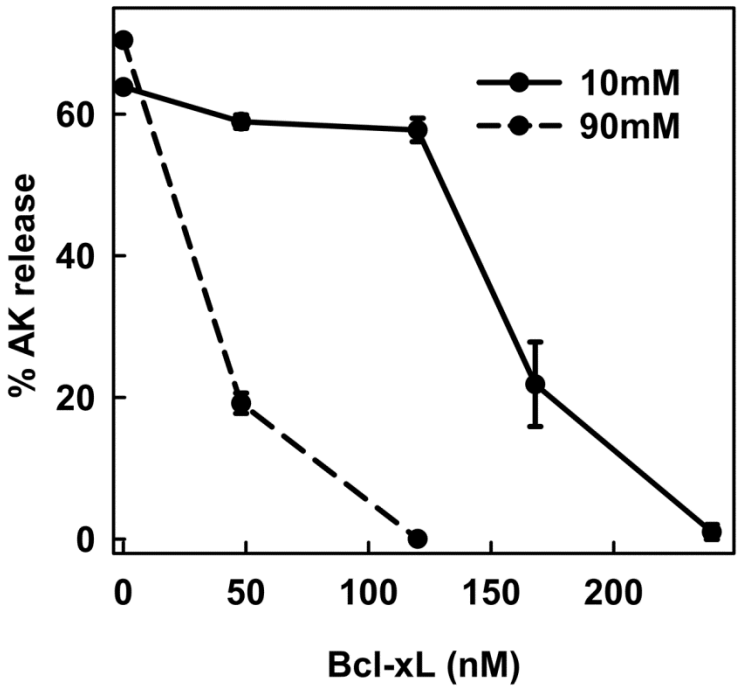

FIGURE 5.10: Increase in ionic strength increases the efficiency of Bcl-xL in inhibiting Bax mediated MOMP. Mitochondrial suspensions were incubated with 17nM Bax, 120nM tBid and varying concentrations of purified Bcl-xL (48, 120, 160 and 240nM) at either 10mM KCl buffer (solid line) or 90mM KCl buffer (dashed line) for 30 minutes at 30^{o}C. Then, the mitochondria were centrifuged and supernatant assayed for AK release. The results are means ± S.E. of 3 experiments.

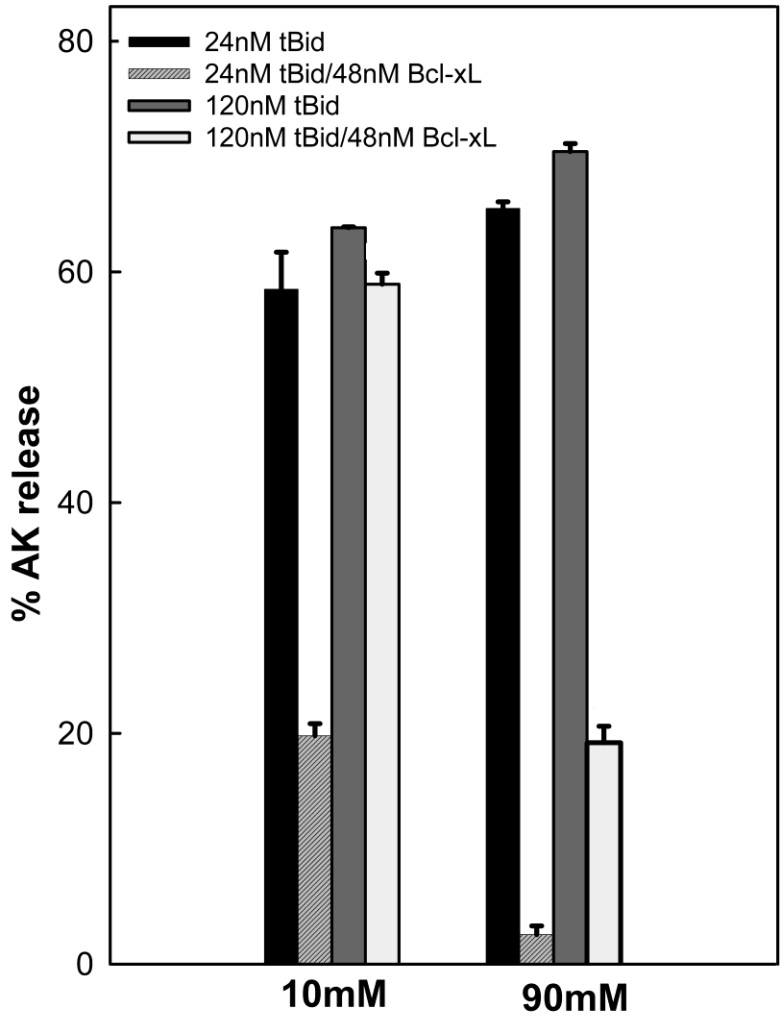

FIGURE 5.11: Bcl-xL mediated inhibition of MOMP is sensitive to tBid concentration. Mitochondrial suspensions were incubated with 17nM monomeric Bax, either 24nM or 120nM tBid, without Bcl-xL or with 48nM Bcl-xL in 10mM KCl buffer or 90mM KCl buffer for 30 minutes at 30^{o}C. Then, the extent of AK release was determined for the different treatments. The differences in the inhibitory effects of Bcl-xL at 10 and 90 mM were statistically significant with P<0.0001 at both tBid concentrations. n = 3.

Change in ionic strength has little effect on membrane insertion of Bax

It is possible that ionic strength could interfere with the extent of Bax insertion into the membrane causing differences in the degree of permeability. Our initial hypothesis was

that more Bax inserts into mitochondria at higher ionic strength causing more mitochondria to be permeabilized hence greater release of AK. To test this hypothesis, mitochondria were incubated with Bax and tBid and the amount of AK released was measured at 10, 20 and 30 minutes of incubation. We found that, although there was an almost 3 fold difference in the amount of AK released at 10 min between 10 and 90mM KCl, the amount of Bax inserted was about the same (Fig 5.12A, B).

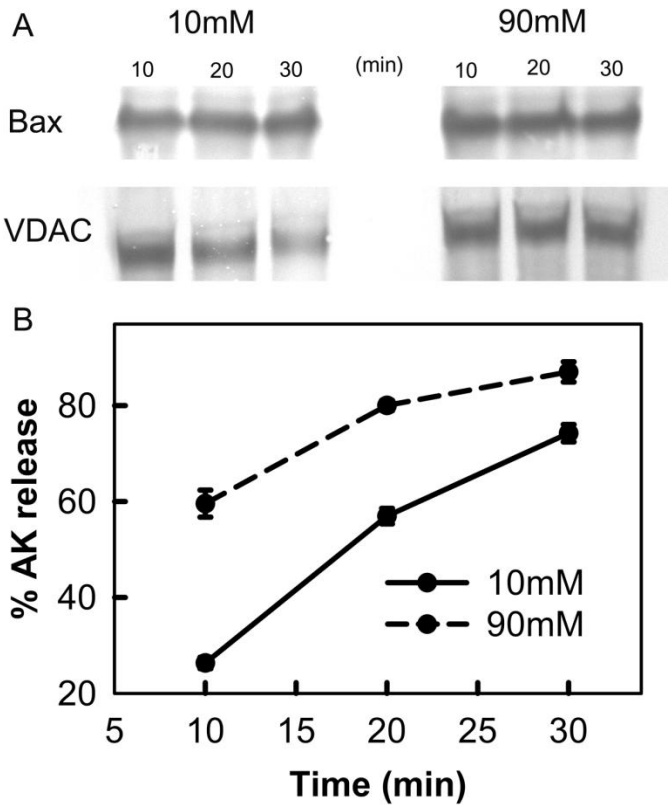

Figure 5.12: Bax insertion into mitochondrial outer membranes is not affected by ionic strength. A. Mitochondrial suspensions (960μg mitochondrial protein/mL) was treated with 50nM Bax and 240nM tBid for increasing amounts of time (10, 20 and 30 minutes) in either 10mM or 90mM KCl buffer. Then the mitochondria were centrifuged and supernatant assayed for AK release. The pellets were subjected to carbonate treatment and probed for Bax insertion by western blot. The carbonate treatment western blots were performed as described in the materials and methods section in the

supporting materials. VDAC served as loading control. B shows the extent of AK release at 10 (solid line) and 90mM KCl buffer (broken line) for each time point corresponding to A.

In our hands, Bax insertion was essentially complete by 10 minutes. Although there was no significant difference in the amount of Bax inserted across the time points tested, AK release increased with time (Fig 5.12B), indicating that new channel formation in more mitochondria continued with time. Thus ionic strength affected the channel formation process rather than Bax insertion. This is consistent with the observation made with purified Bak whose insertion into membranes is not affected by salt concentration (133). To test if ionic strength affected Bcl-xL mediated inhibition of Bax insertion into membranes, mitochondria were incubated with Bax and tBid with or without Bcl-xL. We found that Bcl-xL had little effect on Bax insertion although there was a complete inhibition of AK release (Fig 5.13). Therefore, under these conditions, Bcl-xL inhibits MOMP by interfering with Bax channel formation.

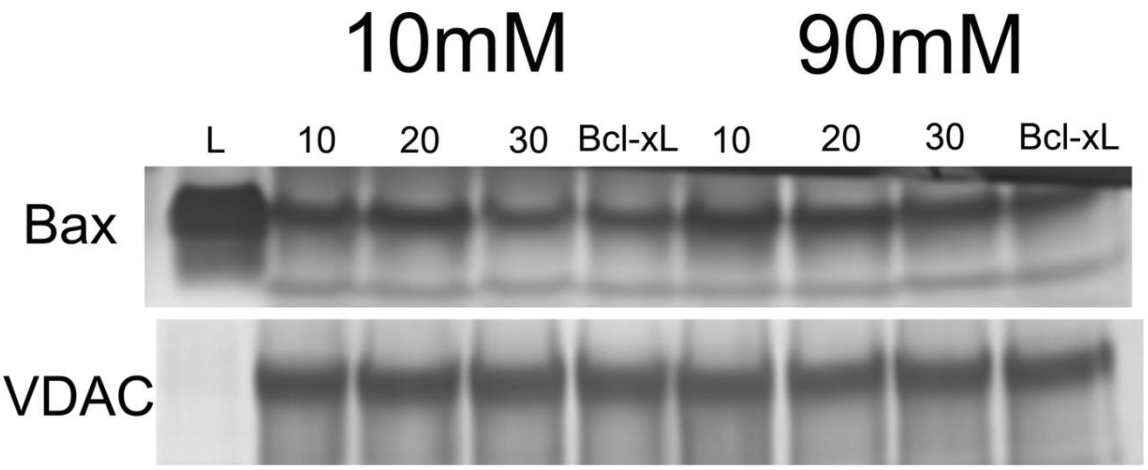

Figure 5.13: Bcl-xL inhibited Bax mediated MOMP without affecting Bax insertion. Mitochondrial suspensions (960μg mitochondrial protein/mL) were treated with 100nM Bax and 240nM tBid for 10, 20 and 30 minutes without Bcl-xL or with 100nM Bcl-xL (for 30 minutes only) in either 10mM KCl buffer or 90mM KCl buffer. The western blots were performed as described in Experimental

Procedures. VDAC served as loading control. Band L corresponds to 10% of the total Bax expected to be present if all the added Bax inserted into the mitochondrial outer membrane.

DISCUSSION

Bax activation and subsequent MOMP occur in multiple steps that are only partially understood. MOMP is a rapid and irreversible process and very stochastic in cell populations (78, 122 - 124). Thus, *in vitro* models have been used to gain insights into this process. Bax is a cytosolic monomeric protein in normal cells, but upon apoptotic induction, translocates to MOM, forms homo-oligomers and hetero-oligomers with Bak and some other proteins (134 – 137) and induces MOMP.

We show that increasing the ionic strength influences the size of the Bax channels, consequently leading to smaller channels.

In summary, our results are consistent with the following conclusions.

1. Bax insertion into MOM is fast and is followed by channel formation and then a slow growth in channel size.
2. The rate of formation of channels, as measured by the kinetics of AK release at different salt concentrations, is faster at higher salt concentration.
3. The rate of expansion of the size of the initial channels is faster at the lower salt concentration, as measured by comparing the kinetics of release of AK and SOX and the time course of growth of real-time MOMP.
4. This effect of salt concentration on the rate of growth of Bax channels explains the differences in the extent of real-time MOMP seen with the cytochrome *c* oxidation assay at different salt concentrations.
5. Increase in ionic strength also makes Bax mediated MOMP more sensitive to inhibition by Bcl-xL.

6. Ionic strength does not affect the insertion of Bax into membranes, suggesting that subsequent steps in channel formation are impeded by an elevated ionic strength.

Key to gaining insight into the dynamics of Bax channel formation and the influence of ionic strength on this dynamics is the measurement of outer membrane permeabilization in two ways: IMS protein release and the rate of cytochrome *c* oxidation. Because of the small volume of the intermembrane space and the long time scale of our experiments, once a channel is formed in one mitochondrion that is large enough to allow the translocation of a particular protein, e.g. AK, all the AK will be released from that mitochondrion within a few milliseconds. Thus the time-dependent release of AK or SOX from a population of mitochondria does not measure the rate of release from each individual mitochondrion but the rate of permeabilization of each of the mitochondria in the population. Thus partial release of AK signifies that only a portion of the mitochondrial population has Bax channels large enough to allow AK release. A difference in the extent of release of AK and SOX in the population means that some mitochondria have channels that are too small to release SOX but are large enough to release AK. It is important to note that release of AK and SOX is independent of ionic strength (138 - 140) hence these proteins may be more suitable for measuring MOMP than cytochrome *c* release. Cytochrome *c*, being a charged protein, binds membranes, especially the inner membrane of mitochondria that is rich in cardiolipin and a separate dissociation step is necessary to facilitate cytochrome *c* release apart from pore formation (138, 140). Thus, assessing permeabilization of the outer membrane becomes more complicated if measuring cytochrome *c* release.

A change in ionic strength is not a very specific tool and thus other possible effects of ionic strength that may influence MOMP were examined. Over a wide concentration range of tBid, the sensitivity to ionic strength did not change suggesting that the interaction between tBid and Bax is not affected by changes in ionic strength. tBid has been reported to remodel cristae in a PTP dependent manner (131) releasing loosely bound IMS proteins from inner membrane into the IMS. Given the catalytic rather than stoichiometric nature of tBid in facilitating Bax mediated MOMP (20, 21) and that Bax mediated cytochrome *c* oxidation rate did not change with tBid at either ionic strength, this is consistent with a model in which the effect of ionic strength is directly on the ability of Bax to form channels in the MOM rather than on the structure of the inner membrane. The inner membrane remodeling induced by tBid was inhibitable by CsA (131) but, in our hands, the exogenous cytochrome *c* oxidation induced by Bax-tBid at either ionic strength was independent of the presence of CsA. This is consistent with other reports (141 - 144) that found MOMP induced by Bax and tBid to be independent of PTP (Fig 5.4).

These observations strongly signify that the cytochrome *c* oxidation rates observed after Bax-tBid treatment are limited by MOM permeability rather than other effects on the structure of inner membrane. Though we do not rule out that changes are caused to the inner membrane by tBid under our conditions, these changes do not affect the interpretation of MOM permeability from the cytochrome *c* oxidation assay. Thus, the rate of oxidation of exogenously-added reduced cytochrome *c* measures the actual permeability of the MOM at any time (real-time permeabilization) and depends on the number of channels and the size of channels present. But it does not distinguish between

many small channels spread out among many mitochondria or a few large channels in just a few mitochondria. Thus each type of assay measures different properties of the permeabilizing pore. By combining the results obtained from the three assays (AK release, SOX release and cytochrome *c* oxidation) one obtains a good picture of the nature of the permeabilization of the MOM.

At low ionic strength, there is general congruency between the permeability measurements (cytochrome *c* oxidation rates) and the amount of protein release but nevertheless the % permeabilization is quite a bit smaller (half in Fig. 5.3A) that the % AK release. Fig. 5.8 shows that at this level of Bax, the release of AK and SOX are the same. Thus the Bax channels are large enough to release SOX but not large enough not to limit the rate of cytochrome *c* oxidation. To allow SOX release the Bax pore must be greater than 3.3 nm in radius. Simple calculations show that such a pore would limit cytochrome *c* translocation rates under the conditions of our experiments. Electron microscopy of Bax channels formed in liposomes show that Bax channel can reach much larger sizes (61, 88) and under those conditions they would certainly not be rate limiting. Thus channel growth requires time both at low and high ionic strength and this is also seen at 8 nM Bax (Fig. 5.8 A and B) when comparing the release of AK and SOX. The quicker release of AK at higher salt suggests that the initial pore formation by Bax is faster at higher ionic strength. However, the release of SOX showed a greater time lag for release at higher ionic strength. This indicates that the Bax channels start out small and grow in size and the expansion is delayed by increasing ionic strength. Thus, the Bax channel-forming process seems to consist of two stages: initial formation of channels capable of releasing AK (stimulated by high ionic strength) and growth of channels

(inhibited by high ionic strength). The small channels limit the rate of cytochrome *c* oxidation resulting in low real-time permeabilization and thus low oxidation rates.

Kluck *et al.* first observed a dichotomy between extent of IMS protein release and real-time permeabilization in mitochondria treated with Bax or tBid (51). The apparent paradoxical finding that the extent of MOMP depended on the technique used to make the measurement is resolved by the experiments reported in this manuscript. MOMP measurement is complicated by the growth in Bax channel size and the marker of permeabilization is influenced by channel size. For protein release to happen, a small pore or a pore with brief open time is sufficient. This is because, after a threshold channel size, protein release is essentially independent of channel size. And since protein diffusion across the MOM is quick (a few milliseconds) compared to the duration of the experiment (order of minutes), all the protein from the IMS will be released as soon as a channel opens in a mitochondrion. But for the real-time flux of cytochrome *c* across the MOM, the pores need to have longer open times. Also, the size of the channel is a critical determinant of the rate of cytochrome *c* flux. In other words, a bigger channel can allow greater flux of cytochrome *c*. Indeed, a detectable cytochrome *c* oxidation rate may involve simultaneous flux of many cytochrome *c* molecules across the membrane. Thus, in spite of cytochrome *c* being smaller than AK, the fractional rates of cytochrome *c* oxidation are lower than the fractional release of AK. This also means that the sensitivity of AK release assay to pore formation is much greater than the cytochrome *c* oxidation assay. But the limitations of the release assays, particularly their independence on channel size and inability to measure real-time changes in the behavior of the channel

require the information from the real-time cytochrome *c* oxidation assay for a more complete understanding of the MOMP pore.

We find that the real-time permeability induced by Bax and tBid increases with time and is influenced by ionic strength. Larger channels formed at lower ionic strength allow greater flux of exogenous cytochrome *c* causing its faster rate of oxidation. A high rate of cytochrome *c* oxidation does not imply unphysiologically high channel sizes as we found that such permeabilities happened when release of AK or SOX was submaximal. In cells, release of most IMS proteins is rapid and complete (78). It is an all-or-none event (78, 122- 124). Thus one can conclude that large channels are present *in vivo* and these have been observed in reconstituted systems (51, 88). We found that Bcl-xL was essentially ineffective at preventing Bax insertion even at concentrations of Bcl-2 proteins when MOMP was completely inhibited. Thus, in the experimental conditions and concentrations of Bcl-2 proteins we used, Bcl-xL may be acting at the level of Bax channel formation. Such an experimental setting provides a platform to study the mechanics of Bax channel assembly downstream of Bax insertion into membranes.

CONCLUSION

In summary, we have identified that decreasing ionic strength results in the formation of large channels that allow high flux rates of cytochrome *c* and synchronously release both small and large proteins. High ionic strength favors the initial formation of small channels and these develop more slowly into the larger structures that were observed much sooner at low ionic strength. Higher ionic strength also increases the sensitivity of Bax mediated MOMP to inhibition by Bcl-xL. Ionic strength can be used as a diagnostic tool to dissect the different steps in Bax mediated MOMP.

Note: Undergraduate honors student Timothy Walsh and fellow graduate student Kai-Ti Chang also contributed to this work. Kai-Ti helped with the purification of the recombinant proteins and Tim helped to perform the enzymatic assays.

CHAPTER 6 GENERAL DISCUSSION AND FUTURE DIRECTIONS

Simplifying the science: The what, why and how

The complexity of cellular processes necessitates both a reductionist approach to mechanistically understand the function of each molecule in the process and a holistic approach to understand how the process occurs by the interplay of these molecules. Either approach presents its own pros and cons. The scientist is constantly required to integrate the insights gained from each approach to develop a comprehensive understanding of the process in study.

A recurring theme of this dissertation has been to understand the structural regulation of molecular assemblies in the reductionist systems of mitochondria, planar membranes and liposomes. Purified mitochondria are simpler than whole cells in that mitochondria are free from the cellular transcription/translation and degradation machinery that can change the concentrations of proteins, among other variables. Planar membranes/liposomes are even simpler and more isolated than mitochondria in that the membrane composition is very well-defined and devoid of any proteins other than the protein of interest. These systems provide an opportunity to study the structural interaction between the constituents whose amounts can be specifically defined, under controlled membrane compositions.

In this chapter, the insights obtained from these studies are discussed in the context of our present knowledge of apoptosis and MOMP from the literature.

This research dissertation has dealt with transport pathways formed in mitochondria that could allow protein flux across the MOM during apoptosis. Specifically, two such pathways have been investigated in detail.

1. Ceramide channels
2. Bax channels

Ceramide and Bax: Till death do them apart

In the first part (chapter 3), the structural regulation of ceramide channels by activated Bax was examined. There is strong evidence in the literature that ceramide and Bcl-2 family proteins interact at multiple levels. At a metabolic level, Bak is necessary to elevate the activity of ceramide synthase to produce ceramide (145). Anti-apoptotic proteins Bcl-2 and Bcl-xL inhibit the synthesis of ceramide. (47 – 49). On a structural level, mitochondrial ceramide and Bax co-localize in the mitochondrial outer membrane upstream of the MOMP resulting in Bax translocation and activation (22, 25, 26, and 46). Based on this observation, it is concluded that ceramide in MOM can activate Bax. Our results with yeast mitochondria and planar membrane indicate that Bax and ceramide interact directly to induce MOMP. More recent work (146) has identified key functional groups of the ceramide molecule that determine the ability of ceramide to interact with Bax. This suggests that the interaction between ceramide and Bax shows molecular specificity and hence is evolutionarily conserved. The exact role of ceramide in the MOM during apoptosis in the physiological context is still debated. Ceramide has been ascribed a predominantly second messenger role in various cellular processes. In the plasma membrane, it is known to form lipid rafts facilitating cell signaling. While the possibility

of ceramide channels being the platform for the Bax interaction is strong (82, 146, and 147), formation of macro-domains of ceramide where Bax co-localizes has also been found (29). Our work further elucidates the cross-talk between ceramide and Bax, suggesting structural mechanisms.

Traditionally, the molecular mechanism of Bcl-xL mediated inhibition of MOMP has been assumed to be entirely mediated by direct and indirect inhibition of Bax activation by the BH3 only proteins, some of which directly activate Bax while some others sequester anti-apoptotic proteins. However, studies with mutants of Bcl-xL that do not bind to any Bcl-2 family proteins (50) which would be expected to not affect permeabilization, still inhibit MOMP, suggesting that additional levels of regulation exist by which Bcl-xL can inhibit MOMP. The effect of Bcl-xL on the ceramide channel (33, 146) qualifies as an additional regulatory step. The interplay between ceramide and Bcl-2 proteins in the highly simplified systems of mitochondria and planar membranes is indeed compelling in that direct molecular interactions between ceramide and the Bcl-2 family proteins are very much possible and hence merit further investigation in the physiological context. A review summarizing our current knowledge of the interaction between Bcl-2 family proteins and ceramide channels was published in the journal, FEBS letters. (147).

Ceramide channel structure: The wonder of structures

In the second part (chapter 4), various analogs of ceramide, representing different modifications in the functional groups of the ceramide molecule, were investigated for their effect on the ability of ceramide to form channels. Ceramide is a unique molecule

with an amide bond. The removal of the C4-C5 trans double bond completely alters the biological function of the resulting dihydroceramide molecule. Ceramide is also at the hub of a complex metabolic pathway that regulates the inter-conversion of sphingolipids into one another. This metabolism must be finely regulated as each sphingolipid has functions strikingly different from their neighbors in the metabolic cross-roads. Various enzymes that metabolize sphingolipids show a great structural specificity. Our results indicate that the structural specificity also operates in the structural stability of the ceramide channel. The insights gained from this study could be used to develop analogs of ceramide that can more potently induce MOMP and can be used as cancer therapeutics. These studies, in light of the ability of Bcl-2 family proteins to regulate ceramide channels (33, 82, 146), indicate that the evolutionary selection pressure that generated and maintains the structure of ceramide is influenced by the need to participate in the onset of apoptosis. The right properties and interactions must be maintained to ensure that apoptosis occurs only when the appropriate conditions are present in the cell. A paper summarizing the ability of different analogs of ceramide to form channels was published in the journal BBA – Bio membranes (148).

Probing Bax channel dynamics with ionic strength: Expanding the *in vitro* inventory

In the last part (chapter 5), the dynamics of Bax channel formation was investigated using ionic strength as a tool. In this study, the ability of higher ionic strength to influence the rate of Bax channel formation was exploited to follow the gradual expansion of Bax channels in real-time. To our knowledge, this is the first study to document the formation and growth of Bax mediated permeabilization of the mitochondria in real-time. Activated Bax can form heterogeneous-sized channels in planar membranes (55). Attempts have

also been made to estimate the stoichiometry of Bax in the channel structure (149) but the estimated numbers have been very different and ambiguous. Our results show that Bax does not form discrete sized channels but rather a continuum and the rate of growth is strongly dependent on experimental conditions of ionic strength. The translocation of Bax from the cytosol to the MOM is fairly well studied but the events subsequent to the insertion leading to the MOMP and the nature of the Bax channel are only partially understood. While *in vitro* studies have strongly established that Bax is a channel former and capable of permeabilizing membranes, there are significant disparities between Bax-induced MOMP *in vitro* and the MOMP seen *in vivo*. For example, *in vitro*, no real-time permeabilization as measured by the bidirectional flux of exogenous cytochrome *c* was detected with Bax (51). But the MOMP that occurs *in vivo* emphatically enables bi-directional flux of proteins across the MOM (78). Our results indicate that this disparity can be resolved by changing the ionic strength of the incubation medium. Obviously, the inhibitory effect of ionic strength seen *in vitro* is overcome *in vivo*. Identifying the molecular components that counteract this inhibitory effect can provide further clues into the process of Bax channel formation. *In vivo*, there is a considerable time gap between Bax translocation to the MOM and the induction of permeabilization (57, 58, 120, 123, 124). *In vitro*, Bax insertion into membranes correlates with the onset of MOMP. Additional signals apart from those that cause Bax translocation are necessary to induce the conformational changes in Bax associated with MOMP (57, 58). Hunting for those missing links provides an interesting line of future research to produce a more comprehensive picture of MOMP. MOMP, being a rapid and stochastic process, has defied any mechanistic investigation in cells and *in vivo*. Thus, *in vitro* tools have been

very effective in understanding MOMP step-by-step. However, the success of *in vitro* models lies in the knowledge of all the factors that influence the process and in the availability of tools to control each one of them precisely. In ionic strength lies one such tool. Keeping this in mind, we have developed ionic strength as a diagnostic to control Bax mediated MOMP in a controlled fashion. Ionic strength can be altered to control the rate of growth of Bax channels real-time.

A few cents for the future: Bequeathing a fortune in science

The complexity of biological systems entails that the researcher must approach his research question from different directions and cross-check the inferences drawn from one line of investigation by different methods. It is also important to have an open mind to accept the need to change the paradigms as more insights are gained. Equally important is the determination to make a constant effort to integrate the results of each line of investigation, howsoever small, into the context of the bigger picture. Indeed, these smaller forays into science provide the finer details that complete the big picture. As with any scientist, it is my earnest hope that this dissertation has added a finer stroke to the picture of apoptosis. I further hope that this effort will open newer avenues of exploration into one of nature's most inspiring exercises, integrating death into life.

References

1. S. Fulda, and Debatin, K.M. 2006. Intrisinc versus extrinsic apoptosis pathways in anticancer chemotherapy. Oncogene. 25:4798-4811.
2. Feng, P., Liang, C., Shin, Y.C., Xiaofie, E., zhang, W., Gravel, R., Wu, T., Sun, R., E. Usherwood, and J.u. Jung. 2007. A novel inhibitory mechanism of mitochondrion-mediated apoptosis by a herpesviral protein. PLoS Pathogens. 3:e174.
3. Blomgran, R., Desvignes, L., V. Briken, and J.D. Ernest. 2012. Mycobacterium tuberculosis inhibits neutrophil apoptosis, leading to delayed activation of naive CD4 T cells. Cell Host Microbe. 11:81 – 90.
4. Miller, J.L., Velmurugan, K., M.J. Cowan, and V. Briken. 2010. The type I NADH dehydrogenase of Mycobacterium tuberculosis counters phagosomal NOX2 activity to inhibit TNF-alpha-mediated host cell apoptosis. PLoS Pathogens. 6: e1000864.
5. Galluzzi, L., Brenner, C., Morselli, E., Z. Touat, and G. Kroemer. 2008. Viral control of mitochondrial apoptosis. PLoS Pathogens. 4: e10000018.
6. D.R. Green and G. Kroemer. 2009. Cytoplasmic functions of p53. Nature. 458: 1127 – 1130.
7. Mohamed, Y. H., H. Gong, and T. Amemiya. 2003. Role of apoptosis in eyelid development. Exp. Eye Res. 76: 115 – 123.
8. Krammer, P.H., R. Arnold, and I.N. Lavrik. 2007. Life and Death in peripheral T cells. 7: 532- 542.

9. R. Youle, and M. Karbowski. Mitochondrial fission in apoptosis. 2005. Nature Rev. Mol. Cell biol. Trends Cell Biol. 6: 657 – 663.

10. Cerveny, K.L., Tamura, Y., Zhang, Z., R.E. Jensen, and H. Sesaki. Regulation of mitochondrial fusion and division. Trends in Cell Biol. 17: 563 – 569.

11. B. Westermann. Mitochondrial fusion and fission in cell life and death. Nature Rev. Mol. Cell Biol. 11: 872 – 884.

12. J. E. Chipuk, and D. R. Green. 2008. How do BCL-2 proteins induce mitochondrial outer membrane permeabilization? Trends Cell Biol.18:157-164.

13. A. Antignani, and R. J. Youle. 2006. How do Bax and Bak lead to permeabilization of the outer mitochondrial membrane? Curr. Opin. Cell Biol.18:685-689.

14. Spierings, D., McStay, G., Saleh, M., Bender, C., Chipuk, J., U. Maurer, U and D. R. Green. 2005. Connected to death: the (unexpurgated) mitochondrial pathway of apoptosis. Science 310:66-67.

15. Cheng, E.H., Sheiko, T. V., Fisher, J. K, W. J. Craigen, and S.J. Korsmeyer. 2003. VDAC2 inhibits Bak activation and mitochondrial apoptosis. Science. 301: 513-517.

16. Llambi, F., Moldoveanu, T., Tait, S.W., Bouchier-Hayes, L., Temirov, J., McCormick, L.L., C. P. Dillon, and D. R. Green. 2011. A unified model of mammalian BCL-2 protein family interactions at the mitochondria. Mol. Cell 44:517-531.

17. Sheridan, C., Delivani, P., S. P. Cullen, and S.J. Martin. 2008. Bax- or Bak-induced mitochondrial fission can be uncoupled from cytochrome *c* release. Mol. Cell. 31: 570 – 585.

18. Suzuki, M., R. J. Youle, and N. Tjandra. 2000. Structure of Bax: Co-regulation of dimmer formation and intracellular localization. Cell. 103: 645-54.

19. Y.T. Hsu and R. J. Youle. 1997. Non-ionic detergents induce dimerization among members of the Bcl-2 family. J. Biol. Chem. 272:13829-13834.

20. Bleicken, S., Classen, M., Padmavathi, P.V., Ishikawa, T., Zeth, K., H. J. Steinhoff, and E. Bordignon. 2010. Molecular details of bax activation, oligomerization, and membrane insertion. J. Biol. Chem. 285:6636-6647.

21. Lovell, J.F., Billen, L.P., Bindner, S., Shamas-Din, A., Fradin, C., B. Leber, and D. W. Andrews. 2008. Membrane binding by tBid initiates an ordered series of events culminating in membrane permeabilization by bax. Cell 135:1074-1084.

22. Y. A. Hannun, and L.M. Obeid. 2008 Principles of bioactive lipid signaling: lessons from sphingolipids. Nat. Rev. Mol. Cell Biol. 9: 139-150.

23. Pettus, B. J., C. E. Chalfant CE, and Y. A. Hannun 2002. Ceramide in apoptosis: An overview and current perspectives. Biochim. Biophys. Acta. 1585: 114-125.

24. L. J. Siskind 2005. Mitochondrial ceramide and induction of apoptosis. J. Bioenerg. Biomembr. 37:143-153.

25. Kashkar, H., Weigmann, K., Yazdanpannah, P., D. Haubert, and M. Kronke. 2005. Acid sphinomyelinase is indispensable for UV-light induced Bax conformational change at the mitochondrial membrane. J. Biol. Chem. 280: 20804-13.

26. Dai, Q., Liu, J., Chen, J., Durrant, D., T.M. McIntyre, and R. M. Lee. 2004. Mitochondrial ceramide increases in UV-irradiated HeLa cells and is mainly derived from hydrolysis of sphingomyelin. Oncogene. 23: 3650-58.

27. Ardail, D., Maalouf, M., Boivin, A., Chaipet, O., Bodennec, J., R. Rousson, and C. Rodriguez-Lafrasse. 2009. Diversity and complexity of ceramide generation after exposure of jurkat leukemia cells to irradiation. Int. J. Radiat. Oncol. Biol. Phys. 73: 1211-18.

28. Birbes, H., Luberto, C., Hsu, Y. T., El Bawab, S., Y. A. Hannun, and L.M. Obeid. 2005. A mitochondrial pool of ceramide is involved in TNF-a induced Bax translocation to mitochondria. biochem. J. 386: 441 - 451.

29. Lee, H., Rotolo, J.A., Mesicek, J., Penate-Medina, T., Rimmer, A., Liao, W.C., Yin, X., Raghupathi, G., Ehleiter, D., Gulbins, E., Zhai, D., Reed, J.C., Haimovitz-Friendman, A., Z. Fuks, and R. Kolesnik. 2011. Mitochondrial ceramide-rich macrodomains functionalize Bax upon irradiation. PLoS One. 6:e19783.

30. L. J. Siskind, and M. Colombini. 2000. The lipids C2 and C16 ceramide form large, stable channels. Implications for apoptosis. J. Biol. Chem. 275: 38640-38644.

31. L. J. Siskind, R. N. Kolesnick, and M. Colombini. 2002. Ceramide channels increase the permeability of the mitochondrial outer membrane to small proteins. J. Biol. Chem. 277: 26796-26803.

32. Siskind, L. J., Davoody, N., Lewin, S., S. Marshall, and M. colombini. 2002. Enlargement and contracture of C2- ceramide channels. Biophys. J. 85:1860-1875.

33. Siskind, L.J., Feinstein, L., Yu, T., Davis, J.S., Jones, D., Choi, J., Zuckerman, J. E., Tan, W., Hill, R. B., J.M. Hardwick and M. Colombini. 2008. Anti-apoptotic Bcl-2 proteins disassemble ceramide channels. J. Biol. Chem. 283:6622-6630.

34. Bionda, C., Portoukalian, J., Schmitt, D., C. Rodriguez-Lafrasse, and D. Ardail. 2004. Subcellular compartmentalization of ceramide metabolism, MAM and/or mitochondria? Biochem. J. 382:527-533.

35. El Bawab, S., Roddy, P., T. Qian, Bielawska, A., Lemasters, J. J. and Y. A. Hannun. 2000. Molecular cloning and characterization of a human mitochondrial ceramidase. J. Biol. Chem. 275: 21508-21513.

36. Siskind, L. J., Fluss, S., M. Bui and M. Colombini. 2005. Sphingosine forms channels in membranes that differ greatly from that of ceramide. J. bioenerg. Biomembr. 27:227-236.

37. Stiban, J., L. Caputo, and M. colombini. 2008. Ceramide synthesis in the endoplasmic reticulum can permeabilize mitochondria to pro-apoptotic proteins. J. Lipid Res. 49:773-780.

38. Stiban, J., D. Fistere Jr and colombini, M. 2006. Dihydroceramide hinders ceramide channel formation. Implications for apoptosis. Apoptosis. 11:773-780.

39. Erlick, M. J., S. Fluss, and M. Colombini. 2006. Sphingosine, a product of dihydroceramide synthesis by ceramidase, influences the formation of ceramide channels. Biophys. J. 99:1749 – 1756.

40. Charles, A.G., Han, T.Y., Liu, Y.Y., Hansen, N., A. E. Giuliano, and M. C. Cabot, 2001. Taxol-induced ceramide generation and apoptosis in human breast cancer cells. Cancer Chemother. Pharmacol. 47: 444-50.

41. Kroesen, B. J., Pettus, B., Luberto, C., Busman, M., Sietsma, H., L. De Leij, and Y. A. Hannun. 2001. Induction of apoptosis through B-cell receptor cross-linking occurs via de novo generated C16-ceramide and involves mitochondria. J. Biol. Chem. 276: 13606-13614.

42. Rodriguez-Lafrasse, C., Alphonse, G., Broquet, P., Aloy, M.T., P. Louisot, and R. Rousson. 2001. Temporal relationships between ceramide production, caspase activation and mitochondrial dysfunction in cell lines with varying sensitivity to anti-Fas-induced apoptosis. Biochem. J. 357: 407-416

43. Thomas, R. L., Matsko, C.M., M. T. Lotze, and A. A. Amoscato, 1999. Mass spectrometric identification of increased C16 ceramide levels during apoptosis. J. Biol. Chem. 274: 30580-30588.

44. Dai, Q., Liu, J., Chen, J., Durrant, D., T. M. McIntyre, and R. M. Lee. 2004. Mitochondrial ceramide increases in UV-irradiated HeLa cells and is mainly derived from hydrolysis of sphingomyelin. Oncogene. 23: 3650-58.

45. Di Paola, M., Zaccagnino, P., Montedoro, G., T. Cocco, and M. Lorusso. 2004. Ceramide induces release of pro-apoptotic proteins from mitochondria by either a Ca2+ dependent or a Ca2+ independent mechanism. J. Bioenerg. Biomembr. 36:165-170.

46. Birbes, H., El Bawab, S., Y. A. Hannun, and L.M. Obeid. 2001. Selective hydrolysis of a mitochondrial pool of sphingomyelin induces apoptosis. FASEB. J. 15: 2669-79.

47. Sawada, M., Nakashima, S., Banno, Y., Yamakawa, H., Takenaka, K., Shinoda, J., Nishimura, Y., N. Sakai, and Y. Nozawa. 2000. Influence of Bax or Bcl-2 overexpression on the ceramide dependent apoptotic pathway in glioma cells. Oncogene. 19:3508 – 3520.

48. Kawatani, M., Uchi, M., Shimizu, S., H. Osada, and M. Imoto. 2003. Transmembrane domain of Bcl-2 is required for inhibition of ceramide synthesis, but not cytochrome *c* release in the pathway of inostamycin-induced apoptosis. Exp. Cell Res. 286:57-66.

49. Okamoto, Y., L.M. Obeid, and Hannun, Y. 2002. Bcl-xL interrupts oxidative activation of neutral sphingomyelinase. FEBS Lett. 350:104-108.

50. Billen, L.P., Kokoski, C.L., Lovell, J.F., B. Leber, and D. W. Andrews. 2008. Bcl-XL inhibits membrane permeabilization by competing with Bax. PLoS Biol. 6, e147.

51. Kluck, R.M., Esposti, M.D., Perkins, G., Renken, C., Kuwana, T., Bossy-Wetzel, E., Goldberg, M., Allen, T., Barber, M.J., D. R. Green, and D. D. Newmeyer. 1999. The pro-apoptotic proteins, Bid and Bax, cause a limited

permeabilization of the mitochondrial outer membrane that is enhanced by cytosol. J. Cell Biol. 147, 809-22.

52. Jürgensmeier, J.M., Xie, Z., Deveraux, Q., Ellerby, L., D. Bredesen, D. and J. C. Reed. 1998. Bax directly induces release of cytochrome *c* from isolated mitochondria. Proc Natl Acad Sci U S A. 95, 4997-5002.

53. Dejean, L.M., Martinez-Caballero, S., Guo, L., Hughes, C., Teijido, O., Ducret, T., Ichas, F., Korsmeyer, S.J., Antonsson, B., E. A. Jonas, and K. W. Kinnally. 2005. Oligomeric Bax is a component of the putative cytochrome *c* release channel MAC, mitochondrial apoptosis-induced channel. Mol. Biol. Cell 16:2424-2432.

54. Heimlich, G., McKinnon, A.D., Bernardo, K., Brdiczka, D., Reed, J.C., Kain, R., M. Krönke, and J.M. Jürgensmeier. 2004. Bax-induced cytochrome *c* release from mitochondria depends on alpha-helices-5 and -6. Biochem. J.378:247-255.

55. Lin, S. H., Perera, M. N., Nguyen, T., Datskovskiy, D., M. Miles, and M. colombini. 2011. Bax forms two types of channels one of which is voltage-gated. Biophys. J. 101:2163-2169.

56. Schlesinger PH, Gross A, Yin XM, Yamamoto K, Saito M., G. Waksman, and S. J. Korsmeyer. 1997. Comparison of the ion channel characteristics of proapoptotic BAX and antiapoptotic BCL-2. Proc Natl Acad Sci U. S. A 94: 11357-11362.

57. Upton, J.P., Valentijn, A.J., L. Zhang, and A. P. Gilmore. 2007. The N-terminal conformation of Bax regulates cell commitment to apoptosis. Cell Death Differ. 14: 932-42.

58. Owens, T.W., Valentijn, A.J., Upton, J.P., Keeble, J., Zhang, L., Lindsay, J., N. K. Zouq, and A. P. Gilmore. 2009. Apoptosis commitment and activation of mitochondrial Bax during anoikis is regulated by p38MAPK. Cell Death Differ. 16: 1551-62.

59. Parsons, D. F., G.R. Williams, and B. Chance. 1996. Characteristics of isolated and purified preparations of the outer and inner membranes of mitochondria Ann. N. Y. Acad. Sci. 137 : 643–666.

60. Basanez, G., Zhang, J., Chau, B.N., Maksaev, G.I., Frolov, V.A., Brandt, T.A., Burch, J., J. M. Hardwick, and J. Zimmerberg. 2001. Pro-apoptotic cleavage products of Bcl-xL form cytochrome *c* conducting pores in pure lipid membranes. J. Biol. Chem. 276:31083-31091.

61. Kuwana, T., Mackey, M. R., Perkins, G., Ellisman, M. H., Latterich, M., Schneiter, R., D. R. Green, and D.D. Newmeyer. 2000. Bid, Bax and lipids cooperate to form supramolecular openings in the mitochondrial outer membrane. Cell 111:331–342.

62. Thuduppathy, G.R., Terrones, O., Craig, J.W., G. Basanez, and R. B. Hill. 2006. The N-terminal domain of Bcl-xL reversibly binds membranes in a pH dependent manner. Biochemistry 45:14533-14542.

63. L. Zhou, D. Chang D. 2006 Dynamics and structure of the Bax-Bak complex responsible for releasing mitochondrial proteins during apoptosis. J Cell Sci 121: 2186-2196.

64. Roucou X., Rostovtseva T., Monessuit S., J. C. Martinou, and B. Antonsson. 2002. Bid induces cytochrome *c*-impermeable Bax channels in liposomes. Biochem. J 363: 547-552.

65. Guihard, G., Bellot G., Moreau, C., Pradal, G., Ferry, N., Thomy, R., Fichet, P., K. Meflah, and F. M. Valette. 2004. The mitochondrial apoptosis-induced channel (MAC) corresponds to a late apoptotic event. J Biol. Chem. 279: 46542-46550.

66. B. Antonsson. 2004. Mitochondria and the Bcl-2 family proteins in apoptosis signaling pathways. (2004). Mol Cell Biochem. 256-257: 141-155.

67. Antonsson, B., Conti, F., Ciavatta, A., Montessuit, S,, Lewis, S., Martinou, I., Bernasconi, L., Bernard, A., Mermod, J.J., Mazzei, G., Maundrell, K., Gambale, F., R. Sadoul, and J. C. Martinou. 1997. Inhibition of Bax channel-forming activity by Bcl-2. Science 277: 370-372.

68. Roucou, X., Rostovtseva, T., Monessuit S., J. C. Martinou, B. Antonsson. 2002. Bid induces cytochrome *c*-impermeable Bax channels in liposomes. Biochem. J 363: 547-552.

69. Yang, Z., Khoury, C., G. Jean-Baptise, and M. T. Greenwood 2006. Identification of mouse sphingomyelin synthase 1 as a suppressor of Bax-mediated cell death in yeast. FEMS Yeast Res 6: 751-762.

70. Neise, D., Graupner, V., Gillissen, B. F., Daniel, P.T., Schulze-Osthoff , K., R. U. Janicke, and F. Essmann. 2008. Activation of the mitochondrial death pathway is commonly mediated by a preferential engagement of Bak. Oncogene 27: 1387-1396.

71. Von Haefen, C., Wieder, T., Gillissen, B., Stärck, L., Graupner, V., B. Dorken, and P.T. Daniel. 2002 Ceramide induces mitochondrial activation and apoptosis via a Bax-dependent pathway in human carcinoma cells. Oncogene 21: 4009-4019.

72. Lee, A.C., Xu, X., Blachly-Dyson, E., M. Forte, and M. Colombini. 1998. The role of yeast VDAC genes on the permeability of the mitochondrial outer membrane. J Membr. Biol. 161: 173-181.

73. Lucken-Ardjomande, S., S. Montessuit, and J.C. Martinou. 2008. Bax activation and stress induced apoptosis delayed by the accumulation of cholesterol in mitochondrial membranes. Cell Death Differ. 15: 484-493.

74. M. Colombini. 1987. Characterization of channels isolated from plant mitochondria. Methods Enzymol 148: 465-475.

75. Ivashyna, O., Garcia-Saez, A.J., Ries, J., Christenson, E.T., P. Schwille, and P. Schlesinger. 2009. Detergent-activated Bax protein is a monomer. J. Biol. Chem. 284:23935–23946.

76. Cartron, P.F., Bellot, G., Oliver, L., Grandier-Vazielle, X., S. Mannon, and F. Vallette. 2008. Bax inserts into mitochondrial outer membrane by different mechanisms. FEBS Lett. 582: 3045-3051.

77. Lazano, J., Menendez, S., Morales, D., Ehletier, D., Liao, W.C., Wagman, R., Haimovitz-Friendman, A., Z. Fuks, and R. Kolesnick. 2001. Cell autonomous apoptosis defects in acid sphingomyelinase knockout fibroblasts. J. Biol. Chem. 276: 442-448.

78. Munoz-Pinedo, C., Guio-Carrion, A., Goldstein, J.C., Fitzgerald, P., D.D. Newmeyer and D. R. Green. 2006. Different intermembrane space proteins are released from mitochondria in a manner that is coordinately initiated but can vary in duration. Proc Natl Acad Sci USA 103:11573–11578.

79. Siskind, L.J., R. N. Kolesnick, and M. Colombini. 2006. Ceramide forms channels in mitochondrial outer membranes at physiologically relevant concentrations. Mitochondrion 6:118–125.

80. Garcia-Suez, C., Colell, A., Mari, M., A. Morales, J.C. Fernandez-Checa. 1997. Direct effect of ceramide on the mitochondrial electron transport chain leads to generation of reactive oxygen species. Role of mitochondrial glutathione. J. Biol. Chem. 272:11369 – 11377.

81. Rodrigues-Lafrasse, C., Alphonse, G., Aloy, M.T., Ardail, D., Gerard, J.P., P. Louisot and R. Rousson. 2002. Increasing endogenous ceramide using inhibitors of sphingolipid metabolism maximizes ionizing radiation-induced mitochondrial injury and apoptotic cell killing. Int. J. Cancer 101:589-598.

82. Ganesan, V., Meenu, N.P., Colombini, D., Datskovskiy, D., K. Chadha and M. Colombini. 2010. Ceramide and activated Bax act synergistically to permeabilize the mitochondrial outer membrane. Apoptosis. 15:553-562.

83. Samanta, S., Stiban, J., T.K. Maugel, and M. Colombini. 2011. Visualization of ceramide channels by transmission electron microscopy Biochim. Biophys. Acta, 1808: 1196–1201.

84. B. Bechninger. 1997. Structure and functions of channel-forming peptides: magainins, cecropins, melittin and alamethicin. J. Membr. Biol. 156: 197–211.

85. M.S.P. Sansom. 1998. Peptides and lipid bilayers: dynamic interactions. Curr. Opin. Colloid Interface Sci. 3:518–524.

86. Qian, S., Wang, W., L. Yang, and H.W. Huang. 2008. Structure of transmembrane pore induced by Bax derived peptide: evidence for lipidic pores. Proc. Natl. Acad. Sci. U. S. A. 105:17375–17383.

87. Basanez, G., Sharpe, J.C., Galanes, J., Brandt, T.B., J.M. Hardwick, and J. Zimmerberg. 2002. Bax type pro-apoptotic proteins porate lipid bilayers through a mechanism sensitive to intrinsic monolayer curvature. J. Biol. Chem. 277:49360–49366.

88. Schafer, B., Quispe, J., Choudhary, V., Chipuk, J.E., Ajero, T.G., Du, H., R. Schneiter, and T. Kuwana. 2009. Mitochondrial outer membrane proteins assist Bid in Bax-mediated lipidic pore formation. Mol. Biol. Cell. 20:2276–2285.

89. Blicher, A., Wodzinska, K., Fidorra, M., M. Winterhalter, and T. Heimburg. 2009. The temperature dependence of lipid membrane permeability, its quantized nature, and the influence of anesthetics. Biophys. J. 96: 4581–4591.

90. Anishkin, A., S. Sukharev, and M. Colombini. 2006. Searching for the molecular arrangement of the ceramide channels. Biophys. J. 90:2414–2426.

91. Usta, J., El-Bawab, S., Szulc, Z.M., Y.A. Hannun, and A. Bielawska. 2001. Structural requirements of ceramide and sphingosine based inhibitors of mitochondrial ceramidase. Biochemistry 40:9657–9668.

92. Chalfant, C.E., Szulc, Z.M., Roddy, P., A. Bielawska, and Y.A. Hannun. 2003. The structural requirements for ceramide activation of serine-threonine protein phosphatases. J. Lipid Res., 45:496–506.

93. Karasavvas, N., Erukulla, R.K., Bittman, R., R. Lockshin, and Z. Zakeri. 1996. Stereospecific induction of apoptosis in U937 cells by N-octanoylsphingosine stereoisomers and N-octylsphingosine. The ceramide amide group is not required for apoptosis. Eur. J. Biochem., 236:729–737.

94. Chun, J., Li, G., H.-S. Byun, and R. Bittman. 2002. Synthesis of new trans double bond sphingolipid analogues: Δ4,6 and Δ6 ceramides. J. Org. Chem. 67:2600–2605.

95. He, L., H.-S. Byun, and R. Bittman. 2000. Stereoselective preparation of ceramide and its skeleton backbone modified analogues via cyclic thionocarbonate intermediates derived by catalytic asymmetric dihydroxylation of alpha, beta-unsaturated ester precursors. J. Org. Chem. 65:7627–7633.

96. Brockman, H.L., Momsen, M.M., Brown, R.E., He, L., Chun, J., H.-S. Byun, and R. Bittman. 2004. The 4,5-double bond of ceramide regulates its dipole potential, elastic properties, and packing behavior. Biophys. J. 87: 1722–1731.

97. He, L., H.-S. Byun, and R. Bittman. 2000. A stereocontrolled, efficient synthetic route to bioactive sphingolipids: synthesis of phytosphingosine and

phytoceramides from unsaturated ester precursors via cyclic sulfate intermediates. J. Org. Chem. 65: 7618–7626.

98. Chun, J., Byun, H.S., G. Arthur, and R. Bittman. 2003. Synthesis and growth inhibitory activity of chiral 5-hydroxy 2-N-acyl-(3E)-sphingenines. Ceramides with unusual sphingoid backbones. J. Org. Chem. 68: 355–359.

99. Bielawski, J., Szulc, Z.M., Y.A. Hannun, and A. Bielawska. 2006. Simultaneous quantitative analysis of bioactive sphingolipids by high performance liquid chromatography-tandem mass spectrometry. Methods. 39:82–91.

100. Bielawski, J., Pierce, J.S., Snider, J., Rembiesa, B., Z.M. Szulc, and A. Bielawska. 2009. Comprehensive quantitative analysis of bioactive sphingolipids by high-performance liquid chromatography-tandem mass spectrometry. Hum. Meth. 579:443–467.

101. M. Montal, and P. Mueller. 1972. Formation of bimolecular membranes from lipid monolayers and study of their electrical properties. Proc. Natl. Acad. Sci. U. S. A., 69:3561–3566.

102. R. Bittman. 2009. Synthetic lipids as bioactive molecules: roles in regulation of cell function. T.P. Begley (Ed.), Wiley Encyclopedia of Chemical Biology, 4Wiley & Sons Inc., New Jersey. 480–504.

103. Pruett, S.T., Bushnev, A., Hagedorn, K., Adiga, M., Haynes, C.A., Sullards, M.C., D.C. Liotta, and A.H. Merrill Jr. 2008. Biodiversity of sphingoid bases (“sphingosines”) and related amino alcohols. J. Lipid Res. 49:1621–1639.

104. P. Megha, P., Sawatzki, T., R. Kolter, and E. Bittman. 2007. Effect of ceramide N-acyl chain and polar headgroup structure on the properties of ordered lipid domains (lipid rafts). Biochim. Biophys. Acta. 1768:2205–2212.

105. Menuz, V., Howell, K.S., Gentina, S., Epstein, S., Riezman, I., Fornallaz-Mulhauser, S., Hengarner, M.O., Gomez, M., H. Riezman, and J.C. Martinou. 2009. Protection of C. elegans from hypoxia by HYL-2 ceramide synthase. Science. 324:381–384.

106. K. Venkataraman, k., C. Reibeling, C., J. Bodennec, J., H. Riezman, H., J.C. Allegood, J.C., M.C. Sullards, M.C., A.H. Merrill Jr., and A.H. Futerman. 2002. Upstream of growth and differentiation factor 1 (uog1), a mammalian homolog of the yeast longevity assurance gene 1 (LAG1), regulates N-stearoyl-sphinganine (C18-(dihydro)ceramide) synthesis in a fumonisin B1-independent manner in mammalian cells. J. Biol. Chem. 277:35642–35649.

107. Mizutani, Y., A. Kihara, and Y. Igarashi. 2006. Mammalian Lass6 and its related family members regulate synthesis of specific ceramides. Biochem. J. 390: 263–271.

108. Laviad, E.L., Albee, L., Pankova-Kholmyansky, I., Epstein, S., Park, H., A.H. Merrill Jr., and A.H. Futerman. 2008. Characterization of ceramide synthase 2: tissue distribution, substrate specificity, and inhibition by sphingosine-1-phosphate. J. Biol. Chem. 283:5677-5683.

109. El Bawab, S., Usta, J., Roddy, P., Szulc, Z.M., A. Bielawska, and Y.A. Hannun. 2002. Substrate specificity of Rat brain ceramidase. J. Lipid Res. 43:141-148.

110. Wijesinghe, D., Masiello, A., Subramanian, P., Szulc, Z.M., A. Bielawska, and C.E. Chalfant. 2005. Substrate specificity of human ceramide kinase. J. Lipid Res. 46:2706 – 2716.

111. Philips, S.C., Triola, G., Fabrias, G., Goni, F.M., D.B. Dupre, and M.C. Yappert. 2009. Cis vs trans ceramides: effects of the double bond on conformation and H bond interactions. J. Phys. Chem. B. 113: 15249–15255.

112. Reed, J.C., J.M. Jurgensmeier, and S. Matsuyama. 1998. Bcl-2 family proteins and mitochondria. Biochim. Biophys. Acta 1366:127-137.

113. Gross, A., J. M. McDonnell, and S. J. Korsmeyer. 1999. BCL-2 family members and the mitochondria in apoptosis. Genes Dev. 13:1899-1911.

114. Petros, A.M., E. T. Olejniczak, and S. W. Fesik. 2004. Structural biology of the Bcl-2 family of proteins. Biochim. Biophys. Acta 1644:83-94.

115. Shamas-Din, A., Brahmbhatt, H., B. Leber, and D. W. Andrews. 2011. BH3-only proteins: orchestrators of apoptosis. Biochim. Biophys. Acta 1813:508-520.

116. Korsmeyer, S.J., Wei, M.C., Saito, M., Weiler, S., K. J. Oh, and P.H. Schlesinger. 2000. Pro-apoptotic cascade activates BID, which oligomerizes BAK or BAX into pores that result in the release of cytochrome *c*. Cell Death Differ. 7:1166-1173.

117. Antonsson, B., Montessuit, S., Lauper, S., R. Eskes, and J. C. Martinou. 2000. Bax oligomerization is required for channel-forming activity in liposomes and to trigger cytochrome *c* release from mitochondria. Biochem. J.345:271-278.

118. Eskes, R., Desagher, S., B. Antonsson, and J. C. Martinou. 2000. Bid induces the oligomerization and insertion of Bax into the outer mitochondrial membrane. Mol. Cell Biol.20:929-935.

119. Gavathiotis, E., Suzuki, M., Davis, M.L., Pitter, K., Bird, G.H., Katz, S.G., Tu, H.C., Kim, H., Cheng, E.H., N. Tjandra, and L. D. Walensky. 2008. Bax activation is initiated at a novel interaction site. Nature 455:1076-1081.

120. Valentijn, A.J., Upton, J.P., N. Bates and A. P. Gilmore. 2008. Bax targeting to mitochondria occurs via both tail anchor dependent and independent mechanisms. Cell Death Differ.15:1243-1254.

121. Zhou, H., Hou, Q., J. L. Hansen, and Y. T. Hsu. Complete activation of Bax by a single site mutation. Oncogene 26:7092-7102.

122. Goldstein, J.C., Muñoz-Pinedo, C., Ricci, J.E., Adams, S.R., Kelekar, A., Schuler, M., R. Y. Tsien, and D. R. Green. 2005. Cytochrome *c* is released in a single step during apoptosis. Cell Death Differ. 12:453-462.

123. Bhola, P.D., and S. M. Simon. 2009. Determinism and divergence of apoptosis susceptibility in mammalian cells. J. Cell Sci.122:4296-4302.

124. Bhola, P.D., A. L. Mattheyses and S.M. Simon. 2009. Spatial and temporal dynamics of mitochondrial membrane permeability waves during apoptosis. Biophys. J.97:2222-2231.

125. Christenson, E., Merlin, S., M. Saito, and P. H. Schlesinger. 2008. Cholesterol effects on bax pore activation. J. Mol. Biol. 381:1168-1183.

126. Montessuit, S., Somasekharan, S.P., Terrones, O., Lucken-Ardjomande, S., Herzig, S., Schwarzenbacher, R., Manstein, D.J., Bossy-Wetzel, E., Basañez,

G., P. Meda and J. C. Martinou. 2010. Membrane remodeling induced by the dynamin-related protein Drp1 stimulates bax oligomerization. Cell 142:889-901.

127. O. Teijido and L. Dejean. 2010. Upregulation of Bcl2 inhibits apoptosis-driven BAX insertion but favors Bax relocalization in mitochondria. FEBS Lett. 584:3305-3310.

128. Ahmed, H. 1959. Principles and Reactions of Protein Extraction, Purification, and Characterization, CRC Press LLC, Boca Raton, FL.

129. Johnson, J.L. and K.V. Rajagopalan. 1976. Purification and properties of sulfite oxidase from human liver. J. Biol. Chem 249:859-866.

130. R. L. Hill, and R. A. Bradshaw. 1969. Fumarase. Methods Enzymol. 13: 91-99.

131. Scorrano, L., Ashiya, M., Buttle, K., Weiler, S., Oakes, S. A., C. A. Mannella, and S. Korsmeyer. 2002. A distinct pathway remodels cristae and mobilizes cytochrome *c* during apoptosis. Developmental Cell. 1:55-67.

132. Gottelieb, E., S. Armour, and C. Thompson. 2002. Mitochondrial respiratory control is lost during growth factor deprivation. Proc. Natl. Acad. Sci. U.S.A. 99: 12801 – 12806.

133. Landeta, O., Landajuela, A., Gil, D., Taneva, S., Di Primo, C., Sot, B., Valle, M., V. A. Frolov, and G. Basañez. 2011. Reconstitution of proapoptotic BAK function in liposomes reveals a dual role for mitochondrial lipids in the BAK-driven membrane permeabilization process. J. Biol. Chem. 286:8213-8230.

134. Valentijn, A.J., J. P. Upton, and A. P. Gilmore. 2008. Analysis of endogenous Bax complexes during apoptosis using blue native PAGE: implications for Bax activation and oligomerization. Biochem. J.412:347-357.

135. Dejean, L.M., Martinez-Caballero, S., S. Manon, and K. W. Kinnally. 2006. Regulation of the mitochondrial apoptosis-induced channel, MAC, by BCL-2 family proteins. Biochim. Biophys. Acta 1762:191-201.

136. Annis, M.G., Soucie, E.L., Dlugosz, P.J., Cruz-Aguado, J.A., Penn, L.Z., B. Leber, and D. W. Andrews. 2005. Bax forms multispanning monomers that oligomerize to permeabilize membranes during apoptosis. EMBO J. 24:2096-2103.

137. Mikhailov, V., Mikhailova, M., Pulkrabek, D.J., Dong, Z., M. A. Venkatachalam, and P. Saikumar. 2001. Bcl-2 prevents Bax oligomerization in the mitochondrial outer membrane. J. Biol. Chem.276:18361-18374.

138. Ott, M., Robertson, J.D., Gogvadze, V., B. Zhivotovsky, and S. Orrenius. 2002. Cytochrome *c* release from mitochondria proceeds by a two-step process. Proc. Natl. Acad. Sci. U.S.A. 99:1259-1263.

139. Uren, R.T., Dewson, G., Bonzon, C., Lithgow, T., D. D. Newmeyer, and R. M. Kluck. 2005. Mitochondrial release of pro-apoptotic proteins: electrostatic interactions can hold cytochrome *c* but not Smac/DIABLO to mitochondrial membranes. J. Biol Chem. 280:2266-2274.

140. Yuan, H., Williams, S.D., Adachi, S., T. Oltersdorf, and R. A. Gottlieb. 2003. Cytochrome *c* dissociation and release from mitochondria by truncated Bid and ceramide. Mitochondrion. 2:237-244.

141. Doran, E., and A. P. Halestrap. 2000. Cytochrome *c* release from isolated rat liver mitochondria can occur independently of outer-membrane rupture: possible role of contact sites. Biochem. J. 348 pt. 2:343-350.

142. Finucane, D.M., Bossy-Wetzel, E., Waterhouse, N.J., T. G. Cotter, and D. R. Green. 1999. Bax-induced caspase activation and apoptosis via cytochrome *c* release from mitochondria is inhibitable by Bcl-xL. J. Biol. Chem. 274:2225-2233.

143. Zhuang, J., and G. M. Cohen. 1998. Release of mitochondrial cytochrome *c* is upstream of caspase activation in chemical-induced apoptosis in human monocytic tumour cells. Toxicol. Lett. 102-103:121-129.

144. Li, T., Brustovetsky, T., B. Antonsson, and N. Brustovetsky. 2010. Dissimilar mechanisms of cytochrome *c* release induced by octyl glucoside-activated BAX and by BAX activated with truncated BID. Biochim. Biophys. Acta 1797:5256.

145. Siskind, L.J., Mullen, T.D., Romero Rosales, K., Clarke, C.J., Hernandes-Corbacho, M.J., A.L. Edinger and L.M. Obeid. 2010. The Bcl-2 protein Bak is required for long chain ceramide generation during apoptosis. J. Biol. Chem. 285: 11818 – 11826.

146. Perera, M.N., Lin, S.H., Peterson, Y.K., Bielawska, A., Szulc, Z.M., R. Bittman, and M. Colombini. 2012. Bax and Bcl-xL exert their influences on different sites of the ceramide channel. Biochem. J. 225: 81 – 91.

147. V. Ganesan, and M. Colombini. 2010. Regulation of ceramide channels by Bcl-2 family proteins. FEBS. Letters 584: 2128 – 2134.

148. Perera, M.N., Ganesan, V., siskind, L.J., Szulc, Z.M., Bielawaski, J., Bielawska, A., R. Bittmann, and M. Colombini. 2012. Ceramide channels: Influence of molecular structure on channel formation in membranes. Biochim. Biophys. Acta. 1818: 1291 – 1301.

149. Martinez-Caballero, S., Dejean, L.M., Kinnally, M.S., Oh, K.J., C.A. Mannella, and K.W. Kinnally. 2009. Assembly of Mitochondrial Apoptosis-induced Channel, MAC. J. Biol. Chem. 12235- 12245.